International Ocean Discovery Program Expedition 368 Preliminary Report

South China Sea Rifted Margin

Testing hypotheses for lithosphere thinning during continental breakup: drilling at the South China Sea rifted margin

9 April–11 June 2017

Zhimin Jian, Hans Christian Larsen, Carlos Alvarez Zarikian,
and the Expedition 368 Scientists

IODP
INTERNATIONAL OCEAN DISCOVERY PROGRAM

Publisher's notes

Core samples and the wider set of data from the science program covered in this report are under moratorium and accessible only to Science Party members until 29 September 2018.

This publication was prepared by the *JOIDES Resolution* Science Operator (JRSO) at Texas A&M University (TAMU) as an account of work performed under the International Ocean Discovery Program (IODP). Funding for IODP is provided by the following international partners:

National Science Foundation (NSF), United States
Ministry of Education, Culture, Sports, Science and Technology (MEXT), Japan
European Consortium for Ocean Research Drilling (ECORD)
Ministry of Science and Technology (MOST), People's Republic of China
Korea Institute of Geoscience and Mineral Resources (KIGAM)
Australia-New Zealand IODP Consortium (ANZIC)
Ministry of Earth Sciences (MoES), India
Coordination for Improvement of Higher Education Personnel (CAPES), Brazil

Portions of this work may have been published in whole or in part in other IODP documents or publications.

Disclaimer

Copyright

Citation

Jian, Z., Larsen, H.C., Alvarez Zarikian, C.A., and the Expedition 368 Scientists, 2018. *Expedition 368 Preliminary Report: South China Sea Rifted Margin.* International Ocean Discovery Program. https://doi.org/10.14379/iodp.pr.368.2018

ISSN
World Wide Web: 2372-9562

August 2018

Expedition 368 participants

Expedition 368 scientists

Zhimin Jian
Co-Chief Scientist
School of Ocean and Earth Science
Tongji University
China
jian@tongji.edu.cn

Hans Christian Larsen
Co-Chief Scientist
Geological Survey of Denmark and Greenland
Denmark
hclarseniodp@gmail.com

Carlos A. Alvarez Zarikian
Expedition Project Manager/Staff Scientist
International Ocean Discovery Program
Texas A&M University
USA
zarikian@iodp.tamu.edu

Stephen A. Bowden
Organic Geochemist
School of Geosciences
University of Aberdeen
United Kingdom
s.a.bowden@abdn.ac.uk

Deniz Cukur
Petrophysics (Physical Properties) Specialist
Marine Geology Department
Petroleum & Marine Research Division
Korea Institute of Geoscience and Mineral Resources (KIGAM)
Republic of Korea
dcukur@kigam.re.kr

Kelsie A. Dadd
Sedimentologist
School of Geosciences
University of Sydney
Australia
kelsie.dadd@sydney.edu.au

Weiwei Ding
Structural Geologist
Key Laboratory of Submarine Geoscience
Second Institute of Oceanography (SIO), State Oceanic Administration (SOA)
China
wwding@sio.org.cn

Eric C. Ferré
Paleomagnetist
Department of Geology
Southern Illinois University at Carbondale
USA
eferre@geo.siu.edu

Fabricio Ferreira
Paleontologist (foraminifers)
Institute for Geosciences, Universidade Federal Fluminense (UFF), Brazil
CAPES Foundation
Ministry of Education of Brazil
ferreira_paleo@hotmail.com

Aaron J. Gewecke
Paleontologist (diatoms)
Earth and Atmospheric Sciences
University of Nebraska, Lincoln
USA
aarongewecke@gmail.com

Enqing Huang
Petrophysics (Physical Properties) Specialist
School of Ocean and Earth Science
Tongji University
China
ehuang@tongji.edu.cn

Shijun Jiang
Paleontologist (nannofossils)
Institute of Groundwater and Earth Sciences
Jinan University
China
sjiang@jnu.edu.cn

Haiyan Jin
Paleontologist (foraminifers)
State Key Laboratory of Marine Geology
Tongji University
China
jinhy@tongji.edu.cn

Robert M. Kurzawski
Petrologist
GEOMAR Helmholtz Center for Ocean Research Kiel
Christian-Albrechts-Universität zu Kiel
Germany
rkurzawski@geomar.de

Yanping Li
Inorganic Geochemist
School of Geographical and Oceanographical Sciences
Nanjing University
China
ypli@nju.edu.cn

Baohua Li
Paleontologist (foraminifers)
Department of Micropalaeontology
Nanjing Institute of Geology and Palaeontology
China
bh-li@nigpas.ac.cn

Jian Lin
Petrophysics (Physical Properties) Specialist
Department of Geology and Geophysics
Woods Hole Oceanographic Institution
USA
jlin@whoi.edu

Chuanlian Liu
Paleontologist (nannofossils)
School of Ocean and Earth Science
Tongji University
China
liucl@tongji.edu.cn

Chang Liu
Sedimentologist
Department of Geology and Geophysics
Louisiana State University
USA
cliu14@lsu.edu

Geoffroy T.F. Mohn
Petrologist
Laboratoire Géosciences et Environnement Cergy (GEC)
Maison Internationale de la Recherche
Université de Cergy-Pontoise
France
Geoffroy.Mohn@u-cergy.fr

Lachit Singh Ningthoujam
Petrophysics (Physical Properties) Specialist
Department of Marine Geophysics
National Centre for Antarctic and Ocean Research (NCAOR)
India
lachit@ncaor.gov.in

Nobuaki Osono
Petrophysics (Physical Properties) Specialist
Faculty of Science
Graduate School of Science and Technology for Innovation,
Yamaguchi University
Japan
t004dg@gmail.com

David W. Peate
Petrologist
Earth & Environmental Sciences
University of Iowa
USA
david-peate@uiowa.edu

Patricia Persaud
Petrophysics (Physical Properties) Specialist
Department of Geology and Geophysics
Louisiana State University
USA
ppersaud@lsu.edu

Ning Qiu
Petrophysics (Physical Properties) Specialist
Key Laboratory of Marginal Sea Geology
Chinese Academy of Sciences
China
ningqiu@scsio.ac.cn

Sara Satolli
Paleomagnetist
Department of Engineering and Geology
University of Chieti-Pescara
Italy
sara.satolli@unich.it

Julie C. Schindlbeck
Sedimentologist
GEOMAR Helmholtz Center for Ocean Research Kiel
Germany
jschindlbeck@geomar.de

Susanne M. Straub
Sedimentologist/Petrologist
Lamont-Doherty Earth Observatory
Columbia University
USA
smstraub@ldeo.columbia.edu

Liyan Tian
Inorganic Geochemist
Institute of Deep-sea Science and Engineering
Chinese Academy of Sciences
China
lytian@idsse.ac.cn

Froukje M. van der Zwan
Petrologist
Institute of Geosciences
Christian Albrechts University Kiel
Germany
fvdz@gpi.uni-kiel.de

Shiming Wan
Sedimentologist
Institute of Oceanology
Chinese Academy of Sciences
China
wanshiming@ms.qdio.ac.cn

Huaichun Wu
Paleomagnetist
School of Ocean Sciences
China University of Geosciences
China
whcgeo@cugb.edu.cn

Guangfa Zhong
Sedimentologist
School of Ocean and Earth Science
Tongji University
China
gfz@tongji.edu.cn

Observers

Pai-Sen Yu
Paleontologist (foraminifers)
National Applied Research Laboratories (NARLabs)
Taiwan Ocean Research Institute (TORI)
Taiwan
epson_yu@narlabs.org.tw

Gailun Zhang
China
jyjj1234567@126.com

Education and outreach

Amanda M. Wolfe
Education/Outreach Officer
USA
wolfe.amanda.marie@gmail.com

Shuhao Xie
Education/Outreach Officer
China
rafaelxie@qq.com

SIEM Offshore AS officials

Steve Bradley
Master of the Drilling Vessel

Wayne Malone
Offshore Installation Manager

Technical support

Susan Boehm
Thin Section Laboratory

Lisa Brandt
Chemistry Laboratory

Lisa Crowder
Assistant Laboratory Officer

Aaron de Loach
Core Laboratory

Keith Dupuis
Underway Geophysics Laboratory

Sheryl Frazier
Physical Properties Laboratory

Timothy Fulton
Senior Imaging Specialist

Clayton Furman
Logging Engineer

Randy Gjesvold
Marine Instrumentation Specialist

Kevin Grigar
Operations Superintendent

Sandra Herrmann
Assistant Laboratory Officer

Michael Hodge
Marine Computer Specialist

Minh Nhut Huynh
Marine Computer Specialist

Nicolette Lawler
X-Ray Laboratory

Brittany Martinez
Curatorial Specialist

Aaron Mechler
Chemistry Laboratory

Mike Meiring
Engineer

William Mills
Laboratory Officer

Algie Morgan
Applications Developer

Beth Novak
Paleomagnetism Laboratory

Garrick Van Rensburg
Marine Instrumentation Specialist

Jean Wulfson
Publications Specialist

Hai (James) Zhao
Applications Developer

Abstract

International Ocean Discovery Program Expedition 368 is the second of two consecutive cruises that form the South China Sea Rifted Margin program. Expeditions 367 and 368 share the common key objectives of testing scientific hypotheses of breakup of the northern South China Sea (SCS) margin and comparing its rifting style and history to other nonvolcanic or magma-poor rifted margins. Four primary sites were selected for the overall program: one in the outer margin high (OMH) and three seaward of the OMH on distinct, margin-parallel basement ridges. These three ridges are informally labeled A, B, and C. They are located within the continent–ocean transition (COT) zone ranging from the OMH to the interpreted steady-state oceanic crust (Ridge C) of the SCS. The main scientific objectives include

1. Determining the nature of the basement within crustal units across the COT of the SCS that are critical to constrain style of rifting,
2. Constraining the time interval from initial crustal extension and plate rupture to the initial generation of igneous ocean crust,
3. Constraining vertical crustal movements during breakup, and
4. Examining the nature of igneous activity from rifting to seafloor spreading.

In addition, the sediment cores from the drill sites targeting primarily tectonic and basement objectives will provide information on the Cenozoic regional environmental development of the Southeast Asia margin.

Expedition 368 was planned to drill at two primary sites (U1501 and U1503) at the OMH and Ridge C, respectively. However, based on drilling results from Expedition 367, Expedition 368 chose to insert an alternate site on Ridge A (Site U1502). In total, the expedition completed operations at four sites (U1501, U1502, U1504, and U1505). Site U1503, however, was not completed beyond casing to 990 m because of mechanical problems with the drilling equipment that limited the expedition from 25 May 2017 to the end of the expedition to operate with a drill string not longer than 3400 m. New alternate Site U1504 proposed during Expedition 367 met this condition. Site U1505 also met the operational constraints of the 3400 m drill string (total) and was an alternate site for the already drilled Site U1501.

At Site U1501, we cored to 697.1 m in 9.4 days, with 78.5% recovery. We also drilled ahead for 433.5 m in Hole U1501D and then logged downhole data from 78.3 to 399.3 m. In 19.3 days at Site U1502, we penetrated 1679.0 m, set 723.7 m of casing and cored a total of 576.3 m with 53.5% recovery, and collected downhole log data from 785.3 to 875.3 m and seismic data through the 10¾ inch casing. At Site U1503, we penetrated 995.1 m, setting 991.5 m of 10¾ inch casing, but no cores were taken. At Site U1504, we took 40 rotary core barrel (RCB) cores over two holes. The cored interval between both holes was 277.3 m with 26.8% recovery. An 88.2 m interval was drilled in Hole U1504B. At Site U1505, we cored 668.0 m with 101.1% recovery. Logging data was collected from 80.1 to 341.2 m. Operations at this site covered 6.1 days. Except for Site U1505, we drilled to acoustic basement, which prior to the expedition, except for Site U1501, had been interpreted to be crystalline basement. A total of 6.65 days were lost due to mechanical breakdown or waiting on spare supplies for repair of drilling equipment.

At Site U1501 on the OMH, coring ~45 m into the acoustic basement sampled highly lithified sandstone to conglomerate of presumed Mesozoic age overlain by siliciclastic Eocene pre- to synrift sediments of Oligocene age and topped by primarily carbonaceous postrift sediments of early Miocene to Pleistocene age. Site U1502 on Ridge A was cased to 723.7 m. At this site, we recovered 180 m of hydrothermally altered brecciated basalts comprising sheet and pillow lavas below deep-marine sediments of Oligocene to late Miocene age. Coring was not performed within the upper 380 m (~Pliocene–Pleistocene) at Site U1502. At Site U1503 on Ridge C, 991.5 m of casing was installed in preparation for the planned deep drilling to ~1800 m, but no coring was performed due to mechanical failures, and the site was abandoned without further activity. Coring at Site U1504 on the OMH ~45 km east of Site U1501 recovered metamorphic schist to gneiss (greenschist facies) below late Eocene (?) carbonate rocks (partly reef debris) and early Miocene to Pleistocene sediments. At Site U1505, we cored to 480.15 m through Pleistocene to late Oligocene mainly carbonaceous ooze followed at depth by early Oligocene to late Eocene siliciclastic sediments.

Efforts were made at every drill site to correlate the core with the seismic data and seismic stratigraphic unconformities interpreted within the Eocene to Plio–Pleistocene sedimentary sequence prior to drilling. The predrilling interpretation of ages of these unconformities was in general confirmed by drilling results.

As a result of the constraints on the length of drill string that could be deployed during the later part of Expedition 368, the secondary expedition objectives addressing the environmental history of the SCS and Southeast Asia received more focus than planned because these sites are located in shallower water depths and required less penetration depth. This forced change in emphasis, however, was without fatal consequences for the primary tectonic objectives. The two expeditions together provided solid evidence for a process of breakup that included vigorous synrift magmatism as opposed to the often-favored interpretation of the SCS margin as a magma-starved margin.

Introduction

The South China Sea (SCS) margin (Figure **F1**) is an accessible and well-imaged location where drilling of synrift sediment and underlying basement will provide key constraints on the processes of rifting and eventual rupturing of the continental lithosphere during breakup at a highly extended rifted margin. Expeditions 367 and 368 were based on International Ocean Discovery Program (IODP) drilling Proposals 878-CPP, 878-Add, 878-Add2, and 878-Add3. This project was implemented as a single science program with 114 days of drilling operations spread across two IODP expeditions as outlined in the Expedition 367/368 Scientific Prospectus (Sun et al., 2016b). Two expeditions were required to drill four deep-penetration sites in a transect across the margin. Three sites targeted acoustic basement in the continent–ocean transition (COT), and one site targeted late prerift to synrift sequences on the landward side of the transect. Although the primary focus of this drilling expedition is to discriminate between possible models for rifting and plate rupture, the drilling, along with results from Ocean Drilling Program (ODP) Leg 184 and IODP Expedition 349, addresses secondary objectives to improve our understanding of the Cenozoic environmental development of the southeast Asian area as recorded within the sediments of the SCS basin. The drilling strategy for Expeditions 367 and 368, however, primarily targeted the deep basement coring and logging objectives.

Background

Global questions regarding formation of rifted margins

The Ocean Drilling Program (1985–2003) made a major effort along the rifted margins of the North Atlantic to understand the processes of continental breakup (ODP Legs 103, 104, 149, 152, 163, 173, and 210). This effort resulted in the recognition of two end-members of rifted margins (see summary of observations in Sun et al., 2016a, 2016b).

The first recognized end-member is volcanic rifted margins, examples of which are characterized by massive igneous activity in a relatively short period of time (~1–3 million years) during breakup and initial seafloor spreading. The pair of conjugate margins of Greenland and northwest Europe is a type example. In these locations, the asthenospheric mantle may have been anomalously hot (e.g., mantle plumes), leading to thermal weakening of the continental lithosphere followed by rapid plate rupture.

The second recognized end-member is magma-poor rifted margins, which are interpreted to endure hyperextension of the continental crust, with tectonic extension at the distal margin eventually exhuming the subcontinental mantle lithosphere and leading to serpentinization of the mantle. The Newfoundland and Iberia conjugate margin, where serpentinite occupies a broad zone within the COT zone, is an example of this type of margin and is the only conjugate margin pair where this interpretation has been confirmed by scientific drilling. The introduction of water to the subcontinental lithospheric mantle is interpreted to have taken place through deep, crust-cutting faults, causing serpentinization that profoundly weakens the mantle lithosphere and facilitates plate rupture. The subsequent ultraslow spreading led to formation of additional serpentinite on the seafloor (e.g., Dick et al., 2003) until sufficient magma production for normal oceanic crust to form was established.

Other examples of highly extended rifted margins have been identified in seismic reflection data elsewhere (e.g., Brune et al., 2017; Doré and Lundin, 2015). However, it is not known if serpentinized mantle plays a critical role in all cases. Modeling by Huismans and Beaumont (2008, 2011) suggests several scenarios for the formation of rifted margins in the absence of anomalously hot asthenospheric mantle. One scenario (Type I of Huismans and Beaumont, 2011) is the Iberia-Newfoundland-type margin described above. In this case, lithospheric thinning initially occurs in the (upper) crust, with extensional faults profoundly thinning the continental crust (hyperextension) and eventually reaching the mantle and causing serpentinization (Whitmarsh et al., 2001; Pérez-Gussinyé and Reston, 2001; Pérez-Gussinyé et al., 2006; Reston, 2009; Sutra and Manatschal, 2012). The schematic model of this type of margin development, shown in Figure **F2**, guided the drilling strategy of Expedition 367/368. Huismans and Beaumont (2008, 2011), however, also suggest that final plate rupture can occur without exhumation of the subcontinental mantle and be followed rather quickly by igneous ocean crust formation, a scenario that our chosen drilling strategy will also test. The highly extended northern margin of the SCS is therefore an excellent location to examine through drilling whether this margin endured magmatism during breakup or its development is closer to the Iberia-type, amagmatic margin.

Geological setting

The SCS is a modestly sized young ocean basin that formed along the eastern boundary of the Eurasian plate during mid- to late Cenozoic time (Figure **F1**). Expeditions 367 and 368 cored and logged a transect of drill sites across the COT in the northern SCS (Figure **F2**).

The continental crust that was rifted to form the SCS was accreted to the Asian margin during the Mesozoic (Zhou and Li, 2000; Zhou et al., 2008; Li et al., 2012a, 2012b). Within ~80 million years, this relatively young continental lithosphere underwent extensive rifting during the Paleogene, likely within the Eocene to early Oligocene (Figure **F3**). Seafloor spreading in the SCS started during the Oligocene, with the oldest interpreted magnetic anomaly in the area of the drilling transect interpreted to be Anomaly C11 (~29.5 Ma) or C12n (~31 Ma) (Briais et al., 1993; Li et al., 2013, 2014; Franke et al., 2013). A later expansion of seafloor spreading into the southwest SCS took place from ~23 Ma (Briais et al., 1993; Barckhausen and Roeser, 2004; Li et al., 2012a, 2012b; Franke et al., 2013).

The initial half-spreading rate was ~3.6 cm/y, later slowing to 1.2 cm/y with seafloor spreading to eventually cease by ~15 Ma (Li et al., 2014). The initial spreading rate in the SCS basin is therefore higher than the ultraslow spreading scenario of the Iberia-Newfoundland margin (Dick, 2003). Subduction of the eastern part of the SCS basin started at or before ~15 Ma along the Manila Trench (Li et al., 2013). For a more complete review of the regional setting and tectonic development of the SCS, see Shi and Li (2012), Li et al. (2013), Sun et al. (2014), and Franke et al. (2013).

The Expedition 367/368 drilling transect is located ~50 km west of IODP Site U1435 (Figures **F1**, **F2**, **F4**) (Li et al., 2015a, 2015b) along the northern SCS margin. A transform fault defines a western boundary of a margin segment that exhibits a broad zone of crustal extension (Figure **F4**). This broad zone of extension (COT) may end to the east somewhere between Sites U1432 and U1435. East of this position, continental crust seems to thin into ocean crust within a much narrower COT.

The segment of the SCS margin addressed by Expeditions 367 and 368 is therefore characterized by a broad COT (~150 km) of crustal stretching and extension prior to breakup. A deep sag basin (midslope basin [MSB]) of presumed Eocene to Oligocene age is present within the midslope area (Figure **F3**) and is bounded seaward by an outer margin high (OMH) forming a quite persistent structure along the margin. Three distinct ridges (A, B, and C in Figures **F3**, **F4**) are found seaward of the OMH within the more distal margin and on progressively thinner crust within the COT. We refer to the continent/ocean boundary (COB) as the much narrower zone in which the outermost, highly thinned continental lithosphere is replaced seaward by new crust that formed within a narrow zone at a spreading ridge in a steady-state fashion. The latter can include continuous tectonic exhumation of rising lithospheric mantle (e.g., Dick et al., 2003), accretion of normal igneous oceanic crust, or a mixture of these two processes. The nature and precise location of the COB at the SCS cannot with any confidence be interpreted from the seismic data without drilling control.

The clear seismic reflections from the Mohorovicic seismic discontinuity (Moho) show distinct thinning of the continental crust (Figure **F3**) across the COT with a thickness of ~6 km around the seaward end of the COT. Separate layers hypothesized to be upper, middle, and lower crust are present within the landward part of

these seismic profiles. The lower crust is acoustically transparent and may in places be as thin as ~6 km. Lower crust with a similar thickness and seismic appearance is reported from the northeastern SCS margin (McIntosh et al., 2013, 2014; Lester et al., 2013). The seaward continuation of this crustal layering into the COB zone is, however, ambiguous, and prevents us from interpreting the exact location and the detailed nature of the COB.

The upper crust shows numerous extensional, low-angle detachment faults soling out at midcrustal level. This fault system generated a number of deep half-grabens filled with synrift sediments that were subsequently covered by postrift sediments. The boundary between synrift sediment and postrift sediments may follow the seismic stratigraphic unconformity named T70 (Figure **F3**). Industry data from distant wells results suggest a breakup unconformity age of ~34 Ma. However, the time of crustal extension is not necessarily synchronous across the margin and could be younger toward the outer margin. A younger, widely distributed unconformity (T60) is also shown in Figure **F3**. The T60 unconformity corresponds to a hiatus at ~23 Ma found at ODP Site U1148 (Wang, Prell, Blum, et al., 2000) and IODP Site U1435. T60 is approximately synchronous with a southward jump of the SCS spreading axis (Briais et al., 1993).

The OMH hosts a number of relatively shallow half-graben basins on top of this broad basement high. The stratigraphy of these smaller basins can be traced seismically into the deeper, central basin sag below the MSB (Figure **F3**). The normal faults bounding these OMH basins are clearly imaged and, for the main part, dip landward. These small rift basins, therefore, offer an opportunity to sample the stratigraphy covering the entire period of rifting and postrift subsidence. The MSB itself is bounded landward by major, seaward-dipping normal fault(s) seemingly forming major detachments soling out at middle to lower crustal levels but not penetrating through the lower crust. If true, this suggests decoupling between the upper and lower crust and, at least within this more landward part of the margin, faults never penetrated the lower curst (remained ductile?).

The lower crust within the COT may thicken seaward (lower crustal flow?), but this possibility is not well constrained (Figure **F3**). Likewise, seismic imaging of the low-angle faults and detachments within the landward part of the COT cannot, with confidence, be traced into the distal margin regime. One possibility is that the main detachment zone was located above what later became Ridge A, effectively implying that Ridge A is a core complex consisting of lower continental crust or subcontinental mantle, depending on how deeply detachments exhumed the lithosphere in the distal margin. Alternatively, if the main detachment underlies Ridge A, this structure would represent upper plate material of upper crustal origin.

Ridge A is for the most part dome-like, showing neither normal faults nor clearly developed synrift half-grabens like the OMH. Excluding sediment, the crust below this outermost basement high is only ~6–8 km thick using the ocean-bottom seismometer (OBS) velocity constraints of Yan et al. (2001), Wang et al. (2006), and Wei et al. (2011). Seaward of Ridge A, the crust has a fairly uniform thickness of ~6 km, which could be consistent with oceanic crust (Yan et al., 2001). Note also that magnetic Anomaly C11 is projected to almost overlap the seaward part of Ridge A (Figures **F3**, **F4**).

Both Ridges B and C consist of fault blocks rotated landward along seaward-dipping normal faults. Some of these faults may be seismically traced to near the base of the crust. Ridge B shows seismic features along strike and within the uppermost crust that could be consistent with a volcanic origin. However, these features could also be consistent with a rotated fault block of upper continental crust (i.e., a distal extensional rider of upper plate origin), in which case the prerift deposits below the seismic unconformity defining the top of acoustic basement at Ridge B should be present. The seismic layered structure of Ridge B makes it less likely to consist of lower crust or serpentinized mantle. Ridge C in many ways is seismically similar to Ridge B. However, an apparent reversed magnetic anomaly strongly suggests that this ridge indeed represents close to if not full igneous ocean crust.

Sampling the basement at Ridges A, B, and C was therefore essential for Expeditions 367 and 368 to distinguish between different tectonic models for breakup along highly extended margins. Ridges A and B help to constrain the style of rifting. In contrast, Ridge C is assumed to represent the early igneous crust and will address another key objective of Expeditions 367 and 368 to constrain the nature of early oceanic crust formation, specifically to determine how quickly a robust igneous system was established, what mantle source is involved (e.g., composition, temperature), what conditions of mantle melting (degree and depth of melting) are present, and, if any, what continental crustal contamination of the igneous material derived from the asthenospheric mantle.

Expedition objectives

The two-expedition drilling transect across the SCS margin set out to understand the timing and process of rifting, eventual rupturing of the continental crust, and onset of igneous oceanic crust at a highly extended rifted margin (Figure **F2**). Four primary and sixteen alternate drill sites across a ~150 km wide COT zone were defined within the *Scientific Prospectus* (Sun et al., 2016b). The four primary sites were planned to target the four main tectonic features (the OMH and its small rift basins) and the nature of the three ridges within the distal margin (Ridges A, B, and C). At each of these sites, the nature of the acoustic basement and the record of synrift and postrift deposits were key targets.

The OMH site (U1501) in particular will address the entire rifting history and provide constraints on the degree of crustal exhumation, if any, within the OMH. Located off the distal margin and at relatively thick crust, the subsidence history at this site can be compared with that of the more distal margin that suffered a much higher degree of crustal stretching. Sampling of late prerift to synrift sediments within the rotated fault block can constrain the timing of rifting and therefore support estimates of the rate of extension. The site is also in a shallower water depth than the other three primary sites and above the present carbonate compensation depth (CCD) and therefore has the potential to yield a rich record of carbonate sediments for detailed paleoclimate studies using stable isotope techniques.

Ridge A in particular would be important for constraining whether this ridge, in effect, is a core complex representing lower plate material, upper plate extensional fault block, or igneous material related to breakup. Ridge B provides a second option to possibly recover unroofed, lower plate material, a highly distal upper plate extensional fault block (i.e., extensional rider), or early igneous material related to incipient seafloor spreading. Ridge C, as described above, targets sampling a time series of early ocean floor magmatism to establish a reference frame for understanding and modeling the entire igneous development of the margin.

Expedition 367 drilled two of the primary sites (U1499 and U1500) on Ridges A and B (Figures **F2**, **F3**, **F4**, **F5**). Coring at Site

U1499 on Ridge A recovered rift-related, syntectonic sediments below the acoustic basement. Because of borehole conditions, however, coring at the site did not penetrate deeply enough to reach crystalline basement (Sun et al., 2017). Coring at Site U1500 successfully sampled 150 m of basaltic lavas, including pillow lavas, below the acoustic basement at Ridge B. Both sites recovered late Oligocene to Pleistocene postrift sedimentary records.

Expedition 368 set out to drill the remaining two primary sites on Ridge C (U1503) and the OMH (Site U1501) (Figures **F2**, **F3**, **F4**, **F5**). However, the Expedition 367 findings of thick, basaltic and submarine lavas at Site U1500 (Ridge B), along with coring at Site U1499 (Ridge A) that did not penetrate to crystalline basement, led Expedition 368 to initially focus on coring the OMH (Site U1501) and pursue a second deep hole on Ridge A (Site U1502) with the potential consequence of not being able to pursue deep drilling at Ridge C (Site U1503). A successful drilling strategy (see below), however, allowed us to eventually pursue Site U1503, but after installation of casing, the hole had to be abandoned for drilling technical reasons. This left time for other, alternate sites with shallower drilling targets (see **Operations**).

Coring and logging strategy

Drilling operations were designed to core and log through thick sediment sections and, significantly, into underlying basement using casing within the upper and unstable part of the sedimentary sections. Initially, the operational approach was to comprise two holes per site (Figure **F6**).

The first hole at each site was to be cored with the advanced piston corer (APC) and extended core barrel (XCB) systems to refusal (or maximum casing depth) and then to be logged with the triple combination (triple combo) and Formation MicroScanner (FMS)-sonic tool strings. The APC/XCB hole was also to document borehole and formation conditions to help determine the length of casing to be drilled into the seafloor in a second hole (B). All full APC cores were intended to be oriented, and formation temperature measurements would be made using the advanced piston corer temperature tool (APCT-3).

The second hole at each site was designed to begin by drilling-in a seafloor reentry system with casing extending to ~650 m or an otherwise defined depth. Casing is drilled down through the reentry cone using an extendable underreamer and mud motor technology (Figure **F6**). Following the installation of casing to the desired depth, coring using the RCB system could then extend from the base of the casing through the sediment and into the underlying basement. Multiple pipe trips to replace hard rock RCB bits were to be made as required by depth of target within basement. Upon completion of the coring objectives, the RCB bit was to be dropped either in the bottom of the hole or on the seafloor before downhole wireline logging data could be collected. For this deeper logging, we planned to use the triple combo and FMS-sonic tool strings as well as the Versatile Seismic Imager (VSI) tool string to conduct check shots.

During Expedition 368, we had to modify this general operational plan in response to borehole conditions and the need to focus our operations time to achieve our highest priority basement objectives. The planned versus implemented operations are shown in Figure **F6**.

At Site U1501, the pilot hole (U1501C) consisted of APC/XCB coring until refusal. From the findings, we concluded that in this location the formation might be stable enough to continue with the deeper RCB Hole U1501D to ~600 m without casing. Logging was therefore not done in Hole U1501C. Hole U1501D was drilled without coring to a slightly shallower depth than Hole U1501C and then RCB cored to the bottom of the hole. Logging was then executed. This approach saved considerable operation time. We drilled in Hole U1502A to 375 m without coring and then cored with the RCB system to identify a proper casing point. Casing was then drilled in Hole U1502B to the desired depth, followed by RCB coring to target. Single-run logging (triple combo) was then executed in the open hole below casing with VSI check shots within both open hole and casing. At Site U1503, we initially drilled in Hole U1503A without coring to a planned casing depth (990 m) estimated on the basis of drilling data from Site U1500 (~20 km away) and seismic correlation between the two sites. A free-fall reentry system was deployed, and casing was subsequently installed in the already established Hole U1503A with the assistance of the underreamer and mud motor. This approach turned out to be very efficient and saved much time. Unfortunately, mechanical problems at the rig floor (see **Operations**) prevented us from further pursuing the site.

With an operational limit of deploying a maximum of 3400 m of drill string for the remainder of Expedition 368, no deep sites requiring casing could be pursued. Site U1504 had a primary basement target below only ~120 m of sediment cover. Hole U1504A was RCB cored to ~150 m. Hole U1504B was drilled without coring to ~90 m and continued with RCB coring to 200 m. No logging was pursued.

Four holes were cored and/or drilled at Site U1505. Hole U1505C was cored with the APC as deep as possible, further cored with the half-length advanced piston corer (HLAPC) system until refusal, extended by XCB coring until the maximum length of the drill string was reached at 480 m, and then logged. Hole U1505D was cored with the APC to 180 m.

Site summaries

Site U1501

Background and objectives

Site U1501 (proposed Site SCSII-41A; 18°53.0923′N, 115°45.9455′E) within the SCS northern margin (Figure **F2**) is located on a broad regional basement high (OMH). The OMH is the most landward of four distinct highs within the COT and is followed seaward by Ridges A, B, and C (Figures **F3**, **F4**, **F7**). Site U1501 is located at 2846 m below sea level (mbsl). Small rift basins of presumed Paleogene age are located on top of the OMH (Figure **F3**). These basins can be traced landward into much deeper half-graben basins that formed during the main phase of crustal extension. The rift basins located on the OMH therefore offer options to recover the stratigraphy of these basins by moderately deep drilling, testing existing stratigraphic interpretations, and extrapolating the findings margin wide. Recovering and characterizing these sequences were key objectives at Site U1501, with the specific goal to constrain the timing and duration of crustal extension, the tectonic vertical movements during rifting, and the subsequent postrift thermal subsidence. The crystalline basement at Site U1501 is most likely located far below the acoustic basement at ≈600 m and was not an objective for this site.

At 2846 mbsl, Site U1501 is one of the few ODP and IODP sites in the SCS above the modern CCD of the SCS. Sites U1504 and U1505, also at the OMH, are situated at <3000 mbsl. The younger stratigraphy is therefore also the focus of some secondary scientific objectives related to Neogene environmental development of the SCS and adjacent landmasses of Southeast Asia. Among these sec-

ondary objectives are to (1) reconstruct the history of the east Asian monsoon evolution and that of deepwater exchanges between the SCS and Pacific Ocean and (2) explore the sedimentary responses to the Cenozoic regional tectonic and environmental development of the Southeast Asia margin.

Operations

We conducted operations in four holes at Site U1501. In Holes U1501A and U1501B, Core 1H missed the sediment–water interface and retrieved full core barrels, indicating that the core was shot from below the seafloor. Hole U1501C (18°53.0919′N, 115°45.9485′E; 2846 mbsl) was APC cored from the seafloor to 461.8 m and recovered 447.8 m (96.3%). Hole U1501D (18°53.0929′N, 115°45.9370′E; 2846 mbsl) was drilled without coring from the seafloor to 433.5 m and then RCB cored to 644.3 m. A total of 78.8 m of core was recovered (37.4%). Hole U1501D was logged with the triple combo tool string from 113 to 299.3 m.

Lithostratigraphy

The sedimentary succession recovered at Site U1501 is composed of clay-rich nannofossil ooze, silty clay, clayey silt, sand, and siltstone and sandstone with minor conglomerate and rare volcanic ash. The succession is divided into three major lithostratigraphic units (I, II, and III) distinguished on the basis of sediment composition, particularly the relative abundance of the calcareous and siliciclastic fractions (Figure **F8**).

Unit I is a 303 m thick, Holocene–late Oligocene succession dominated by clay-rich nannofossil ooze and nannofossil ooze with clay, with minor amounts of nannofossil-rich foraminifer sand or silty sand. A felsic volcanic ash layer occurs in Section 368-U1501A-1H-7, and an ash pod was observed in Section 368-U1501C-3H-1. Unit I is divided into six subunits: IA (0–25.47 m), IB (25.47–66.17 m), IC (66.30–156.70 m), ID (156.80–191.99 m), IE (191.99–293.09 m), and IF (293.90–303.01 m), based on changes in lithology, particularly the clay to nannofossil ratio and the presence and abundance of foraminifers, and/or physical properties. The lower contact of Unit I is erosional and marked by the emplacement of a poorly sorted sandy layer. At the boundary, marked changes in *P*-wave velocity, natural gamma radiation (NGR), magnetic susceptibility, porosity, moisture and density, color, carbonate content, and biostratigraphy indicate a small hiatus (Figure **F8**). Unit I was deposited in a deep-marine environment, and lithologic changes between subunits likely reflect the amount of terrigenous input into a relatively open ocean setting. This input may be delivered as buoyant sediment plumes from shallower shelf environments and rarely by weak (distal) turbidity currents. Soft-sediment deformation in Subunit IB indicates slumping downslope of parts of the sequence.

Unit II is 296 m thick and late Oligocene to late Eocene in age. The unit consists of variable amounts of clay, silt, and sand with minor nannofossil-rich clay, nannofossil ooze, and silt with organic matter. Gravel-size grains occur, including shell fragments and glauconite, as well as carbonate and pyrite concretions. Unit II is divided into six subunits: IIA (303.01–385.26 m), IIB (388.80–448.24 m), IIC (452.60–482.33 m), IID (491.00–519.80 m), IIE (529.80–548.64 m), and IIF (548.64–598.91 m). The uppermost two subunits define a fining-upward succession of glauconite-sand dominated to siltstone and clay overlain by clay with nannofossils. Subunits IIC and IE are dominated by sandstone with calcite and Subunit IID has more fine-grained, organic-rich lithologies, whereas Subunit IIF is similar to Subunit IIB but has more coarse-grained sediment and distinctive weak red and reddish gray intervals within the green glauconite-bearing sands. Coarse sand– to pebble-size shell fragments are common in Unit II, and coral fragments occasionally were observed in the upper part of the unit. Glauconite and quartz minerals dominate the siliciclastic grain component. Diagenetic pyrite is common. Unit II most likely represents a gradual change upward from shallow (outer shelf or upper continental slope) to deepwater (lower slope) depositional environments. The Unit II/III boundary was not recovered but is marked by an abrupt change in magnetic susceptibility, NGR, and *P*-wave velocity. A change in the apparent dip of strata from near horizontal in Unit II to ~20° in Unit III suggests that the contact is unconformable.

Unit III (598.91 m to the bottom of the hole) is well lithified and composed of poorly sorted, feldspar-rich sandstone interbedded with moderately to well-sorted, medium- to fine-grained sandstone and rarely siltstone and poorly sorted conglomerate. The age is unknown because no fossils were recognized. Unit III is divided into two subunits: IIIA (598.91–629.79 m) and IIIB (629.79–643.56 m). Subunit IIIA is composed of coarse-grained heterolithic sandstone, sandstone with calcite clasts, and minor conglomerate and siltstone. Pebble- to cobble-size clasts include felsic intrusive and volcanic rocks, sedimentary rocks, metamorphic rocks, and rare gabbro. Subunit IIIB consists of sandstone and minor sandstone with organic matter. The subunit is finer grained than Subunit IIIA and has finely laminated intervals. We speculate that Unit III was formed in continental to littoral environments with a provenance not far from the site.

Structural geology

Unit I shows predominantly horizontal to subhorizontal bedding with local soft-sediment deformation structures such as slump folds. Unit I is devoid of any structures related to tectonic deformation, apart from some rare normal faults with minor offsets.

Unit II is characterized by subhorizontal to gently dipping bedding. Steep dips up to 40° are locally observed in close relation to parallel lamination and are therefore interpreted as cross-laminae. In contrast to Unit I, deformation structures were observed within Unit II, although their occurrence is rather heterogeneously distributed. Planar to irregular millimeter-scale normal faults and joints were observed in Subunit IIA, typically with offsets ranging from 0.1 to 0.5 cm and apparent dips of 10°–40°. Striations and slickensides were documented locally where the surfaces of such structures are exposed. Deformation in the underlying Subunits IIC–IIF is essentially characterized by randomly distributed occurrence of single to branched uniform calcite and quartz veins. Recognition of deformational structures was difficult due to drilling disturbance throughout this unit.

The acoustic basement marks the top of Unit III. This unit shows a weak tilting of stratified beds expressed in apparent dips on split core surfaces up to ~20°. Again, deformation structures remain scarce and heterogeneously distributed in Unit III. The recognized structures consist of veins, fractures, and local microfaults associated with cataclastic fault gouge.

In conclusion, despite the various tilting of reflectors (~5°) and the vicinity of extensional structures observed on seismic profiles, only weak evidence of bedding tilting and/or deformation structures were observed at this site, possibly due to the nature of the sediments.

Biostratigraphy

All core catcher samples at Site U1501 were analyzed for calcareous nannofossils, diatoms, and foraminifers, with select core

catchers examined for ostracods. Additional samples were taken from the split working-half sections when necessary to refine the ages between core catcher samples. Preservation of calcareous microfossils varies from good in Unit I (Cores 368-U1501A-1H, 368-U1501B-1H, and 368-U1501C-1H through 44X) to poor in Units II and III (Cores 368-U1501C-45X through 62X and 368-U1501D-2R through 5R). Planktonic foraminifers and calcareous nannofossils are abundant in Unit I, common to rare in Unit II and upper Unit III, and barren in the rest of Unit III (Cores 368-U1501D-6R though 27R). Diatoms are few with moderate preservation in Samples 368-U1501A-1H-CC, 368-U1501B-1H-CC, and 368-U1501C-1H-CC and 2H-CC. The rest of the core catcher samples are barren of diatoms, with the exception of Samples 368-U1501C-3H-CC, 4H-CC, 33F-CC through 35F-CC, and 46X-CC, in which diatoms are rare with poor preservation. Diatoms are common in burrows found in interval 368-U1501C-35F-1, 118–119 cm, with poor preservation.

Twenty-eight biostratigraphic datums were identified in a mostly continuous succession from the middle Eocene to Holocene with indications that Holes U1501C and U1501D penetrated into strata older than the middle Eocene (Figure **F8**). The Pleistocene/Pliocene boundary (~2.6 Ma) is placed within Core 368-U1501C-7H, the Pliocene/Miocene boundary (~5.3 Ma) within Core 9H, the Miocene/Oligocene boundary (~23.0 Ma) between Cores 41X and 42X, and the Oligocene/Eocene boundary (~33.9 Ma) deeper than Core 45X. Sedimentation rates varied from ~11 mm/ky in the Miocene to ~14 mm/ky in the Pliocene and 24 mm/ky in the Pleistocene. Low sediment accumulation rates (~3.6 cm/ky) during the late Eocene through the early Oligocene and in the late Miocene suggest the presence of hiatuses in the sedimentary record during these periods. In contrast, higher sediment accumulation rates (35 mm/ky) existed during the late Oligocene and the early Miocene.

Predominance of shallow-water benthic foraminifer and ostracod assemblages in Cores 368-U1501C-45X through 62X and 368-U1501D-2R through 6R indicate an upper bathyal to continental shelf paleoenvironment during the Eocene to the early Oligocene. Predominantly abyssal benthic foraminifers and ostracods shallower than Cores 368-U1501C-44X indicate that deepwater conditions existed in this part of the SCS since the early Oligocene.

Paleomagnetism

Paleomagnetic investigations combined measurement and in-line alternating field (AF) demagnetization of archive-half sections on the 2G Enterprises superconducting rock magnetometer (SRM) with the measurement of discrete samples demagnetized thermally or with AF.

The rock magnetic experiments on six representative samples from Hole U1501C show SIRM/χ ratios between 12.8 and 14.6 kA/m, indicating the predominance of greigite in Unit I of Hole U1501C, documented by scanning electron microscopy (SEM) in 2–10 μm grains. Thermal demagnetization behaviors also show that greigite dominates the natural remanent magnetization (NRM), at least downhole to 83 m. However, the magnetic remanence left above 575°C further suggests contributions from additional phases such as maghemite (Curie Temperature [TC] = ~590°–675°C) or hematite (TC = ~675°C).

Both AF and thermal treatments on discrete samples successfully removed the steep low-temperature/coercivity component that represents the drilling overprint. The mean inclination gathered from the high-temperature component is 37.3° ± 6.6°, corresponding to a paleolatitude of 20.8° ± 3.3° for Unit I (see **Lithostratigraphy**). Many of the AF-demagnetized discrete samples reveal trends showing reversed or normal polarity in the last step of demagnetization (50 mT) and are more difficult to interpret.

The magnetostratigraphy in Holes U1501C and U1501D is based on directions derived from the raw moments measured by the SRM at 25 mT and from the corroborative evidence from discrete samples. Magnetostratigraphy was correlated to the standard timescale and plotted along with the tie points from the microfossil ages from shipboard paleontologists. The paleomagnetic and paleontological age constraints match well over most of the section (Figure **F8**). A succession of eight normal and five reverse events was recognized in Hole U1501D. However, the lack of biostratigraphic constraints throughout Hole U1501D prevented even a tentative correlation of these events with the standard timescale.

Geochemistry

Interstitial water samples were obtained from depths to 450 m (Subunit IIB). Within Unit I, variations are mainly the result of diagenetic and microbial processes, and measurements of alkalinity, phosphate, ammonia, and sulfate are within the typical ranges for the region (3.5–5 mM alkalinity, 250–510 μM phosphate, <30 μM ammonia, and <26 μM sulfate). However, more atypically (particularly when compared with Expedition 367 Site U1499), the main changes associated with microbial processes are notable only within the uppermost 25 m in Subunit IA and are typical of organic matter degradation. Deeper than this within Unit I, changes in interstitial water chemistry appear inhibited until 300 m. These changes may be a consequence of the low organic carbon concentration and high carbonate content (~50%) of Unit I. Decreases in sulfate concentrations with depth are more pronounced in Unit II (>300 m), and within this zone there is heavy pyritization and total sulfur contents are high, suggesting sulfate reduction has taken place. Within the uppermost part of Unit II (300–370 m), chloride, bromide, and sodium are notably lower (chloride = 500 mM, cf. 565 mM; bromide = 0.75 mM, cf. 0.9 mM; and sodium = 410 mM, cf. 480 mM). This difference in interstitial water chemical composition is sharp and could result from pressure-isolated units retaining a distinct formation water chemistry or from the migration of chloride-poor formation water.

Headspace gas concentrations are below background laboratory levels in all samples collected from Site U1501 (<1% ppmv). Total organic carbon (TOC) content is typically <0.5% in Unit I, except from 0 to 50 m (Subunit IA). Within this interval, a typical black marine mud has a TOC of ~1%. TOC was also typically <0.5% in Units II and III, except for a few carbonaceous lithologies: sandstones with plant phytoclasts associated with an ash-rich boghead coal in Unit II (interval 368-U1501D-9R-1, 10–15 cm) and a bitumen-impregnated sandstone in Unit III (interval 27R-1, 12–16 cm). Total sulfur content is low in Unit I: ~1% in Subunit IA and below effective shipboard detection limits of 0.01% for the rest of Unit I. Total sulfur content is higher in Unit II; the muddier uppermost part of Unit II has values >1%, whereas the sandier deeper part averages ~0.5%.

Elemental compositions primarily reflect geological units and changes in lithology. Within Unit I, carbonate contents are high and exceed 50% within foraminifer-rich intervals (compositionally a limestone). Within Units II and III, carbonate is less common, and the units are predominantly siliciclastic with a distinction between units that are mud rich and feldspathic and sandier units toward the base of the hole. Calcium, along with strontium, is associated with

biogenic sediments in Unit I, but in deeper units they covary with aluminum. Within the base of Units II and III, sodium and potassium are both high, which is consistent with the dominant presence of feldspathic sediments. The higher aluminum proportion within the uppermost part of Unit II is consistent with the muddier, clay-rich lithologies present here.

Physical properties

Hole U150A is divided into four units based on the sediment and rock physical properties. Physical properties (PP) Unit 1 (0–300 m) experienced the most evident changes in sediment compaction, which is expressed by increasing bulk density (from 1.4 to 2.0 g/cm^3) and *P*-wave velocities (from 1450 to 1930 m/s) and decreasing porosity (from 85% to 45%) with depth. Because PP Unit 1 consists mostly of calcareous ooze, it has relatively low NGR (between 20 and 40 counts/s) and magnetic susceptibility (between 10^{-6} and 10^{-5} SI). The onset of PP Unit 2 (300–450 m) is marked by a rapid increase in NGR and porosity values and a rapid decrease in bulk densities and *P*-wave velocities, corresponding to a shift to a different lithologic unit with sand, silt, and clay-enriched sediments. Within the entire unit, NGR is persistently high (60–80 counts/s), whereas magnetic susceptibility values remain as low as 10×10^{-5} SI. *P*-wave velocities and bulk densities continue to increase with core depth. Most physical properties of PP Unit 3 (450–600 m) have similar values as those of Unit 2, except that *P*-wave velocities are extremely high, up to 4000–6000 m/s at some interbeds, and bulk densities and porosities increase and decrease to 2.6 g/cm^3 and 2%–3%, respectively, at parallel depths. PP Unit 4 (600–657 m) is distinct from other units due to higher mean values of NGR (80 counts/s), bulk density (2.6 g/cm^3), magnetic susceptibility (500×10^{-5} SI), and *P*-wave velocity (4500 m/s). Throughout the hole (0–657 m), thermal conductivities increase from 0.7 to 3.4 W/(m·K), most likely as a result of increasing sediment compaction and changes in sediment compositions. L* reflectance values are highly relevant to percent carbonate in sediments, which exhibit relatively high L* values between 100 and 160 in the upper 300 m and thereafter remain as low as 90.

Downhole measurements

Wireline logging was conducted in Hole U1501D using a modified triple combo tool string that included the Hostile Environment Natural Gamma Ray Sonde (HNGS), Hostile Environment Litho-Density Sonde (HLDS), High-Resolution Laterolog Array (HRLA), and magnetic susceptibility sonde (MSS). The triple combo run collected good data between 115.1 m (base of the drill pipe) to 300 m, where it encountered an impenetrable obstruction. Four logging units are defined: logging Unit 1 (base of the drill pipe to 190 m wireline depth below seafloor [WSF]) is characterized by intervals of large hole diameter and relatively high variability in NGR and magnetic susceptibility. Logging Unit 2 (190–260 m WSF) is characterized by a relatively constant hole diameter, relatively homogeneous logs, and submeter-scale layering. Logging Unit 3 (260–275 m WSF) again shows a relatively large hole diameter, as well high variability in NGR, density, and resistivity logs. Logging Unit 4 (275–300 m WSF) exhibits relatively large values of resistivity and magnetic susceptibility. The upward log pass indicated a collapsed hole at ~156.3 m drilling depth below seafloor (DSF) on the caliper curve, and for safety reasons no further attempts to descend deeper than that undergauge spot were made. Because the interval of the collapsed hole was located only ~40 m below the base of the pipe, the originally planned FMS-sonic tool string was not run. Four in situ formation temperature measurements were made in Hole U1501C, yielding a geothermal gradient of 81.4°C/km and a calculated heat flow of 100.1 mW/m^2. These values are comparable to the relatively high values observed at some ODP and IODP sites in this part of the SCS.

Site U1502

Background and objectives

Site U1502 (proposed Site SCSII-17A) within the SCS northern margin (Figures **F2**, **F9**) is located at 3764 mbsl on a prominent basement ridge (A) within the COT (Figure **F3**). Ridge A is one of four distinct basement highs found across the COT. The OMH is the most landward of these highs and is followed seaward by the nearly parallel Ridges A, B, and C. A key objective of Expeditions 367 and 368 is to examine the nature of the crust within Ridge A. This ridge is considered to be a pivotal element in the transition from continental to oceanic crust. Hence, the main objective of Site U1502 was to drill through synrift deposits overlying an interpreted shallow-dipping (~20°) fault zone and into the crystalline basement below the fault. Information on the nature and age of the synrift deposits overlying the fault, as well as the nature and age of the overlying sediments and associated seismic unconformities, formed another target with the objective of constraining basin subsidence.

Operations

We conducted operations in two holes at Site U1502. Hole U1502A is located at 18°27.8720′N, 116°13.8381′E, at 3763 mbsl. Our operations in Hole U1502A were designed to provide information on formation characteristics and drilling conditions so that we could decide the length of casing to drill into the seafloor in deep-penetration Hole U1502B. Given this purpose and the amount of time to drill the second, deep hole, we did not core continuously in Hole U1502A. Instead, we drilled without coring from the seafloor to 375.0 m and cored with the RCB system from 375.0 to 758.2 m, recovering 176.81 m (46%). Hole U1502B is located at 18°27.8798′N, 116°13.8409′E, at 3763.6 mbsl. In Hole U1502B, we drilled a reentry funnel and 727.7 m of 10¾ inch casing into the seafloor; cored with the RCB system through the sediment–basalt transition (727.7–739.16 m) and 180 m into the underlying basalt (739.16–920.95 m), recovering 128 m (70%); and collected downhole log data with the triple combo tool string and a check shot with the VSI tool string.

Lithostratigraphy

The sedimentary succession recovered at Site U1502 extends from the late Eocene to the late Miocene. The succession includes four sedimentary units (I and III–V) that are composed of mainly clay, nannofossil-rich clay, biosiliceous-rich clay, limestone, and clast-rich clay and two igneous units (II and VI) that are mainly composed of basalt. The base of the sedimentary succession is a sequence of clay and metasediments (dolomite marble and dolomitic limestone) possibly forming the contact with a unit of altered basalt (Unit VI) (Figure **F10**).

Late Miocene to late Oligocene lithostratigraphic Unit I is divided into five subunits. Subunit IA (Hole U1502A: 375.00–486.82 m) is composed of dark gray, gray, dark greenish gray, and greenish gray silty clay, clay with nannofossils, and nannofossil-rich clay intercalated with dark grayish brown, grayish brown, and brown clay with nannofossils, with minor dark greenish gray sandy clay with calcite. Subunit IB (Hole U1502A: 490.20–599.57 m) is composed of alternating intervals of brown and greenish gray clay, silty clay, and clayey silt. Sandy intervals are rare. Recovery in Subunits IA and IB

was very poor, which might be due to the occurrence of thick sand beds that were washed out. Subunit IC (Hole U1502A: 599.57–602.39 m) is composed of greenish gray and reddish gray foraminifer-rich clayey siltstone to sandstone with parallel lamination and convolute bedding, with thin layers of pinkish gray foraminiferal chalk. Subunit ID (Hole U1502A: 602.39–724.03 m) is mainly composed of alternating greenish and brownish gray and grayish brown clay, silty clay, clayey silt, and clay with silt (Cores 368-U1502A-25R through 32R), but brown colors dominate from Core 33R through 38R. Nannofossils are abundant within the lowermost ~4 m of this subunit. Subunit IE (Hole U1502A: 724.03–734.87 m; Hole U1502B: 727.79–727.96 m) is composed of brown nannofossil-rich clay with foraminifers and nannofossil-rich clay with pale green colors as haloes around fractures. The sediments of Unit I are interpreted as having been deposited in a deep-marine environment. Fining-upward intervals in Subunits IA–IC are interpreted as turbidites.

Unit II is a highly altered greenish gray basalt clast recovered from Hole U1502B at 727.96–728.04 m. The primary mineral phases are replaced by an alteration-mineral assemblage.

Unit III (Hole U1502A: 739.10–739.16 m; Hole U1502B: 728.04–733.82 m) is composed of a brownish yellow, very hard, poorly sorted breccia. The granule- to pebble-size siliceous clasts consist of alteration minerals (Fe hydroxides) cemented by a matrix of annealed quartz in various grain sizes.

Unit IV consists of biosiliceous-rich silty clay. Diatoms, sponge spicules, and radiolarians are abundant in the upper part, but the abundance of both nannofossils and diatoms decreases rapidly downhole from Section 368-U1502A-40R-1 to 40R-3. Pyrite occurs as centimeter-size patches and along cracks. The layering in Unit IV is inclined and may be slightly deformed.

Unit V (Hole U1502A: 747.20–749.01 m; Hole U1502B: 733.82–739.16 m) is an interval of alternating metasediments (dolomite marble, dolomitic limestone, and clast-rich clay). The dolomite marble is dominated by very fine grained dolomite (~95%) with minor amounts of magnetite (~3%) and calcite (~2%). The annealing texture is equigranular and crossed by fine-grained dark gray bands. The presence of magnetite explains the extraordinarily high magnetic susceptibility of this unit. The gray, fine-grained dolomitic limestone in Hole U1502B is intercalated with well-consolidated, very dark greenish gray clay with 10%–15% igneous clasts. The sediment is partially overprinted with alteration caused by secondary high-temperature processes (e.g., hydrothermal fluid sediment interaction or contact metamorphism).

Unit VI (Hole U1502A: 749.01–750.67 m; Hole U1502B: 739.16–920.95 m) consists of highly altered basaltic breccia, brecciated basalt, pillow basalt, and sheet basalt. The unit is divided into two subunits. Subunit VIA is composed of highly altered basaltic breccia and brecciated basalt with minor sheet basalt, chert, and claystone and very minor pillow basalt. Subunit VIB is dominated by pillow basalt and sheet flows and is less brecciated than Subunit VIA.

Igneous petrology

At Site U1502, we recovered two igneous lithologic units. Unit 1 (lithostratigraphic Unit II) is represented by just three small, aphanitic, fine-grained basalt fragments that contain rare plagioclase phenocrysts (Figure **F11**). Alteration of Unit 1 is intense, with most of the groundmass replaced by green clay minerals, clinozoisite, zeolites, and Fe (hydr)oxides.

Unit 2 (lithostratigraphic Unit VI) comprises a 182 m thick sequence of highly altered aphyric to highly plagioclase porphyritic basalts, with minor chert (Figure **F11**). These basalts are divided into two igneous subunits (2a and 2b) based on flow morphology and alteration style: an upper brecciated and fractured massive lava flow sequence (Subunit 2a) and a lower sequence of interbedded pillow flows with lobate and sheet lava flows in which the alteration style is characterized by intense veining (Subunit 2b). Subunit 2a is characterized by highly altered breccia clasts of sparsely to moderately phyric basalt in a matrix of carbonates, epidote, chlorite, Fe (hydr)oxides, quartz, zeolite minerals, and clay minerals. The clasts show an alteration assemblage similar to the matrix, with remnant plagioclase and secondary pyrite. Subunit 2b consists of aphyric to highly plagioclase phyric (>30%) basalts with abundant chlorite and sulfides, as well as epidote, clay minerals, carbonates, zeolites, and opaque minerals.

All of Unit 2 has undergone some degree of hydrothermal alteration. This alteration varies from complete replacement of the rock, where the original composition and texture are difficult to determine, to replacement of mineral phases with little change to the texture. Glassy pillow rinds are completely replaced, and multiple phases of veining and haloes are ubiquitous throughout the rocks. Three vein types were observed: (1) white to green to black silica-epidote veins (2) apple green pyrite-epidote veins, and (3) white silica and/or calcite veins. Sulfide mineralization (disseminated and veined) is widespread throughout Unit 2 and is dominated by pyrite, with minor sphalerite, chalcopyrite, and covellite.

Handheld X-ray fluorescence (pXRF) analyses show no significant differences in contents of alteration-resistant elements such as TiO_2 and Zr within Unit 2, but Subunit 2a has lower MgO, FeO, and MnO than Subunit 2b, which is consistent with the higher degree of alteration. Subunit 2b is also strongly affected by secondary alteration, but areas of less intense alteration are indicated by higher magnetic susceptibility and high CaO and Fe_2O_3 values. Unit 1 appears to be compositionally distinct from Unit 2, and has, for example, higher Ti/Zr ratios.

Structural geology

Deformation structures are scarce in Unit I above Core 368-U1502A-37R, with only a local, convolutely bedded sequence in Core 25R. Downhole from Core 37R at ~700 m, a gradual increase in deformation structures was observed (Figure **F11**). Cores 37R through 39R are characterized by microfaults, as evidenced by downward-dip plunging striations and slickensides on exposed fracture surfaces, systematically associated with greenish halos. No deformation structures were encountered in Unit II. Unit III consists of an extremely silicified breccia that was poorly recovered. The nature of this breccia, however, as sedimentary, tectonic, or hydrothermal remains unconstrained at the moment. In Unit IV, a small-scale transition from distributed to localized shear in unlithified sediments was documented. No deformation structures were encountered in Unit V. Unit VI is essentially composed of basalts that were heterogeneously affected by brecciation and veining associated with the circulation of hydrothermal fluids. Subunit VIA is dominated by brecciated basalt/basaltic breccias, whereas Subunit VIB comprises a rather coherent series of lava flows crosscut by a multistage network of polymineralic veins.

The uppermost part of Unit VI contains severely fractured and fragmented basalt locally filled by fine-grained unconsolidated greenish rock. Subunit VIA is characterized by diverse brecciation horizons associated with veins and microcracks. Depending on the intensity of fragmentation and the clast/matrix ratio, the rocks are referred to as brecciated basalt or basaltic breccia. A typically ob-

served feature is the jigsaw-puzzle structure, suggesting possible in situ fragmentation. Macro- and microscopic observations show that the breccia-clasts consist mainly of sparsely to moderately plagioclase phyric basalts that were hydrothermally altered to variable degrees. Thus, formation of such breccias likely involved fluid-assisted fracturing of basalt. In contrast, Subunit VIB is characterized by a progressive decrease of breccia horizons and the development of different vein types, almost always polymineralic. Notably, vein composition and their orientation changes through Subunit VIB. Although numerous small-scale veins often related with major veins were observed, three first-order vein types were categorized: (1) composite silica-rich veins, (2) composite epidote-rich veins, and (3) composite carbonate- and/or silica-rich veins.

Biostratigraphy

All core catcher samples from Hole U1502A and selected samples from Hole U1502B were analyzed for calcareous nannofossils, foraminifers, diatoms, and ostracods. Additional samples were taken from intervals within the working-half cores when necessary to refine the ages. The preservation of calcareous microfossils is mostly good to moderate in the upper sections (Cores 368-U1502A-2R through 13R) and moderate to poor in the lower sections (Cores 14R through 41R). Planktonic foraminifers and calcareous nannofossils are abundant to common in Cores 2R through 10R, 25R, and 37R through 39R and rare to barren in all other sections. Diatoms were only observed in Sections 368-U1502A-40R-1 through 40R-3. In Hole U1502B, foraminifers were observed only in Section 368-U1502B-3R-1 and are represented by well-preserved, agglutinated deepwater taxa. Ostracods are extremely rare, and single occurrences were observed only in three samples in Hole U1502A (Samples 3R-CC, 4R-CC, and 5R-CC).

Fourteen planktonic foraminifer and calcareous nannofossil biostratigraphic events were used to provide an age-depth model for Site U1502 from the late Miocene to late Oligocene. The Pliocene/Miocene boundary is placed tentatively within Core 368-U1502A-2R, but it may be shallower than the cored section. The Miocene/Oligocene boundary was determined to lie between Samples 368-U1502A-39R-CC and 40R-1, 7 cm. Sedimentation rates vary from ~39 mm/ky in the late Miocene to ~10 mm/ky in the middle and early Miocene. No planktonic microfossils were found in Hole U1502B, but a sample from a sandy interval in Core 368-U1502B-3R revealed abundant and diverse abyssal agglutinated benthic foraminifers. The composition of this agglutinated benthic foraminifer assemblage provides a possible age of late Eocene for this interval.

Paleomagnetism

The magnetic behavior of sediments at Site U1502 correlates with their color (greenish gray or reddish brown). Reddish brown sediments show AF magnetization indicative of magnetite or titanomagnetite and hematite (responsible for the color). In contrast, greenish gray sediments host magnetite or titanomagnetite and pyrrhotite. The predominance of steep normal inclinations (~75°; Figure **F12**) across all late Oligocene to late Miocene units (375.00–750.67 m) affects the SRM section measurements and prevents any reliable magnetostratigraphy to be established for both Holes U1502A and U1502B.

The basalt has NRM intensities one order of magnitude higher than sediment. The main magnetically remanent phase is titanomagnetite, but its alteration produces maghemite or hematite. Magnetic susceptibility (κ) shows a bimodal distribution with a median at 327 × 10^{-6} SI. κ does not show any strong correlation with any chemical (R^2 = 0.343 for Fe^2O^3 wt%). Intervals of high κ values might correspond to the bottoms of flows with a massive, less altered structure. Altered basalts have higher Koenisberger ratios (Q = 1–10) than fresher basalts (Q = 0.001–1). The mean dip of magnetic foliation is 8°. Cores 368-U1502B-9R and 10R show less-pervasive drilling overprint and two discrete samples show both a normal (soft) component and a reverse (hard) component, suggesting a possible reversal.

Geochemistry

Site U1502 contains very low high-hydrocarbon gas abundances and TOC, nitrogen, and sulfur contents, likely reflecting the poor preservation of organic matter. Instances of high carbonate content are associated with siderite, and on occasion this mineral comprises >50% by mass of intervals of lithostratigraphic Subunit ID. The interstitial water at Site U1502 is enriched in Ca, Mg, and K; has notably high alkalinity; but is depleted in Na, Cl, and Br. The linear decrease and increase of major anion and cation contents implies upward movement of fluid from deeper sediments. The hemipelagic sediments within Unit I have some similarities to the geochemical characteristics of the hemipelagic and pelagic units at Sites U1501 and U1505, but Site U1502 sediments are enriched in Fe, K, and clay concentrations, likely as a result of regions of increased alteration. All of the analyzed igneous rocks from Units II–VI were heavily altered, although samples from igneous lithologic Subunit 2b were altered to a lesser degree than those from Subunit 2a.

Physical properties

Physical property data acquired at Site U1502 include density, magnetic susceptibility, *P*-wave velocity, NGR, color reflectance, and thermal conductivity (Figure **F13**). These data allow us to characterize four physical property units. PP Unit 1 (375–740 m) corresponds to the nannofossil-rich and biosiliceous-rich clay lithologies and exhibits small variations in NGR between 50 and 70 counts/s and uniformly increasing *P*-wave velocities with depth that are on average <2500 m/s. Unit 1 sediments show similar porosities to those recorded at nearby Sites U1499 and U1500 in the same depth interval, suggesting the same compaction history. A significant increase in bulk density (up to 2.7 g/cm^3) in Core 368-U1502B-3R is associated with strongly lithified limestone beds. Variations of high and low magnetic susceptibility values correspond to sediment color changes in Unit 1 and may be controlled by the amount of pyrrhotite within the sediments.

PP Unit 2 (740–750 m) in Hole U1502A is characterized by lower *P*-wave velocities and bulk densities and higher NGR than the strata above. Low densities and *P*-wave velocities found in Unit 2 reflect the clast-rich claystone from lithostratigraphic Unit V.

PP Units 3 and 4 represent the basaltic basement and are characterized by relatively low NGR values (<10 counts/s), high densities, and *P*-wave velocities that vary over a broad range (3000–6000 m/s). The boundary between Units 3 and 4 is marked by an abrupt increase in density, *P*-wave velocity, and thermal conductivity and coincides with the change from igneous lithologic Subunit 2a to 2b. Prominent magnetic susceptibility peaks (up to 4000 × 10^{-5} SI) in Units 3 and 4 correspond to relatively less altered basalt. Thermal conductivity in Units 3 and 4 is variable but generally increases in line with decreasing porosity with depth.

Downhole measurements

Wireline logging was conducted in Hole U1502B using a modified triple combo tool string and the VSI tool string. The modified triple combo tool string included the HNGS, HLDS, and Dipole Sonic Imager (DSI) for acoustic velocity. The triple combo run collected good data downhole from 875.3 m (~45 m above the bottom of Hole U1502B) and allowed us to define eight logging units, which correlate in great part to the lithostratigraphic units and core physical properties. Logging Units 1–5 are defined by data collected through the casing and drill pipe. Unit 6 data was collected outside the casing but inside the drill pipe, whereas data in Units 7 and 8 were collected in the open hole. For measurements inside the casing and/or drill pipe, only NGR and the associated K, Th, and U components provide meaningful data, although they are highly attenuated by the casing and/or drill pipe. Open-borehole conditions from the bottom of the casing at 723 m to 875.3 m were generally good, with measured diameters from 12 to 14.5 inches. Log and core data generally show good agreement, and downhole measurements provide information in zones of poor core recovery in Hole U1502B. The log data exhibit increasing densities and *P*-wave velocities with depth. The amplitude of NGR increases gradually with depth throughout Units 1–3 (seafloor to ~630 m), with an interval of relatively constant values between 150 and 350 m. NGR values are lowest in Units 4–8 (~630–850 m).

The VSI tool string was run only inside casing because the tool could not pass through an obstruction encountered at the end of the casing. Eight stations were attempted. The two deepest stations (at 715.1 and 695.2 m) are associated with large noise levels possibly caused by poor mechanical coupling of the casing with the surrounding formation. The remaining upper six stations, located at 290.2, 350.3, 450.3, 550.1, 590.3, and 630.3 m, recorded good quality waveforms.

Site U1503

Background and objectives

Site U1503 (proposed Site SCSII-9B) is located at 3868 mbsl near the top of the structural high named Ridge C (Figures **F2**, **F14**). Ridge C is the most seaward ridge of the three margin-parallel Ridges A, B, and C that characterize the lower continental slope underlain by thin (5–7 km) crust. Ridge C is believed to represent at least partly, if not full, igneous crust and hence the completion of continental breakup along this margin segment of the northern SCS.

A key operational objective of Site U1503 was to sample the lowermost ~300 m of sediments on top of basement to constrain the age and subsidence history of the crust at this location, the timing of normal faulting, and the environment of the early half-graben fill. A second and most important goal was to sample the igneous stratigraphy to at least 100 m below the basement. Because of a rig floor equipment failure (drawworks), we abandoned the site after installing casing in Hole U1503A to 991.5 m.

Deep, representative sampling of the basaltic material at this site would have provided an important reference frame for the modeling of breakup. With an estimated sediment thickness of 1640 m overlying basement, obtaining basement samples and log data at this site represented a challenging operation.

Operations

To reach our objectives, we conducted operations in one hole (U1503A; 18°08.6300′N, 116°18.8456′E; 3868 mbsl). We successfully installed a reentry system and 991.5 m of 10¾ inch casing in Hole U1503A. However, we were unable to deepen the hole below the casing because of repeated breakdowns of the low clutch diaphragm in the drawworks and concerns that we did not have enough spares to last the remainder of the expedition. Without the drawworks low clutch, we could not conduct drilling operations deeper than 3400 m (water depth plus penetration depth). Because Site U1503 had a planned depth of 5695 m (water depth plus penetration depth), we abandoned Hole U1503A without addressing any scientific objectives. Hole U1503A remains cased and open for possible future occupation.

Site U1504

Background and objectives

Site U1504 (alternate Site SCSII-27A) was proposed during Expedition 367 and approved by the Environmental Protection and Safety Panel during Expedition 368 as an alternate site should there be time left following completion of the high-priority sites included in the *Scientific Prospectus*. Expedition 368 decided to occupy Site U1504 following the inability to continue drilling below the 990 m deep cased Hole U1503A. Most of our remaining approved sites were in water deeper than 3400 m and/or required deep penetration. One exception was Site U1504, located at 2823 mbsl, ~45 km east of Site U1501 on the OMH, and with a shallow coring target (Figures **F2**, **F15**).

Operations

Two holes were drilled at Site U1504. In Hole U1504A (18°50.9199′N, 116°14.5397′E; 2816.6 mbsl), we cored with the RCB system from the seafloor to metamorphic basement at 134.8 m and then into basement to 165.5 m, recovering 52.77 m (32%). In Hole U1504B (~200 m southeast of Hole U1504A; 18°50.8213′N, 116°14.5978′E; 2843.0 mbsl), we drilled without recovery to 88.2 m, cored with the RCB system to metamorphic basement at 107.9 m, and then cored into basement to 200 m, recovering 21.48 m (19%).

Lithostratigraphy

The succession recovered at Site U1504 includes two sedimentary units (I and II) underlain by a metamorphic unit (III). Lithostratigraphic Unit I is dominated by nannofossil and foraminiferal ooze and minor nannofossil-rich clay and is divided into four subunits (IA–ID). Subunit IA (Hole U1504A: 17.50–46.59 m) is composed of nannofossil-rich clay, nannofossil ooze, nannofossil ooze with biogenic silica, and clay-rich nannofossil ooze. The color of the ooze gradually changes downhole from dark greenish gray to greenish gray and gray. Distinct intervals contain more silt. Thin silt laminations are often disrupted by bioturbation. Layering is contorted at the base of the subunit. Subunit IB (Hole U1504A: 46.59–59.73 m) is composed of light brown foraminifer-rich nannofossil ooze and pale brown nannofossil ooze with foraminifers. Subunit IC (Hole U1504A: 65.80–104.99 m) is composed of light greenish gray, greenish gray, light brownish gray, pale brown, and light gray nannofossil ooze with clay and greenish gray clay-rich nannofossil ooze, intercalated with light gray nannofossil-rich foraminiferal ooze with clay, light brownish gray foraminifer-rich nannofossil ooze, and foraminifer-rich nannofossil ooze with clay. Subunit ID (Hole U1504A: 104.99–112.66 m; Hole U1504B: 88.20–92.31 m) is composed of light brown to yellowish brown nannofossil ooze with foraminifers, intercalated with pink or brownish yellow foraminifer-rich nannofossil ooze.

Unit II (Hole U1504A: 114.72–134.80 m; Hole U1504B: 97.90–107.91 m) is clast supported, bioclast-rich limestone with larger

benthic foraminifers (up to 15 mm). The contact between Units I and II was not recovered.

Unit III (Hole U1504A: 136.40–163.70 m; Hole U1504B: 117.40–196.28 m) is composed of fine- to coarse-grained epidote-chlorite schist (Subunit IIIA) and calc-silicate schist (Subunit IIIB), with granofels clasts.

Metamorphic petrology

We recovered 27 m (Hole U1504A) and 79 m (Hole U1504B) of a variety of mylonitic epidote-chlorite to calc-silicate schists containing granofels clasts. Recovery was <20% in this unit. Lithologic changes with depth and between the two holes were observed, and the unit is divided based on a change in the predominant metamorphic lithology (Figure **F16**). Lithostratigraphic Subunit IIIA was recovered in both Holes U1504A and U1504B and consists of greenish gray, microcrystalline to coarse-grained epidote-chlorite schist with dark greenish gray granofels clasts (<10 cm) and epidote-chlorite breccia. The schists show a strong mylonitic foliation, whereas the clasts have generally isotropic textures showing local weakly developed foliation. Both the schist and the granofels clasts show, in general, a comparable mineral assemblage consisting of epidote, chlorite, feldspar, and quartz ± other phyllosilicates and accessory minerals and locally isolated subhedral dark minerals (pyroxene?). The granofels clasts are often crosscut by a network of quartz veins. Subunit IIIB contains an alternation of calc-silicate schist and epidote-chlorite schist with granofels clasts, epidote and/or chlorite granofels, chlorite schist with epidote, epidote-chlorite gneiss, and minor marble. The lithologies are fine- to coarse-grained with mostly an inequigranular texture and some bimodal or equigranular textures, and the schistose sections show a strong mylonitic foliation. Several of the schists show a reddish brown alteration, and late calcite veins crosscut the foliation of the deepest schists recovered (e.g., in Core 368-U1504-20R). Minerals observed are epidote, quartz, chlorite, calcite and feldspar. Metamorphic Subunit IIIB contains numerous clasts with variable lithologies: cryptocrystalline granofels either with or without quartz and/or calcite veins, porphyritic rocks with tabular phenocrysts (possibly altered plagioclase), brecciated (epidote, calcite and/or quartz) veins, and foliated granofels.

Handheld pXRF analyses show an average mafic igneous composition for both the schist and the clasts but with a spread toward ultramafic (in Hole U1504B Subunit IIIA) and more felsic compositions (in Subunit IIIB). A clear change in sulfur contents occurs between Subunits IIIA and IIIB, the latter of which is below the detection limit. High Nb contents compared to mid-ocean-ridge basalt (MORB) indicate a potentially enriched source for the protolith.

Lithostratigraphic Unit III consists of mylonitic, greenschist facies metamorphic rocks, indicated by the presence of epidote and chlorite. We infer that the protolith most likely was a breccia, based on the different clast sizes and types and styles of deformation. The protolith likely had a mafic igneous composition. It is, however, unclear if this breccia with mafic clasts has a sedimentary origin (e.g., volcaniclastic) or represents a potentially hydrothermally altered form of basalt, gabbro, or ultramafic protolith. At present, the metamorphic evolution of this unit and its connection with the opening of the SCS is unknown.

Structural geology

Lithostratigraphic Unit I shows subhorizontal bedding and locally some minor possible slump folds, as observed in Section 368-U1504A-5R-1. Unit II is devoid of any deformation structures. The metamorphic basement at Site U1504 is formed by greenschist facies mylonitic epidote-chlorite schists and calc-silicate schists (Unit III). The rocks preserve distinct deformation structures resulting from changes in the mode of deformation (brittle/ductile); the modal amount of quartz + feldspar governing the (local) rheological behavior; the amount of accumulated strain; the occurrence of variably sized (up to decimeter scale), prekinematic, heterolithic clasts that mostly form rigid (i.e., internally undeformed) bodies within the ductile foliation; and/or superimposed multiple deformation phases. The steeply dipping (up to 75°) mylonitic foliation is characterized by distinct morphologies: (1) a widely spaced anastomosing foliation associated with leucocratic bands; (2) a tight, closely spaced, and often crenulated foliation associated with more melanocratic schist variations; and (3) a tight anastomosing foliation associated with calc-silicate schists enclosing angular to rounded heterolithic granofels clasts. Locally, the sense of shear is indicated by shear bands and sigma clasts. In Subunit IIIA (Figure **F16**), granofels clasts are consistently microcrystalline (chlorite + epidote) and dismembered by a network of mostly parallel and perpendicular quartz veins cutting each other. Often they form apparently stretched, elongated bodies oriented parallel to the foliation. Subunit IIIB shows a wide range of prekinematic (mostly mafic) clasts enclosed by the foliation. Encountered varieties encompass highly phyric to aphyric rocks, as well as fragmented former (epidote/calcite/quartz) vein fillings. In some cases, such clasts show ductile internal deformation. Clast boundaries can be either distinctly sharp or diffuse, the latter indicating mechanical and/or chemical interactions with the surrounding foliation. Deformation in Subunit IIIB is presumably strongly controlled by an inherited (protolithic) brecciated structure.

Biostratigraphy

All core catcher samples at Site U1504 were analyzed for calcareous nannofossils, foraminifers, and diatoms. Additional samples were taken from intervals within the working-half cores when necessary to refine the ages. Preservation of calcareous microfossils is good to very good in Cores 368-U1504A-2R through 12R and 368-U1504B-2R and is poorly preserved deeper in the section due to recrystallization in the reefal limestone. Diatoms are poorly preserved in Cores 368-U1504A-2R through 5R, and they are rare or barren in other core catcher samples. Planktonic foraminifers and calcareous nannofossils are abundant in Cores 368-U1504A-2R through 12R and 368-U1504B-2R and barren in Cores 368-U1504A-13R through 15R. Twenty biostratigraphic datums were identified in a succession from the late Pleistocene to the early Miocene.

A hiatus between the early Pleistocene and late Miocene was determined within Core 368-U1504A-6R, with abrupt planktonic foraminiferal and nannofossil assemblage changes. Sedimentation rates at this site varied from ~22 mm/ky during the Pleistocene to ~6 mm/ky in the early middle Miocene.

Cores 368-U1504A-13R through 15R are mainly composed of reefal limestone with abundant larger benthic foraminifers occurring in Cores 14R and 15R. Thin section examination of these carbonate rocks indicates the presence of abundant *Nummulites*, suggesting an Eocene age. The abundant larger benthic foraminifers indicate deposition in a warm shallow-marine environment. In contrast, the abundant planktonic foraminifers and calcareous nannofossils in the carbonate ooze in the overlying sedimentary section (Cores 2R through 12R) indicate a deepwater environment since the early Miocene.

Paleomagnetism

Most of the 14 discrete sedimentary samples show an initial soft magnetic behavior attributed to titanomagnetite followed by a gyroremanent magnetization greater than 70 mT attributed to greigite, a mineral already identified at Site U1501. Consistently steep normal inclinations (~60°) across all sedimentary units indicate a significant drilling overprint that is removed by AF demagnetization up to 15 mT. A succession of nine normal and eight reversal polarities can be defined, particularly in the upper part of the cores (Figure **F17**).

Discrete samples show low κ values, a moderate degree of magnetic anisotropy, and a strongly oblate symmetry, probably of depositional origin. This subhorizontal planar fabric indicates deposition in a calm, pelagic environment with moderate traction.

NRM intensities of metamorphic rocks, measured on the SRM and on four discrete cubes, are relatively weak and indicate a complex magnetic assemblage composed of magnetite and hematite in one specimen. The anisotropy of magnetic susceptibility fabrics consistently dip steeply and show a moderate to high degree of magnetic anisotropy, oblate symmetries, and oblique magnetic lineations, possibly indicating an oblique motion within this high-strain shear zone.

Geochemistry

Hydrocarbon gases were not detected above background levels at Site U1504, and TOC, nitrogen, and sulfur contents were low (<0.5%). Instances of high carbonate content were associated with bioclast-rich and clast-supported limestone. The upper part of the sediment was not cored; therefore, present-day early diagenetic processes were not constrained. Interstitial water data are broadly comparable to other sites.

Physical properties

Four petrophysical units are identified at Site U1504 according to variations in the core physical properties. Core material in PP Units 1 and 2 consists of soft sediments. In general, with respect to Unit 2, Unit 1 has a higher average NGR count (~30 versus 20 counts/s), a weaker color reflectance (mean L* of ~40 versus 50), and a lower average RGB value (100 versus 150). These changes in physical properties between Units 1 and 2 correspond to a switch of sediment compositions from nannofossil-rich clay to nannofossil ooze. A general increase in bulk (from ~1.4 to 1.8 g/cm^3) and dry (from ~0.7 to 1.2 g/cm^3) densities and a downhole decrease in porosities (from 75% to 56%) in Units 1 and 2 mainly indicate sediment compaction with time. The boundary between Units 1 and 2 is marked by a relatively rapid increase in *P*-wave velocity and bulk density and a rapid decrease in porosity compared with the general trends mentioned above. This physical property boundary corresponds to an unconformity in the seismic profile and also to a hiatus confirmed by the biostratigraphic data.

P-wave velocities and bulk densities increase from ~3800 to 5000 m/s and from ~2.4 to 2.9 g/cm^3, respectively, within Unit 3, which corresponds to a transition in lithology from coral-rich limestone to clast-supported limestone. Coral-rich limestone in the upper portion of Unit 3 is also associated with a moderately high porosity of ~23%. Unit 4 is characterized by uniformly high velocities of ~5500 m/s, high bulk densities of ~2.9 g/cm^3, and low porosities of ~3%, which correspond to the epidote-chlorite schist. A large increase in both velocities and densities at the boundaries between Units 2 and 3 and also Units 3 and 4, corresponds to strong reflectors in the seismic data. The gradual downhole increase in thermal conductivity values at shallow depths is likely due to progressive compaction of the sediments.

Site U1505

Background and objectives

Site U1505 (proposed Site SCSII-3D) is located at 2916.6 mbsl on a broad regional basement high (Figure **F18**). This site was an alternate to Site U1501, should time be left for drilling following completion of the high-priority sites included in the *Scientific Prospectus* (Sun et al., 2017). Site U1505 was included in Expedition 368 because it might complement findings at Site U1501 and it was within the operational limits of 3400 m drill string imposed by the failure of the drawworks (see **Operations** for details).

Both Sites U1505 and U1501 are located on the same structural high at similar water depths and are 10.5 km apart (Figure **F2**). The seismic section at Site U1505 generally shows a more horizontal orientation of the seismic reflectors and concordant relationship of the strata than at Site U1501, indicating the sediment sequence here should be more complete. The key objective at Site U1505 was to sample the stratigraphic record above seismic unconformity T80 (inferred to be ~38 Ma), with specific goals to constrain both the sediment responses to the tectonic events and basin evolution since the Eocene and Neogene paleoceanographic and paleoclimatological changes along the northern SCS margin.

The relatively shallow water depth of 2916.6 m at Site U1505 makes it one of the few ODP/IODP sites above the modern CCD of the SCS. Its hemipelagic deposits, rich in calcareous microfossils, enable the application of stable isotopes, faunal analyses, and other multidisciplinary methods. Key objectives were to reconstruct the east Asian monsoonal climate record in the SCS and upper- and deep-water variations in the western Pacific. Site U1505 will, for the first time, provide an almost continuous sequence of paleoceanographic studies at orbital and millennial timescales since the late Eocene in the SCS. We cored two holes at this site with the APC system to obtain a continuous record for the Pliocene–Pleistocene interval for high-resolution paleoceanographic studies.

Operations

Four holes were cored with the APC/XCB systems at Site U1505. In Hole U1505A (18°55.0560′N, 115°51.5369′E; 2916.6 mbsl), Core 1H misfired and recovered only 0.3 m. In Hole U1505B (18°55.0562′N, 115°51.5370′E; 2918.6 mbsl), a 3.23 m long mudline core was recovered for future education and outreach activities. Hole U1505C (18°55.0570′N, 115°51.5370′E; 2917.4 mbsl) was APC cored to 317 m and then XCB cored to 480.2 m, recovering 480.15 m (100%). Hole U1505D (18°55.0485′N, 115°51.5501′E; 2917.5 mbsl) was APC cored to 184.5 m and recovered 191.43 m (104%). Downhole logging with a modified triple combo tool string was conducted in Hole U1505C from 341.2 m uphole. The maximum drilling depth of 480.2 m was determined by the possible maximum total length (3400 m) of drill string deployment.

Lithostratigraphy

The sediment succession recovered at Site U1505 extends from the late Eocene to the Pleistocene. Two sedimentary units (I and II) were observed (Figure **F19**). Lithostratigraphic Unit I is dominated by nannofossil ooze with varying amounts of foraminifers and clay as well as, in the upper interval of the hole, with biogenic silica. Unit I is divided into three subunits (IA–IC). Subunit IA (Hole U1505C: 0.00–27.76 m) is composed of dark greenish gray and greenish gray

biosiliceous-rich clay with nannofossils, nannofossil-rich clay with biogenic silica, and nannofossil-rich biosiliceous ooze with clay. The abundance of biogenic silica decreases downhole. A pinkish gray, ~6 cm thick, slightly fining upward ash layer occurs at 20.8 m (Hole U1505C), and ash pods were observed at 20.3 m in Hole U1505D. Subunit IB (Hole U1505C: 27.76–273.39 m) is composed of gray to brown nannofossil ooze with minor silty intervals. The color change reflects the varying abundance of foraminifers and clay. Subunit IC (Hole U1505C: 273.39–403.79 m) is composed of gray, greenish gray, and light brownish gray clay-rich nannofossil ooze (with foraminifers) and foraminifer-rich nannofossil ooze with clay and minor amounts of nannofossil-rich clay. Unit II (Hole U1505C: 403.50–480.54 m) is dominated by dark greenish gray, well-consolidated silty clay and clayey silt (with nannofossils).

Biostratigraphy

All core catcher samples from Holes U1505A–U1505C were analyzed for calcareous nannofossils, planktonic foraminifers, and diatoms. Additional samples were taken from intervals within the working-half sections when necessary to refine the ages. Hole U1505D was not sampled continuously for biostratigraphic analyses because of time constraints at the end of the expedition, but the sequence recovered spans from the late Miocene to the present (Figure **F19**). Preservation of calcareous microfossils is good in Cores 368-U1505C-1H through 48X and moderate to poor in Cores 49X through 64X. Planktonic foraminifers are abundant or common in Cores 1H through 56X and 59X through 62X and rare in Cores 57X, 58X, 63X, and 64X. Calcareous nannofossils are generally abundant to common in most samples from Hole U1505C, except for those from the upper part of Core 57X.

Forty-five biostratigraphic datums identified in Hole U1505C suggest a continuous succession from the early Oligocene to the Holocene (Figure **F19**). The Pleistocene/Pliocene boundary is placed within Core 7H, the Pliocene/Miocene boundary is placed between Cores 11H and 13H, and the Miocene/Oligocene boundary is placed between Cores 54X and 55X. Sedimentation rates are ~7 mm/ky in the Oligocene, ~15 mm/ky during the Miocene–Pliocene, and ~24 mm/ky during the Pleistocene.

Relatively low abundances of planktonic foraminifers deeper than Core 57X indicate bathyal depths during the early Oligocene, whereas much higher abundances of planktonic foraminifers shallower than Core 56X suggest a deeper water environment since the late Oligocene.

Paleomagnetism

Only NRM was measured with the SRM in Hole U1505C, except for Sections 368-U1505C-1H-1 through 3H-1, which were inline AF demagnetized in three steps. Most of the 55 AF demagnetized discrete samples show very soft magnetic behavior responsible for the acquisition of a strong, vertical drilling overprint (average inclination = ~81°) that was removed by demagnetization to 10–15 mT. This soft behavior shows that magnetic remanence is dominated by multidomain to pseudosingle-domain titanomagnetite or magnetite. The drilling overprint appears to impact discrete samples far less than core sections (Figure **F20**). The lower part of the hole (Cores 368-U1505C-48X through 64X) is characterized by severe drilling disturbance, which causes a large scatter of NRM directions and inclinations.

Magnetostratigraphic data is based on polarities assigned to the archive-half sections and corroborated by directions obtained from oriented discrete samples. The lower boundary of the Brunhes (C1n) normal chron is at 37.4 m (0.781 Ma). The lower boundary (57.4 m) of the reverse polarity r1 is the base of Subchron C1r.3r with an age of 1.778 Ma.

Geochemistry

Low but measurable hydrocarbon gases were detected only in Cores 368-U1505C-53X through 60X (371–438 m). The base of the hole has methane distributions similar to those at Site U1499, whereas the uppermost section is barren of methane, similar to Site U1501. Except for the shallowest 30 m of sediment, TOC, nitrogen, and sulfur contents are mostly low in lithostratigraphic Unit I, but sulfur and TOC are slightly higher in Unit II; however, in all cases they are typically <1% (Figure **F21**). Interstitial water chemistry has two important features. The upper part of the hole exhibits patterns similar to those at Site U1501, with inhibited sulfate reduction, and low chlorine, bromine, and salinity suggest the presence of freshwater at depth. Freshwater at >400 m coincides with the presence of low quantities of methane and the T60 regional seismic unconformity.

Physical properties and downhole measurements

Physical property data were acquired from cores from Holes U1505C (0–480.5 m) and U1505D (0–184 m), including density, magnetic susceptibility, *P*-wave velocity, NGR, color reflectance, and thermal conductivity. Physical property trends allow us to define two physical property units, PP Units 1 (0–403 m) and 2 (403–480 m). The boundary between Units 1 and 2 displays a distinct color change from greenish and light brownish gray to dark greenish gray. This boundary, which corresponds to seismic stratigraphic unconformity T60, is associated with a sharp change in the physical properties. In Unit 1, sediments are composed of foraminifer-rich nannofossil ooze with clay in the upper part that gradually changes to clay-rich nannofossil ooze in the lower part. This change is well reflected in the NGR, which increases with depth. The higher NGR values in Unit 2 are related to sediment that primarily consists of silty clay. Magnetic susceptibilities overall gradually decrease with depth. The boundary between Units 1 and 2 shows that densities and *P*-wave velocities drop sharply from ~2.2 to ~1.8 g/cm^3 and from ~2250 to 1750 m/s, respectively. Porosities abruptly increase from ~35% to ~50%. Thermal conductivity also shows a sharp change at the boundary. Reflectance parameter L* and RGB data are well correlated with carbonate content.

Wireline logging was conducted in Hole U1505C using the triple combo tool string, which included the HNGS, HLDS, DSI, and MSS. This logging string collected good data from 341.2 m (139.1 m above the bottom of Hole U1505C), which allows the definition of six logging units that mostly correlate with the lithostratigraphic units and core physical property data. Logging Unit 1 extends from the seafloor to the base of the drill pipe at 78 m. NGR is highly attenuated inside the drill pipe. Logging Unit 2 (base of the drill pipe to 96 m) exhibits NGR values that are ~50% lower than the underlying logging Unit 3. In Unit 3 (96–136 m), NGR increases with depth. Logging Unit 4 (136–220 m) exhibits relatively constant V_P and V_S. In logging Unit 5 (200–296 m), resistivity increases with depth, whereas most of the other physical properties are relatively constant. Logging Unit 6 (296–341.2 m) has higher magnetic susceptibilities than logging Unit 5.

Four downhole temperature measurements were conducted in Hole U1505C using the APCT-3. The temperature values range from 4.7°C at 36.7 m to 11.7°C at 122.8 m, giving a geothermal gradient of 84.6°C/km. A heat flow of 94.0 mW/m^2 was obtained from

the linear fit between temperature and thermal resistance. The geothermal gradient and heat flow at Site U1505 are comparable to the relatively high values observed in a number of ODP and IODP sites in this part of the SCS.

Preliminary scientific assessment

In this section, we assess the achievements of Expedition 368 within the SCS toward meeting the four specific objectives of Expeditions 367 and 368 as stated in the *Scientific Prospectus*. Based on Expedition 367 results, Expedition 368 chose to follow a modified drilling plan from that described in the proposal (Sun et al., 2016b). Based on findings made during Expedition 368, new, alternate sites were proposed to further adjust drilling plans. However, because of equipment failure, the drilling capability of the R/V *JOIDES Resolution* was limited to a maximum 3400 m drill string deployment, severely affecting our possible choice of targets from 25 May 2017 to the end of the expedition on 11 June. Furthermore, expedition time spent from 14 to 25 May installing casing to 990 m for primary Site U1503 was de facto time wasted for the expedition but left an important drill site ready for coring in the future. The overall effect of this operational constraint is that it directed efforts more toward Objective 4 (below) than originally planned.

1. *To determine the nature of the basement within critical crustal units across the COT of the SCS rifted margin to discriminate between different competing models of breakup at magma-poor rifted margins. Specifically, to determine whether the subcontinental lithospheric mantle was exhumed during plate rupture.*

This objective was partly achieved during Expedition 368 with the potential for completion following postexpedition research.

Following the partly successful attempt during Expedition 367 to identify the nature of the basement within the critical Ridge A (Site U1499), we decided to pursue a second and alternate drill site (Site U1502) at this important ridge structure within the COT during Expedition 368. To give this site priority over the planned deep site (proposed Site SCSII-9B) on the distal Ridge C was a significant decision and deviation from the drilling plan in the *Scientific Prospectus*, which proposed Site SCSII-9B (Site U1503) as the initial priority of Expedition 368.

At Site U1502, we recovered ~180 m of basalt of possible late Eocene age overlain by late Eocene to Miocene deepwater sediments. The basalt shows pillow structures, confirming subaqueous deposition, found in a seismic stratigraphic position where we expected synrift deposits to be present on the seaward flank of a continental fault block. Onboard preliminary inductively coupled plasma–atomic emission spectroscopy element analyses indicate they are tholeiitic basalt and are comparable to samples from the ocean crust within the SCS collected during Expedition 349 and from Site U1500 of Expedition 367. The shipboard data suggest that the basalts may be slightly enriched, but this will need to be constrained by postexpedition work.

The recovered ~180 m basalt section shows strong fracturing and alteration by hydrothermal activity, including mineralization (e.g., massive pyrite). One zone (40 cm) of potential fault gauge separates an upper and lower series and may suggest that syn- to postbasaltic tectonism was active. This high-temperature hydrothermal alteration requires that a significant heat source capable of driving the hydrothermal system was present and that the deeper crust might comprise plutonic bodies.

Combining the findings at Site U1502 with the recovery at Site U1499 (Expedition 367; Ridge A) of rift-related syntectonic sediments of Oligocene age suggests that Ridge A is a complex structure comprising both syntectonic sediments and syntectonic igneous material. These findings do not constitute a complete understanding of the deep crustal nature of Ridge A, including the specific question of whether lower crust or subcontinental lithospheric mantle is present at depth. Detailed examination of the recovered basalts will help to constrain the specific nature of the deeper crust.

We believe that to further advance our understanding of the detailed and deeper nature of Ridge A, future dedicated geophysical surveying and one or two more deep drill holes are required.

The nature of the crust at the OMH was well addressed during Expedition 368. Operations at Site U1501 drilled ~45 m into the basement below the Cenozoic sedimentary section and recovered lithified, coarse-grained sedimentary rocks of presumed Mesozoic age. This finding verified our predrilling interpretation of the OMH as comprising upper continental crustal material. The basement of the most eastward extension of the OMH was also sampled at Site U1504. In this location, greenschist facies metamorphic rock was found within the uppermost part of the OMH basement, suggesting that only a moderate amount (~5 km) of upper crust was removed prior to deposition of the thin, mainly postbreakup sediments that overlie the basement. The timing of the removal of the uppermost crust is constrained to be of at least pre-early Miocene to pre-late Eocene age and very likely much older (Mesozoic or older). If the cored material allows, postexpedition work on age determination and thermobarometry may suggest a plausible exhumation history and if this timing is indeed directly related to the Cenozoic rifting.

Our inability to pursue deep drilling at Site U1503 obviously prevents us from characterizing the nature of the crust at Ridge C based on in situ drilling data.

2. *To determine the time lag between plate rupture and asthenospheric upwelling that allowed decompression melting to generate igneous ocean crust.*

This objective was achieved during Expedition 368.

The simple answer to Objective 2 is that there was no time lag between (final) plate rupture and asthenospheric upwelling supporting the generation of igneous material with a basaltic, MORB-type composition. The well-constrained pre-Oligocene age of the basaltic basement rocks at Ridge A rules out any time lag. In fact, a potential late Eocene age for the basalt may indicate that asthenospheric mantle melting slightly preceded final breakup. Postexpedition work on mantle melting history may detail the status of lithospheric thinning at this point of breakup (i.e., thickness of residual subcontinental lithosphere). Age determination and detailed geochemical work and modelling, however, will be challenging because of the highly altered nature of the basalts.

Our findings also rule out that the margin in this location within the COT was overprinted by late-stage magmatism. The failure to pursue Site U1503, located on the interpreted earliest full ocean crust, did not very seriously affect the accomplishment of the specific objective of constraining a possible time lag. However, the failure to recover basement rocks at this location means that establishing a well-defined reference frame for assessing mantle composition and mantle melting conditions during steady-state accretion of igneous crust might be difficult. Likewise, the possible modelling based on basalt composition of the decreasing thickness of the lithosphere from incipient breakup to full spreading may be

hampered. Site U1500 basalt samples collected during Expedition 367 possibly can help in this regard. Reoccupation of Site U1503 is, however, highly recommended to provide a benchmark against which the earlier breakup magmatism can be compared. Similarly, if in the future it would be possible to recover more fresh basaltic material from Ridge A, it would greatly benefit the study of the SCS margin in terms of age determination of the earliest basaltic magmatism and its detailed geochemical elemental and isotopic composition.

3. *To constrain the rate of extension and vertical crustal movements.*

This objective was achieved, but postexpedition work is needed to further develop our findings.

Important stratigraphic control on the synrift sediments related to breakup was achieved at Sites U1501, U1502, and U1505. At Site U1501, located on the OMH, the entire sequence of synrift sediments down to (presumed) Mesozoic basement was recovered. The sequence shows development from deltaic to shallow marine with terrigenous sedimentation (Eocene) through deepening water, yet still predominantly clastic detrital sediments (~early Oligocene), to deepwater marine calcareous sediments (~late Oligocene to Miocene). Biostratigraphic constraints on the Eocene deposits are lacking below the late Eocene. An almost similar evolution was documented at Site U1505 for the late Eocene to Miocene interval. Site U1502, located seaward of the OMH within Ridge A of the distal margin, shows (minor) deepwater deposits of late Eocene age followed exclusively by deepwater deposits of Oligocene to Miocene age. Site U1504, also at the OMH and slightly more elevated, penetrated a 120 m thick postrift sedimentary sequence above crystalline basement. Deepwater conditions were established by lowermost early Miocene time. The presence of a carbonate reef debris deposit (very shallow marine water) with an age of ~late Eocene suggests that the ~3 km subsidence experienced by these sediments was initiated post-late Eocene. The inability to pursue coring at Site U1503 prevented Expedition 368 from extending subsidence studies seaward of Ridge B (Site U1500). However, the most serious lack of data needed for constraining rate of extension is the lack of biostratigraphic control within the deeper part of the Eocene section at Site U1501. Similar deltaic to shallow-marine sediments of Eocene age were found at Site U1435 (Expedition 349), and, although similarly barren of microfossils, detrital zircon was present in the sediment. If present in the Site U1501 samples, age determination on a population of these might provide maximum ages. The amount of extension will be determined through a detailed tectonic interpretation of the regional seismic data (courtesy of the Chinese National Offshore Oil Corporation [CNOOC]) that the entire Expedition 367/368 program is based on.

4. *To improve the understanding of the Cenozoic regional tectonic and environmental development of the Southeast Asia margin and SCS by combining Expedition 367/368 results with existing ODP/IODP sediment records and regional seismic data.*

This objective was achieved and was even more successful than originally planned, but intensive multidisciplinary postexpedition work is needed to maximize our findings.

One of the most important achievements during Expedition 368 was recovering a relatively continuous sequence of the prerift, synrift, and postrift sediments since the Eocene at Site U1501. This sequence will greatly help us to understand the sedimentary processes associated with tectonic events and paleoenvironmental development at the SCS northern margin. Together with micropaleontological evidence of late Eocene age deposits at Site U1502, Expedition 368 findings provide the possible tectonic links between the SCS and the western Pacific in the aspects of the SCS formation history.

Based on the coring/drilling results of Expedition 368, new time-depth constraints on some of the major seismic stratigraphic unconformities that are mapped regionally throughout the basin were done by integrating microfossil ages, petrophysics, and borehole logging data with the existing seismic reflection data. Among these seismic unconformities, the T60 unconformity is the most prominent. It is easily recognized basin-wide and is present at Sites U1501, U1502 and U1505. Exploring its nature (e.g., timing and duration, processes, and mechanisms) is very important for understanding the regional geological evolution, but this objective will need further postexpedition work.

The high-quality postrift sediments cored during Expedition 368 will provide major contributions to our understanding of the late Cenozoic tectonic and environmental history of the SCS. An early to middle Miocene succession of red claystone was found at Site U1502 and at Expedition 367 Sites U1499 and U1500, all located below 3500 mbsl. The red claystone deposits near the acoustic basement (e.g., basalt or altered basalt or gravel) extending over all of these sites indicates that the SCS basin was deep and the sedimentation rate was extremely low at that time. These conditions may correlate to a basin-wide event related to deep circulation of oxygenated water from the western Pacific prior to the closure of the Luzon Strait.

A late Miocene succession of hemipelagic and turbidite deposits was observed at deeper Site U1502 and likely recorded the processes that delivered sediment from the shallow shelf or slope of the northern SCS to the deeper parts of the basin. A high sedimentation rate at Site U1502 during the late Miocene and a nearly 10 Ma hiatus from the middle Miocene to Pleistocene observed at Site U1504 indicate strong erosion from source areas and efficient transport to the deep basin.

The Pliocene–Pleistocene sequence was recovered by double APC holes at Site U1505 that aimed to establish a continuous record at this site for high-resolution paleoceanographic and paleoclimatic studies. The hemipelagic deposits, rich in calcareous microfossils, at this site above the modern CCD of the SCS will enable us to reconstruct the east Asian monsoonal climate and paleoceanographic changes in the SCS at orbital and millennial timescales.

Postexpedition research using samples from Expeditions 367 and 368 together with seismic stratigraphic correlations will continue to improve the contributions to Objective 4. This research should be channeled into four general avenues:

1. To reconstruct the early stage history of the SCS, including paleonvironmental changes from land to deep sea and new data (e.g., detrital zircon geochronology) to constrain the sedimentary provenance.
2. To explore the paleoceanographic conditions favorable for early to middle Miocene pelagic red clay and late Miocene turbidite deposition through geochemical and geophysical techniques.
3. To correlate the chronostratigraphic records between Sites U1501, U1502, and U1505; previous IODP Expedition 349 and 367 sites; and ODP Leg 184 sites in the SCS.
4. To conduct high-resolution paleoceanographic study of Pliocene- and Pleistocene-related monsoonal climate changes and deepwater exchange between the SCS and the Pacific.

Integration of drilling results with seismic data

The large regional set of high-quality seismic data provided by the CNOOC formed an essential basis for the planning, scheduling, and implementation of Expeditions 367 and 368. The continued availability of these data to the scientific party will be pivotal for postexpedition research on most of the scientific objectives discussed above.

Operations

Hong Kong port call

Expedition 368 started at 0754 h (all times in this report are in ship local time [the same as in Hong Kong], or UTC + 8 h) on 9 April 2017 with the first line ashore at the China Merchants Wharf in Hong Kong. After the ship cleared immigration and customs, the Expedition 368 Co-Chief Scientists, IODP staff, and a group of 11 scientists, each representing each ship laboratory, moved onto the ship and started crossover with their Expedition 367 counterparts. Loading and offloading operations began after clearance was issued. Sixty tons of barite were loaded. The rig crew began breaking down 68 stands of 5½ inch drill pipe and laying them out on the riser hold hatch. All life rafts were offloaded for inspection to be returned prior to sailing.

The rest of the Expedition 368 scientists boarded the ship on the morning of 10 April and got settled in their rooms. Later that morning they were introduced to life on board the *JOIDES Resolution* and participated in an initial laboratory and ship safety tour. Loading and offloading operations continued with the loading of 40 short tons of sepiolite and the containerized science ocean freight along with fresh and refrigerated food products and 300 metric tons of potable water. Expedition 366 and 367 cores were offloaded from the vessel and loaded into refrigerated containers for shipment to the Kochi Core Center and Gulf Coast Repository, respectively. Ninety joints of 5½ inch drill pipe were offloaded to the pier, and another 72 joints were broken down and stowed on the riser hold hatch.

On 11 April, major port call activities included loading 1212 metric tons of marine gas oil and 40 short tons of sepiolite mud (total = ~80 short tons). All dry food for Expedition 368 was loaded. The rest of the 204 joints of 5½ inch drill pipe were broken down and offloaded to the pier to be returned for inspection and refurbishment. The vessel continued to conduct annual class, radio, and lifeboat surveys. Tours were conducted for members of the Hong Kong Sea Cadet Corps and Hong Kong Baptist University.

On 12 April, casing loading operations were initiated and tours were conducted for students and faculty from the Southern University of Science and Technology. On 13 April, casing loading operations were completed. Mud motors, underreamers, and reentry equipment were all loaded and stowed for transit. Annual life boat inspections and all other certifications were completed. All equipment was secured for sailing.

At 0600 h on 14 April, immigration authorities boarded the ship and cleared the personnel and vessel for departure. The harbor pilot arrived on board shortly after 0900 h, and with the assistance from two harbor tugs the *JOIDES Resolution* was underway, with the last line released at 0912 h. We proceeded to the pilot station, and after a 6 nmi transit the pilot disembarked the ship at 0954 h. The sea voyage continued for the next 24 h. During the transit, the Co-Chief Scientists presented the scientific objectives for Site U1501 and the Captain held the first fire and boat safety drill. Later that day, the Co-Chief Scientists, key *JOIDES Resolution* Science Operator (JRSO) staff, and the ship's crew met to review the coring and logging plan for Site U1501. The scientists began their working shifts, and the noon-to-midnight shift resumed laboratory activities. The 255 nmi transit from Hong Kong to Site U1501 was completed at 0837 h on 15 April at an average speed of 10.6 kt.

Site U1501

We conducted operations in four holes at Site U1501. The original plan included two holes, the first to ~650 m with the APC/XCB system followed by downhole measurements with the triple combo and FMS-sonic tool strings. The second hole was to have a reentry system to ~640 m and coring to ~1063 m followed by logging with the triple combo, FMS-sonic, and VSI tool strings. Actual operations differed significantly from the original plan. Mudlines were missed in Holes U1501A and U1501B, with Core 1H for each hole retrieving a full core barrel. Hole U1501C was cored from the seafloor to 461.8 m and recovered 447.8 (96.3%). Hole U1501D was drilled without coring from the seafloor to 433.5 m and then cored to 644.3 m. A total of 78.8 m of core was recovered (37.4%). See Table **T1** for the operations summary.

Holes U1501A–U1501C

After arriving at Site U1501, we lowered the thrusters, deployed a seafloor beacon, put together the APC/XCB bottom-hole assembly (BHA), and started lowering it to the seafloor (2857 mbsl) in preparation for coring. The calculated precision depth recorder (PDR) depth for the seafloor at Site U1501 was 2873.4 m below rig floor (mbrf), and we chose to place the bit at 2868 mbrf to take the first core. An APC core barrel was lowered to the bit, and coring in Hole U1501A started at 2345 h on 15 April 2017. The mudline core recovered 9.5 m of sediment, and seafloor was calculated to be 2868 mbrf (2857.1 mbsl). Hole U1501A was terminated at 0025h on 16 April to attempt to core a better mudline at this site. The drill string was with the bit at 2863 mbrf. We started Hole U1501B at 0100 h, again recovering a full core barrel, indicating once again that the APC system was fired at or below the seafloor, and Hole U1501B was terminated. The vessel was offset 10 m east of the site coordinates, and the bit was raised to 2843 mbrf in an attempt to start Hole U1501C, but the core barrel was retrieved empty. We then lowered the bit to 2848 mbrf for a second spud attempt at 0300 h, and another empty core barrel was retrieved. We lowered the bit to 2856.4 mbrf, and Hole U1501C was successfully spudded at 0510 h, recovering 9.3 m of core and establishing a seafloor depth at 2856.7 mbrf (2845.8 mbsl).

Hole U1501C was cored to 156.8 m using the full-length APC coring system. The HLAPC system was deployed to deepen the hole to HLAPC refusal at 257 m. We changed to the XCB system and deepened the hole to a final depth of 469.1 m. Nonmagnetic core barrels were used on all cores. All full-length APC cores were oriented using the Icefield MI-5 tool. The APC recovered 156.5 m of core (99.8%). Temperature measurements were taken on Cores 368-U1501C-5H (47.3 m), 8H (75.8 m), 11H (104.3 m) and 14H (132.8 m). Partial strokes were recorded on Cores 16H and 17H (151.8 and 156.8 m, respectively). The HLAPC system cored a 100.2 m interval with 88.54 m of recovery (88.4%). Partial strokes were recorded on Cores 22F (180.3 m) and 25F through 39F (189.7–257 m). The bit was advanced 4.7 m after each core despite the partial strokes. The bit was advanced 1.5 m after Core 39F.

The XCB system was deployed to core to refusal, recovering 199.5 m (97.4%). A hard layer was met at 383.5 m (Core 53X), and a

small piece of sandstone was recovered in the cutting shoe after retrieving the core barrel. Core recovery after that consisted of mudstone. Three more hard layers were found at 447.1, 454, and 460 m. Refusal was reached after no advancement was accomplished for ~10 min at 469.1 m. There were no indications that casing would be needed to core deeper using the RCB system at this site. The bit was then retrieved to the rig floor, clearing seafloor at 0935 h and clearing the rotary at 1420 h. Overall, 62 cores were taken over a 461.9 m interval with 444.8 m recovery (96.3%). Time spent on Hole U1501C was 84.75 h (3.5 days).

Hole U1501D

The vessel was offset 20 m west of Hole U1501D. The RCB outer core barrel was set up in the rotary table, and the core barrels were spaced out to the outer core barrel. While making up the BHA, a leak was detected in the low clutch diaphragm. The diaphragm was replaced and back on line by 0500 h on 20 April. Once the diaphragm was on line, the core barrels were prepped and spaced out, the remainder of the RCB BHA was made up, and the drill string was run in the hole to 2816 mbrf. The top drive was picked up and the bit spaced out to spud Hole U1501D.

Hole U1501D was drilled to 433.5 m, and the center bit was retrieved. An RCB core barrel was dropped, and coring began from that depth. Coring continued to 644.3 m using the RCB, and the hole was conditioned for logging. The rotary shifting tool was run in to release the bit, and heavy mud was spotted at the bottom of the hole. The top drive was set back, and the bit was raised to 113 m for logging.

The rig floor was set up for logging. The average heave was estimated to be <1 m just prior to logging. A modified triple combo tool string was made up and run into the open hole. The tool string hung up at ~3030 mbrf (173.3 m). After six attempts, the tool finally passed through that depth with significant drag and then continued downhole smoothly until it reached 3156 mbrf (299.3 m). At that depth, the full weight of the tool hung up and would no longer advance. The consensus among the wireline engineer, drilling department, and operations department was that the hole was collapsed and logging would have to be conducted from that point upward.

There was a significant overpull at ~173.3 m. The caliper log indicated that the hole was collapsed to approximately the same diameter as the tool itself. It was deemed unsafe to attempt to go below that depth with any subsequent passes, and the rest of the logging program was terminated. The drill pipe was recovered to the rig floor, clearing the seafloor at 1225h on 24 April and the rotary at 1715 h on 24 April.

A total of 90 cores were recorded for the site. The APC system was deployed 19 times with the full APC core barrel. The HLAPC system was deployed 22 times, the XCB system was deployed 23 times, and the RCB system was deployed 26 times. The total drilled interval was 433.5 m without recovery. The APC cored interval was 175.8 m with a recovery of 176.6 m of core (100.1%). The HLAPC cored interval was 100.2 m with a recovery of 88.54 m (88.4%). The XCB cored interval was 204.9 m with a recovery of 199.53 m of core (97.4%). The RCB cored 210.8 m and recovered 78.77 m of core (37.4%). Total core recovered at Site U1501 was 543.10 m. The overall recovery for Site U1501 was 78.5%. Total time spent at Site U1501 was 224.75 h (9.4 days).

Site U1502

We conducted operations in two holes at Site U1502 with the objective of sampling the lowermost sediment and underlying basalt. At Site U1502, we successfully penetrated from the seafloor to the sediment–basalt contact at 728 m and 180 m into the underlying basalt. The sedimentary section was not continuously cored, and recovery in the cored intervals was highly variable (46%). In contrast, core recovery in the basalt was significantly better (70%). Downhole logging was conducted in Hole U1502B with the triple combo and VSI tool strings.

Our operations in Hole U1502A were designed to provide information on formation characteristics and drilling conditions so that we could decide the length of casing to drill into the seafloor at deep-penetration Hole U1502B. Given this purpose and the amount of time to drill the second, deep hole, we did not core continuously in Hole U1502A. Instead, we drilled without coring from the seafloor to 375 m and cored with the RCB from 375 to 758.2 m, recovering 176.81 m (46%).

In Hole U1502B, we drilled a reentry funnel and 727.7 m of 10¾ inch casing into the seafloor, continuously cored a sediment sequence from 727.7 to 739.16 m (11.46 m cored; 3.55 m recovered; 30.9%) with the RCB system, continuously cored 180 m into the underlying basalt from 739.16 to 920.95 m (128 m recovered; 70%) with the RCB system, and collected downhole log data with the triple combo and VSI tool strings.

See Table **T1** for the operations summary. A diagram of the reentry cone and casing in Hole U1502B is shown in Figure **F22**.

Hole U1502A

After laying out the knobbies, the drill string was pulled out of the hole, clearing the seafloor at 1225 h on 24 April 2017. The acoustic beacon was recovered at 1511 h. The recovery of the pipe continued, and at 1715 h on 24 April, the end of the mechanical bit release (MBR) cleared the rig floor, ending Hole U1501D and Site U1501.

The *JOIDES Resolution* made the 36.5 nmi transit from Site U1501 to U1502 in 3.6 h, averaging 10.1 kt. The vessel arrived over the site coordinates at 2142 h on 24 April. At 2240 h, an acoustic beacon was deployed ~100 m west of the site coordinates. Upon arrival at Site U1502, a new C-4 RCB bit with a MBR was assembled onto the bottom of the BHA. The core barrel space out was checked, and the BHA was lowered to 161 mbsl. A PDR depth was taken on arrival, showing a calculated seafloor depth of 3768.4 mbsl.

The bit was lowered to 3733 mbsl, stopping every 20 stands to fill the pipe with water. The upper guide horn (UGH) was pulled, and the underwater camera system was deployed to the seafloor to observe the seafloor tag. While the camera was being lowered, 115 ft of drill line was slipped and cut. Next, the bit was spaced out to 3750.7 mbsl and slowly lowered until it tagged the seafloor. Seafloor was determined to be at 3763.7 mbsl. The bit was again spaced out to 3750.7 mbsl, and the top drive was picked up. The UGH was raised, and the underwater camera was recovered at 1215 h. A center bit was dropped and landed in the BHA, the bit was lowered, and Hole U1502A was spudded at 1300 h on 25 April. The hole was advanced without coring to 375 m in 18 h. The center bit was pulled, and an RCB bit was dropped to begin coring operations. One of the main objectives in Hole U1502A was to core with the RCB system to a depth in the formation that would provide a good and stable casing set point for the next hole.

Cores 368-U1502A-2R through 7R were drilled very quickly and had little recovery. This interval was interpreted as unconsolidated sand. Penetration rates slowed for Cores 8R through 14R, with the bit taking ~15,000 lb of weight during coring operations. Recovery improved through this mudstone interval but dropped off in what

was interpreted as another unconsolidated sand interval from 499.5 to 585.9 m (Cores 15R through 23R). A second mudstone interval was sampled, with very good recovery from Core 24R at 585.9 m to Core 39R at 739.1 m. The last 2 m of the following core (40R) drilled very slowly, indicating a major change in formation. One more core was drilled to confirm the continuity of the formation change. At that point, it was decided to terminate coring in Hole U1502A in favor of continuing to core in a cased hole. The drill string was pulled to the surface, clearing the seafloor at 0330 h on 30 April, ending Hole U1502A, and beginning Hole U1502B.

Total time spent in Hole U1502A was 125.25 h (5.2 days). The RCB system was used exclusively for the hole. A total of 40 cores were taken over a 383.2 m interval with 176.81 m of recovery (46.1%). There was one drilled interval from the mudline to 375.0 m.

Hole U1502B

The RCB components of the BHA were laid out and secured, and the rig floor was cleared for reentry and casing operations. The vessel was offset to the coordinates provided from the science office, and the UGH was removed and laid out to the drill collar racks.

The hydraulic release tool (HRT) was made up to a landing stand and racked back in the derrick. The prepared mud skirt was moved onto the moonpool doors and centered underneath the rotary table. After rigging-up to run 10¾ inch casing, 62 joints of 10¾ inch casing (723.7 m) were run through the mud skirt. The landing stand was picked up, and the casing was lowered to the moonpool and latched into the mud skirt. The adapter flange was unbolted, and the landing stand was pulled back to the rig floor and racked back in the derrick.

The bit, bit sub, underreamer, and mud motor were assembled, and a pump-in sub was connected to the top of the mud motor. The mud motor and underreamer were function-tested in the moonpool with good results. The remainder of the stinger was assembled. The landing joint was again picked up, and the mock hanger and HRT were attached to the top of the casing and mud skirt. The adapter flange was again bolted up and torqued up with a torque wrench to the recommended torque. The reentry funnel was picked up in the moonpool and securely welded to the mock hanger.

The drilling and casing assembly were lowered to the seafloor. Every 20 stands, the drill string was secured and filled water to prevent collapse from differential pressure. After running-in to 3744 m, the subsea camera was lowered to the bottom of the pipe to observe the drilling activity. While the camera descended, the top drive was picked up and the rig was serviced. The drill string was spaced out, and slow circulating rates were recorded. Hole U1502B was spudded at 3763.7 mbsl at 1255 h on 1 May. The drilling and casing installation continued until the mud skirt landed on the seafloor. After successfully drilling the 723.7 m long casing string into the seafloor, the go-devil was inserted into the drill pipe and pumped down to release the casing at 2220 h on 2 May. The drill string was released from the casing assembly, and the bit and underreamer were pulled back through the casing to the rig floor. The bit cleared the seafloor at 0115h on 3 May. The remainder of the drill string was pulled back to the rig floor, and the bit cleared the rotary table at 1130 h on 3 May.

After removing the tricone bit, the mud motor and underreamer were flushed with freshwater and laid out. The UGH was reinstalled, and the drill floor was reassembled. The RCB outer core barrel was set up in the rotary table, and the core barrels were spaced out to the outer core barrel. The remainder of the RCB BHA was made up, and the drill string was lowered to 3732 mbsl. The subsea camera system was deployed and run to near bottom in preparation for reentering Hole U1502B and beginning coring operations. While the subsea camera was lowered to the seafloor, 115 ft of drill line was slipped and cut. After a 3.5 h search, we found the Hole U1502B reentry cone and reentered the hole at 0400 h on 4 May. The camera was pulled back to the surface and secured.

The bit was lowered through the casing until encountering fill at 715.3 m, 12.4 m above the total depth of the hole. The top drive was picked up, a core barrel was dropped, and the hole was washed and reamed to bottom. A 20 bbl mud sweep was circulated to help clean cuttings from the hole. Once the hole was clean, coring began in Hole U1502B from 727.7 m. Coring continued to Core 368-U1502B-21R at 846.8 m. While cutting Core 21R, the driller noticed some excessive torque while on bottom. With 48.8 h on the bit, it was decided to pull out of the hole for a bit change. The bit was found to be in relatively good condition.

The drill string was pulled inside the casing before setting back the top drive. Overpull of 60,000 lb was noted between 740.3 m and the casing shoe. The bit was then pulled to the mouth of the reentry cone, and the vibration isolated television (VIT) camera was run to the seafloor to verify the condition of the base and cone. The cone was visible but below the surface. Sea water was circulated in a successful attempt to clear the funnel of cuttings, and the VIT was retrieved to the moonpool. The bit was then pulled to surface, clearing the seafloor at 0600 h and clearing the rotary at 1345 h on 8 May.

A new 9⅞ inch C-7 RCB bit and a MBR were installed in the BHA, and the bit was run back to seafloor, followed by the subsea camera, for reentry. The cone was clearly visible, and Hole U1502B was reentered at 0240 h on 9 May. The camera was recovered, and the bit was lowered to 728.3 m, ~0.5 m below the casing shoe. The top drive was picked up, and a center bit was dropped. The hole was then washed to total depth with the fill holding 10,000 lb weight on bit from 733.3 to 770.3 m.

A mud sweep was circulated, and the center bit was retrieved prior to resuming coring operations.

Coring continued to 858.4 m when the low clutch diaphragm failed for a second time during the expedition at 0115 h on 10 May. The bit was pulled inside the casing and up to 715.3 m, and the drill pipe was hung off the elevators. The clutch diaphragm was replaced, and the drill string was lowered again by 0945 h on 10 May.

The driller noticed a spike in pressure while running in hole, and a deplugger was dropped to clear any obstruction in the bit. The deplugger was retrieved, and a center bit was deployed so that the bit could be worked to the bottom of the hole. A total of 3 m of fill were cleared before reaching the total depth of the hole. The center bit was recovered, and coring resumed from 858.4 m (Core 25R) to a final depth of 920.8 m (Core 37R). Recovery was generally high over this interval (82%–101%), except for Cores 28R and 29R, which had only 33% and 45% recovery and a higher rate of penetration of 2.76 and 3.75 m/h, respectively. The hole was then prepared for logging operations by circulating a high-viscosity mud sweep and performing a wiper trip. The bit was then released in the bottom of the hole, and the end of pipe was raised to a logging depth of 747.3 m to ensure that the logging tools could bypass obstructions encountered by the bit when reentering the hole below casing.

Downhole logging

Two logging tool strings were deployed in Hole U1502B: a modified triple combo and the VSI. The triple combo tool string was rigged up, zeroed, presurvey calibrated, and deployed in the hole

with the DSI, HLDS (with source), HNGS, Enhanced Digital Telemetry Cartridge (EDTC), and Logging Equipment Head (LEHQT).

The string made it into the open hole without any issue, but it stopped at a maximum depth of 4639 m, roughly 45.5 m higher than the driller's total depth. Based on an unexpected drop in NGR readings through casing, material at this depth was believed to be fill from above that had slumped and fallen to the bottom of the hole.

The repeat pass was taken from that depth up to the point where the logging head was just outside the pipe. The tool was then returned to maximum depth, which remained firmly at 4639 m. The main log was started there and continued up past the seafloor to provide a continuous NGR log of the entire interval. The caliper was closed at 4549 m to facilitate pipe entry, which proceeded without any problems. The tools were pulled to surface with ease until the final joint of pipe at the top.

With the EDTC already sticking out of the top of the pump-in sub during the process of pulling the tool up to remove the density source, a large overpull was observed, causing the tension alarms to trip and disable winch function. Several attempts to free the tool were made, but they only resulted in it becoming too stuck to move up or down significantly. An alternate plan of disconnecting the first joint of drill pipe to permit access to the tool inside and then disassembling whichever portion was free to move worked, and the radioactive source along with the majority of the string was rigged down. The portion remaining stuck in the top single consisted only of the LEHQT and EDTC, which were extracted relatively quickly and easily from the bottom of that single using an air tugger.

There was no sign of damage to the tool string itself nor any sign of a problem in the affected joint of pipe, so the cause is believed to have been a fragment of shear pin from coring or other item of small debris such as a pebble. The offending item was never located, but the string was safely rigged down with only about 0.5 h of additional time required. The wireline was extracted from the travelling blocks to facilitate pulling the pipe up to ~69 mbsl for the seismic run, and wireline operations were paused for that action.

The VSI tool string was rigged up, zeroed, presurvey calibrated, and lowered in Hole U1502B with the VSI tool, EDTC, and LEHQT.

While pulling up the pipe, the drill crew observed that the hole was beginning to flow and had to make an unplanned break in the trip to pump down some seawater to stop the flow. Once that was done, the seismic string was rigged up and lowered inside the hole without finishing the pull-out because the pipe was already at 4023 mbsl (259 m), which was sufficiently high to avoid any major complication with the seismic experiment, and it was getting too late to raise the pipe any higher and still have sufficient time to finish the survey before dark.

The tool was rigged up as quickly as was safe to do so and run in the hole at a somewhat accelerated rate to make as much use as possible of the remaining daylight. The depth was correlated and adjusted to be on-depth in real time using a distinct NGR peak at 4413 mbrf (corrected depth based on field pick of sea bed; raw depth of 4411.3 mbrf on main pass of first run). With the seismic tool on-depth, several attempts were made to get out of the casing and down to the bottom of the hole so that the deepest requested stations for the survey could be recorded, but the tool appeared to be hanging up on a ledge and was unable to pass into the open-hole section.

Having very little daylight remaining in which to complete the rest of the survey, the decision was made to abandon the open-hole stations and concentrate on getting as many of the cased-hole stations as time would permit. In all, eight stations were attempted, all in casing, and of those, the deepest two did not produce any useful signal, but the upper six all resulted in good seismic arrivals. The seismic survey was concluded roughly at sunset, and the tool was pulled out of hole and rigged down in the usual manner. The heave compensator was not required for any portion of the logging because the total heave was approximately ±2 inches throughout the entire operating time.

The Schlumberger equipment was then rigged down, and the crew began recovering the drill string. The bit cleared the seafloor at 2235 h on 13 May. The beacon was recovered at 0015 h on 14 May, and the vessel began moving toward Site U1503 in dynamic positioning mode. The bit cleared the rotary at 0445 h on 14 May, ending Hole U1502B and Site U1502.

Total time spent in Hole U1502B was 337.25 h (14.1 days). The RCB system was used exclusively for the hole. Overall, 36 cores were taken over a 193.1 m interval with 126.94 m of recovery (65.7%). There was one drilled interval from the mudline to 727.7 m with 10¾ inch casing installed to 723.7 m.

Site U1503

We conducted operations in one hole at Site U1503 with the objective of sampling the lowermost sediment and 150 m into the underlying basalt. In this hole, we installed a reentry system and 991.5 m of casing (10¾ inch), but we were unable to continue deepening the hole because of mechanical problems with the drawworks: (1) fourth clutch diaphragm failure, (2) failure of the aft shaft bearing on one of the Elmagco brakes, and (3) inability of the ship drilling equipment to operate deeper than 3400 m without the low clutch. Therefore, Site U1503 was abandoned without achieving any scientific objectives. Despite this major setback to the expedition and the South China Sea Rifted Margin program, Hole U1503A remains a legacy hole for future occupation.

Hole U1503A

The *JOIDES Resolution* began the transit from Site U1502 to Site U1503 in dynamic positioning mode while pipe was being tripped. The mud skirt and reentry cone to be used at Site U1503 was moved to the center of the moonpool and stationed on the moonpool doors. With this equipment secured, the thrusters were pulled and the vessel was underway at full speed at 0806 h on 14 May 2017.

The vessel arrived on site at 0930 h on 14 May to find the Chinese R/V *Shiyan 2*, operated by the South China Sea Institute of Oceanology, conducting a seismic survey in the area. Because of this, the *JOIDES Resolution* was unable to occupy the site until 1130 h on 14 May. The vessel completed the 19.8 nmi voyage from Site U1502 in 8.6 h (7.2 h in dynamic positioning mode and 1.4 h at cruise speed).

Once on site, a positioning beacon was deployed and the crew made up the BHA with a 14¾ inch bit to drill a hole without coring to 1000 m for installation of 10¾ inch casing. The bit was lowered through the reentry cone and base that was assembled and placed in the moonpool. A PDR depth was taken upon arrival, placing the seafloor at 3873.1 mbsl. The bit was lowered to 3846 mbsl, the top drive was picked up, and the bit was spaced out to spud Hole U1503A. The hole was started at 2010 h on 14 May and was advanced to a depth of 902.8 m at 0100 h on 16 May. At this time, the rig mechanic noticed a leak in the low clutch diaphragm, which had already been replaced twice during the expedition. It was decided to pull the bit to the surface before the diaphragm failed completely. The bit was pulled to 97.6 m, and the reentry cone assembly was free-fall deployed. The subsea camera was lowered to observe the

landing orientation of the cone (Figure **F23A**). Once the camera was near the sea bottom, the bit was pulled out of the hole, clearing the seafloor at 0750 h on 16 May. The bit tagged the internal aperture of the cone to establish a seafloor depth of 3867.7 m, 5.4 m higher than previously thought. The hole depth was adjusted to 908.2 m.

The bit was then pulled to 3846 m, and 215 ft of drill line was slipped and cut. The bit was pulled to the surface, clearing the rotary at 1655 h. With no spare clutch diaphragms on board and delivery of spare diaphragms not until ~20 May, it was decided to move along with all possible operations without using the low drive on the drawworks.

The drill crew ran 85 joints (989.3 m) of 10¾ inch casing and crossed over to a 16 inch casing hanger. While attempting to engage the DrilQuip running tools, it was noted that the seal diameter on the casing hanger was too small. The crew modified the hanger to enlarge the seal diameter and engaged the running tool. The casing was then lowered into the moonpool and hung off the moonpool doors.

The crew then picked up the mud motor and underreamer, lowered the drilling assembly into the moonpool, and tested them. The rest of the drilling assembly was made up and lowered through the casing. The running tool was then reengaged into the casing hanger, and the entire casing string and drilling assembly was lowered as far as possible (2379 m) without using the drawworks low clutch and then hung off the traveling blocks. Our last operation was to make up three stands of knobbies and pump a pig through each stand to clean any rust; these were then racked back in the derrick for use when drilling-in the casing.

The rig then went on downtime on Thursday 18 May at 0915 h until the replacement parts (low clutch diaphragms) were delivered to the ship at 2310 h on 20 May. The seagoing tug *Taikoo* arrived on site with three spare low clutch diaphragms. The tug stationed itself on the port aft side of the *JOIDES Resolution*. Supplies were offloaded, and the tug departed by 2320 h. At the end of the week, the crew began replacing the low clutch diaphragm.

Repairs were complete by 0415 h on 21 May. The driller continued lowering the casing string from 2379 mbsl to the seafloor, filling the pipe with seawater every 25 stands. The subsea camera was deployed, and Hole U1503A was reentered at 1005 h on 21 May with the 10¾ inch casing string. The casing began taking weight at 342 m; thus, it was pulled back, the top drive was installed, and the mud motor, bit, and underreamer were used to drill the casing to the bottom of the predrilled hole at 908.2 m. We continued drilling-in the last 86.9 m of casing, reaching 991.5 m. The casing was released at 0915 h on 22 May, and the camera and the drilling assembly were recovered. The mud motor and underreamer were flushed with freshwater and laid out. The casing running tool was detorqued and laid out.

The UGH was installed, and the drill crew began making up and deploying an RCB BHA. The bit was lowered to 1232 mbsl, when the drill crew noticed a loud noise coming from the forward Elmagco brake. The aft bearing on the forward Elmagco brake had failed. The crew began working to replace the brake with a reconditioned unit that was loaded on board in Hong Kong. This job was scheduled for the maintenance period following Expedition 368. We were lucky that the seas were calm, as this typically can't be done at sea.

Repairs began at ~0530 h on 23 May. Because of the calm seas, the crew was able to make the heavy crane lifts required. The forward brake was disconnected and moved to the rig floor where the hub could be removed for use on the replacement. The 28,000 lb (12.7 metric tons) nonfunctioning brake was then transferred to the main deck, and the replacement was moved to the rig floor to have the hub fitted and be installed on the forward end of the drawworks. The brake was moved into place, the electrical and water connections were made, and the shaft was aligned by 0600 h on 25 May.

Operations resumed, and the bit was lowered to 3819 mbsl at 1100 h on 25 May, when it was noticed that the low clutch diaphragm was leaking again. The diaphragm was replaced for the fourth time during this expedition (completed at 2100 h on 25 May). Because of the deep water depth along with the planned deep penetration at Site U1503, we would need to extensively use the low clutch. Because of the number of diaphragm failures so far and with only one more spare left on board, it was determined that the safest action would be to terminate operations in Hole U1503A without reentering the cased hole. An optimistic delivery date for additional clutch diaphragm spares, if available, was estimated for 2 June. If we were to reenter Hole U1503A and had an additional clutch failure while coring below the casing, the remaining spare would be enough only to get the drill string out of the hole, and any failed operations in the open hole could have prevented a future reentry operation. This was a very difficult decision to make, but with two more weeks left of the expedition the decision was made to switch to operations at sites with shallower water depths and penetration that did not require the use of the low clutch while drilling or coring. Therefore, we decided to transit to Site U1504 and continue operations there.

Before departing from Site U1503, the subsea camera was deployed to the seafloor to inspect the Hole U1503A reentry. The cone appeared to be 1–2 m below the seafloor but was clearly visible and expected to be available for reentry at a later date (Figure **F23B**, **F24**). Consequently, the site can be considered a legacy site for future expeditions. The camera was retrieved, the bit was recovered, and the rig was secured for transit. The thrusters were up at 0930 h on 26 May, and the vessel began the 42.5 nmi transit to Site U1504.

Site U1504

We drilled two holes at Site U1504. In Hole U1504A, we cored with the RCB system from the seafloor to 165.5 m and recovered 52.77 m (31.9%). In Hole U1504B, we drilled without recovery to 88.2 m and then cored 111.8 m with the RCB system with 21.48 m of recovery (19.2%).

Transit to Site U1504

The *JOIDES Resolution* began the transit from Site U1503 to Site U1504 at 0948 h on 26 May 2017 and arrived on site at 1400 h the same day. The thrusters were lowered, and we switched to dynamic positioning mode at 1432 h, beginning operational time at Site U1504. An RCB BHA was made up and deployed to 1720 mbsl before a failure of the pipe spinner on the iron roughneck. The spinner was replaced, and the crew continued to lower the pipe to 2776 mbsl. The underwater camera was deployed, and the bit was placed at 2813 mbsl for a short seafloor survey to verify that no seafloor cables were in the area. The seafloor was tagged after the survey, determining a water depth of 2816.6 m. The camera was retrieved, and the top drive was picked up for starting Hole U1504A. Coring in Hole U1504A started at 0215 h, and the bit reached the sediment/basement contact at 136.4 m (at 1455 h on 27 May). Coring continued to 165.5 m, where erratic torque and overpull caused us to terminate coring operations in this hole at 1100 h on 28 May. The bit was recovered to the surface, clearing the seafloor at 1220 h and the rotary at 1740 h. The rig floor was secured for the 22 nmi transit

to Site U1505 by 1825 h on 28 May, ending (temporarily) operations at Site U1504.

Total time spent in Hole U1504A was 50.5 h (2.1 days). The RCB coring system was used exclusively for the hole. Overall, 21 cores were taken over a 165.5 m interval with 52.77 m of recovery (31.9%).

Return to Site U1504

We returned to Site U1504 after completing Site U1505. The 22.2 nmi transit from Site U1505 to Site U1504 was completed at 0048 h on 3 June. The thrusters were lowered, and the heading was controlled at 0357 h, beginning operational time at Site U1504.

An RCB BHA was made up, and core barrels were spaced out. A center bit was installed, and the bit was deployed to 2776 m. The underwater camera was deployed to the bit, and the drill string was hung off the elevator stool. The low clutch was then dismantled, and the low clutch diaphragm was replaced. The diaphragm had failed during operations at Site U1505 but was not replaced then because it was not necessary for operations at that site and the crew wanted to have a new diaphragm installed at seafloor in case it was necessary during operations in Hole U1504B. The replacement took 7.75 h. Once completed, the top drive was picked up and the bit was lowered to the seafloor.

Seafloor was tagged at 2843.0 mbsl. The underwater camera was recovered to the moonpool, and Hole U1504B was spudded at 2250 h on 4 June. The hole was advanced without coring to 88.2 m.

The center bit was recovered using the core line, and an RCB core barrel was dropped to begin coring. Sediments were recovered in Core 368-U1504B-2R. The following two cores, 3R and 4R, contained coral and reefal limestone fragments. Basement rubble was recovered from Core 4R downhole. RCB coring continued through Core 20R at 200.0 m. Torque was erratic throughout basement coring operations, and half cores were cut for all basement cores except Core 19R.

Coring was terminated due to time after Core 20R, and the bit was recovered to the surface, clearing the seafloor at 0455 h and the rotary at 1040 h on 7 June. The rig floor was secured and made ready for the 946 nmi transit to Shanghai, China, by 1130 h on 7 June. The vessel was underway at 1200 h, ending Hole U1504B and Site U1504.

Total time spent in Hole U1504B was 80.0 h (3.3 days). The RCB coring system was used exclusively for the hole. Overall, 19 cores were taken over a 111.8 m interval with 21.48 m of recovery (19.2%).

Site U1505

Four holes were APC/XCB cored at Site U1505 with the objective of recovering a complete sedimentary succession from the early Miocene to Holocene that can supplement the interval sampled at Site U1501 for postexpedition paleoceanographic and paleoclimatological studies. Core 368-U1505A-1H misfired (failed shear pins) and recovered only 0.3 m. Core 368-U1505B-1H penetrated 3 m into the seafloor, recovering 3.23 m of core (107%). With a good mudline core, the hole was terminated. Hole U1505C was cored to 480.2 m, recovering 480.15 m (100%). Hole U1505D was cored to 184.5 m, recovering 191.43 m (104%). Downhole logging with a modified triple combo tool string was conducted in Hole U1505C.

Transit to Site U1505

The *JOIDES Resolution* began the transit from Site U1504 to Site U1505 at 1854 h on 28 May 2017 and arrived on site at 2112 h the same day. The thrusters were lowered, and the heading was controlled at 2148 h, beginning operational time at Site U1505.

Holes U1505A and U1505B

An APC/XCB BHA was made up, and a PDR depth was taken to help determine seafloor. By 0000 h, the drill string was being lowered to the seafloor followed by the subsea camera system to observe the end of the pipe tag the seafloor and start APC coring in Hole U1505A. At 0545 h, 29 May, a water depth of 2916.6 mbsl was established. Before retrieving the underwater camera, we conducted required routine rig servicing, which consisted of slipping and cutting 115 ft of drilling line. The top drive was picked up while recovering the subsea camera, and the bit was spaced out to 2911.2 m to spud Hole U1505A. There was an apparent misfire (failed shear pins) of the APC, and the core barrel was recovered to surface. The barrel had 0.38 m of core, far less than anticipated, and the hole was terminated at 1200 h in order to attempt a better mudline.

The bit was spaced out to 2912.1 mbsl, and Hole U1505B was spudded at 1235 h on 29 May. The core was recovered with 3.23 m of sediment. With a good mudline core, Hole U1505B was terminated at 1300 h.

Hole U1505C

The vessel was offset 20 m east of Hole U1505B, and the bit was spaced out to 2916.1 mbsl. The decision was made to core to XCB refusal or to the maximum drill string weight that could be lifted using the high clutch (whichever came first) due to a leak in the newly replaced low clutch diaphragm. Hole U1505C was started at 1340 h on 29 May. Seafloor was calculated at 2917.4 mbsl based on recovery from Core 368-U1505C-1H. The full-length APC system was used to refusal at 207.1 m, with APCT-3 temperature measurements taken on Cores 4H, 7H, 10H, and 13H. All four deployments produced good temperature data. APC refusal was determined after partial strokes on five consecutive cores (19H through Core 23H). The HLAPC was then deployed and used to recover 24 cores, 24F through 47F. All HLAPC cores were considered partial strokes, with the standpipe retaining pressure after each core. The residual pressure in the standpipe was bled off using the Cameron Orbit valve. HLAPC refusal was determined with recovery of 3.14 and 2.60 m in Cores 46F and 47F, respectively. While bleeding pressure on Core 47F, the diaphragm on the pneumatic actuation for the Orbit valve failed. The pressure was bled by manually opening the valve. The valve was taken out of service and repaired.

The XCB system was then deployed and used to core to 480.2 m before drill string weight dictated the end of coring operations. The hole was displaced using heavy mud, and the bit was spaced out to a depth of 80.1 m below the seafloor in preparation for logging.

A modified triple combo tool string was rigged up and lowered into the hole. The tool string was exceptionally long, consisting of all tools typically run as part of the triple combo (MSS, HLRA, HLDS [with source], HNGS, EDTC, and LEHQT) with the addition of the DSI for acoustic velocity. The DSI was added to the first run in anticipation of potential hole problems that might prevent subsequent runs based on experience at nearby sites with similar lithology. The tool string began collecting data a few meters above the seafloor and recorded continuously to the deepest point the tools could reach, which was a firm hole obstruction at 341.2 m. The tool string was unable to pass below that depth even after several attempts. Accordingly, the repeat pass was conducted from that depth for a length of ~110 m, and the main pass was also conducted from that depth up to just above the seafloor. During the run, the tool string collected NGR, density (with caliper), acoustic velocity, neutron porosity, and magnetic susceptibility. The caliper indicated that the hole diameter was too large (>14 inches) for effectively col-

lecting useful data with the FMS-sonic and VSI tool strings. Therefore, the decision was made to end downhole logging operations in Hole U1505C. The tools were pulled to the surface after logging was completed. After rigging down the logging equipment, the bit was raised, clearing the seafloor at 1755 h on 2 June and ending Hole U1505C.

Total time spent in Hole U1505C was 103.0 h (4.3 days). The APC, HLAPC, and XCB systems were deployed in the hole, coring a 480.2 m interval and recovering 480.15 m (100.0%).

The APC system was used to cut 23 cores over a 207.1 m interval with 99.9% recovery. The HLAPC system was used to cut 24 cores over a 109.9 m interval, recovering 112.9 m (102.7%). The XCB system recovered 160.4 m of sediment (98.3%) over a 163.2 m interval.

Nonmagnetic core barrels were used on all cores for the hole. All full-length APC cores were oriented. APCT-3 temperature measurements were taken on Cores 4H, 7H, 10H, and 13H.

Hole U1505D

The vessel was offset 20 m south of Hole U1505C, and the bit was spaced out to 2911.6 m. Hole U1505D was spudded at 2200 h on 2 June 2017. Seafloor was calculated at 2917.5 mbsl based on recovery from Core 368-U1505D-1H. The hole was then cored to a total depth of 184.5 m using the APC system. Then the bit was recovered to surface, clearing the seafloor at 1800 h and the rotary table at 2310 h. The beacon was recovered while raising pipe and was on deck at 1953 h. The thrusters were raised, and the rig floor was secured for transit. The vessel was underway to return to Site U1504 at 0048 h on 3 June, ending Hole U1505D and Site U1505. The plan was to drill a second hole to basement at Site U1504 with the time remaining on the expedition.

Overall, 20 APC cores were taken in Hole U1505D over a 184.5 m interval with 191.43 m recovered (103.8%). Nonmagnetic core barrels were used for all cores and all cores were oriented using the Icefield MI-5 tool.

Education and outreach

Expedition 368 had a team of three Onboard Outreach Officers: one teacher from the United States and two journalists from China. The Officers communicated the goals of their jobs on the ship to all scientists at the beginning of the expedition. This presentation gave examples of how the Onboard Outreach team could be a resource for the scientists to share the process of science during the expedition to the general public. The three Onboard Outreach Officers had different approaches and targets for their products and in their responsibilities, as well as working together to support the webcast program and a collaborative music video project; this report includes a summary of their work.

Webcasts

The Onboard Outreach Officers used a direct satellite link, iPad, and videoconferencing software (Zoom) to interact with K–12 classrooms, organizations, and universities around the world. The video connection schedule was prepared using a public Google calendar, direct contact with teachers to advertise the opportunity, and requests from scientists on board the *JOIDES Resolution*. Each webcast was led by the Officer who spoke in English or Mandarin depending on the language of the shore-based attendees. On occasions where the native language of the attendees was different, a scientist who was fluent in that language led the webcast (e.g., Italian or Dutch). The connections were used to reach students from primary schools to universities (both graduate and undergraduate levels), as well as with organizations who wished to learn more about the program. A typical session was approximately 1 h and was divided into the following parts:

- Identification of the geographical location and presentation of the geological questions addressed by the expedition;
- Brief review of plate tectonics and the rifting margin;
- Tour of the ship with a close look at the derrick, the rig floor, and the catwalk;
- Tour of the laboratories with questions to the scientists present (usually core describers, geophysicists, paleomagnetists, and paleontologists); and
- Opportunity for the students to ask questions.

A total of 53 events reached ~2500 students in 8 different countries (USA, China, Italy, Spain, The Netherlands, France, Japan, and Argentina). Before every video connection, the Onboard Outreach Officer interacted with the schools by sending the teachers some selected educational materials about the *JOIDES Resolution*, the seafloor drilling research, and the scientific topics related to Expedition 368. Before each week of webcasts, the Officer would communicate the schedule of broadcasts to the science party, Marine Computer Specialists, and Expedition Program Manager. Before the start of the broadcasts, the Officers would check in with scientists and IODP technicians to make sure that the broadcasts did not interrupt their workflow. After the video connection, a survey was sent to all of the teachers and participants (from Europe and USA).

Music video production

The Onboard Outreach Officer team worked with the Science Party and IODP technicians to produce a short music video to be used for promotion of the IODP program. This video was filmed over the course of 1 day by the Chinese Officer/Videographer and edited by the US Officer. It was shown at the postexpedition celebration in Shanghai.

Social media

The US Onboard Outreach Officer maintained four social media accounts during the expedition: the *JOIDES Resolution*'s blog at **http://joidesresolution.org**, Facebook page, Twitter feed, and Instagram account. Additionally, she produced 14 short videos that were posted on the *JOIDES Resolution* YouTube channel and received 1329 views during the course of the expedition. The total number of posts on the blog was 34, with 7044 read by the general public. The blog posts were divided into different areas: science as a process and highlights of areas of research, educational activities and reflections, scientist interview series, and ship life. Each post was crafted over the course of 1–2 days through interviews with scientists and observations and, when needed, were reviewed by scientists or technicians for accuracy before posting. The total number of Facebook posts was 57. The posts reached ~111,150 people with 21,600 post clicks and 2455 reactions, shares, or comments. A total of 31 tweets on Twitter were made with 36,373 impressions and 808 engagements. A total of 17 posts on Instagram were made and received 951 likes.

The US Onboard Outreach Officer also hosted a Reddit Science "Ask Me Anything" session, answering 15 questions from the public over the course of 2 h. Four members of the night shift science party participated in answering the questions. This session is permanently

archived at **https://www.reddit.com/r/science/comments/6dgfih/science_ama_series_scientists_are_on_board_the/**.

Educational material

The US Onboard Outreach Officer produced several scientist interview products discussing the process of science and careers in science. These scientists' interviews are intended to be a product that educators can use to lead discussions about career paths in science. Additionally the Officer worked with the paleontology team and other scientists on shore to do background research for future curriculum development projects.

The US Officer worked with several different outreach tools: webcasts (Zoom), blog posts through the *JOIDES Resolution* website (**http://joidesresolution.org/**), video production for YouTube, and other social media accounts for outreach (Facebook, Twitter, and Instagram).

Chinese media outreach

During the 2 months of Expedition 368, the journalist from *Science and Technology Daily* wrote about 30 news articles, including 4 videos and some photos, and the SMG News broadcasted 7 articles with Short Videos and 6 TV News, including a music video about the *JOIDES Resolution*.

These reports highlighted the importance of ocean drilling, the history and achievements of IODP, and the research progress of this expedition. The reports also told the stories of the scientists on board, explaining their work and showing their life on board. These reports were widely distributed in Chinese media and networks. They also helped enhance the public's awareness of IODP and scientific research in the SCS.

The Chinese journalists and scientists also did 26 education outreach broadcasts.

References

Barckhausen, U., and Roeser, H.A., 2004. Seafloor spreading anomalies in the South China Sea revisited. *In* Clift, P., Wang, P., Kuhnt, W., and Hayes, D. (Eds.), *Continent-Ocean Interactions within East Asian Marginal Seas.* Geophysical Monograph, 149:121–125. **http://dx.doi.org/10.1029/149GM07**

Briais, A., Patriat, P., and Tapponnier, P., 1993. Updated interpretation of magnetic anomalies and seafloor spreading stages in the South China Sea: implications for the Tertiary tectonics of Southeast Asia. *Journal of Geophysical Research: Solid Earth,* 98(B4):6299–6328. **http://dx.doi.org/10.1029/92JB02280**

Brune, S., Heine, C., Clift P.D., and Pérez-Gussinyé, M., 2017. Rifted margin architecture and crustal rheology: reviewing Iberia-Newfoundland, central South Atlantic, and South China Sea. *Marine and Petroleum Geology,* 79:257–281. **https://doi.org/10.1016/j.marpetgeo.2016.10.018**

Dick, H.J.B., Lin, J., and Schouten, H., 2003. An ultraslow-spreading class of ocean ridge. *Nature,* 426(6965):405–412. **http://dx.doi.org/10.1038/nature02128**

Doré, T., and Lundin, E., 2015. Research focus: hyperextended continental margins—knowns and unknowns. *Geology,* 43(1):95–96. **https://doi.org/10.1130/focus012015.1**

Franke, D., Savva, D., Pubellier, M., Steuer, S., Mouly, B., Auxietre J.-L., Meresse, F., and Chamot-Rooke, N., 2013. The final rifting evolution in the South China Sea. *Marine and Petroleum Geology,* 58(Part B):704–720. **http://dx.doi.org/10.1016/j.marpetgeo.2013.11.020**

Huismans, R., and Beaumont, C., 2011. Depth-dependent extension, two-stage breakup and cratonic underplating at rifted margins. *Nature,* 473(7345):74–78. **http://dx.doi.org/10.1038/nature09988**

Huismans, R.S., and Beaumont, C., 2008. Complex rifted continental margins explained by dynamical models of depth-dependent lithospheric extension. *Geology,* 36(2):163–166. **http://dx.doi.org/10.1130/G24231A.1**

Lester, R., McIntosh, K., Van Avendonk, H.J.A., Lavier, L., Liu, C.-S., and Wang, T.K., 2013. Crustal accretion in the Manila trench accretionary wedge at the transition from subduction to mountain-building in Taiwan. *Earth and Planetary Science Letters,* 375:430–440. **http://dx.doi.org/10.1016/j.epsl.2013.06.007**

Li, C.-F., Lin, J., and Kulhanek, D.K., 2013. *Expedition 349 Scientific Prospectus: South China Sea Tectonics.* International Ocean Discovery Program. **http://dx.doi.org/10.2204/iodp.sp.349.2013**

Li, C.-F., Lin, J., Kulhanek, D.K., Williams, T., Bao, R., Briais, A., Brown, E.A., Chen, Y., Clift, P.D., Colwell, F.S., Dadd, K.A., Ding, W., Hernández-Almeida, I., Huang, X.-L., Hyun, S., Jiang, T., Koppers, A.A.P., Li, Q., Liu, C., Liu, Q., Liu, Z., Nagai, R.H., Peleo-Alampay, A., Su, X., Sun, Z., Tejada, M.L.G., Trinh, H.S., Yeh, Y.-C., Zhang, C., Zhang, F., Zhang, G.-L., and Zhao, X., 2015a. Expedition 349 summary. *In* Li, C.-F., Lin, J., Kulhanek, D.K., and the Expedition 349 Scientists, *South China Sea Tectonics.* Proceedings of the International Ocean Discovery Program, 349: College Station, TX (International Ocean Discovery Program). **http://dx.doi.org/10.14379/iodp.proc.349.101.2015**

Li, C.-F., Lin, J., Kulhanek, D.K., Williams, T., Bao, R., Briais, A., Brown, E.A., Chen, Y., Clift, P.D., Colwell, F.S., Dadd, K.A., Ding, W., Hernández-Almeida, I., Huang, X.-L., Hyun, S., Jiang, T., Koppers, A.A.P., Li, Q., Liu, C., Liu, Q., Liu, Z., Nagai, R.H., Peleo-Alampay, A., Su, X., Sun, Z., Tejada, M.L.G., Trinh, H.S., Yeh, Y.-C., Zhang, C., Zhang, F., Zhang, G.-L., and Zhao, X., 2015b. Site U1435. *In* Li, C.-F., Lin, J., Kulhanek, D.K., and the Expedition 349 Scientists, *South China Sea Tectonics.* Proceedings of the International Ocean Discovery Program, 349: College Station, TX (International Ocean Discovery Program). **http://dx.doi.org/10.14379/iodp.proc.349.107.2015**

Li, C.-F., Wang, P., Franke, D., Lin, J., and Tian, J., 2012a. Unlocking the opening processes of the South China Sea. *Scientific Drilling,* 14:55–59. **http://dx.doi.org/10.2204/iodp.sd.14.07.2012**

Li, C.-F., Xu, X., Lin J., Sun, Z., Zhu, J., Yao, Y., Zhao, X., Liu, Q., Kulhanek, D.K., Wang, J., Song, T., Zhao, J., Qiu, N., Guan, Y., Zhou, Z, Williams, T., Bao, R., Briais, A., Brown, E.A., Chen, Y., Clift, P.D., Colwell, F.S., Dadd, K.A., Ding, W., Hernández Almeida, I., Huang, X.-L., Hyun, S., Jiang, T., Koppers, A.A.P., Li, Q., Liu, C., Liu, Z., Nagai, R.H., Peleo-Alampay, A., Su, X., Tejada, M.L.G., Trinh, H.S., Yeh, Y.-C., Zhang, C., Zhang, F., and Zhang, G.-L., 2014. Ages and magnetic structures of the South China Sea constrained by deep tow magnetic surveys and IODP Expedition 349. *Geochemistry, Geophysics, Geosystems,* 15(12):4958–4983. **http://dx.doi.org/10.1002/2014GC005567**

Li, J., Ding, W., Wu, Z., Zhang, J., and Dong, C., 2012b. The propagation of seafloor spreading in the southwestern subbasin, South China Sea. *Chinese Science Bulletin,* 57(24):3182–3191. **http://dx.doi.org/10.1007/s11434-012-5329-2**

McIntosh, K., Lavier, L., van Avendonk, H., Lester, R., Eakin, D., and Liu, C.-S., 2014. Crustal structure and inferred rifting processes in the northeast South China Sea. *Marine and Petroleum Geology,* 58(Part B):612–626. **http://dx.doi.org/10.1016/j.marpetgeo.2014.03.012**

McIntosh, K., van Avendonk, H., Lavier, L., Lester, W.R., Eakin, D., Wu, F., Liu, C.-S., and Lee, C.-S., 2013. Inversion of a hyper-extended rifted margin in the southern Central Range of Taiwan. *Geology,* 41(8):871–874. **http://dx.doi.org/10.1130/G34402.1**

Pérez-Gussinyé, M., Phipps Morgan, J., Reston, T.J., and Ranero, C.R., 2006. The rift to drift transition at non-volcanic margins: insights from numerical modelling. *Earth and Planetary Science Letters,* 244(1–2):458–473. **http://dx.doi.org/10.1016/j.epsl.2006.01.059**

Pérez-Gussinyé, M., and Reston, T.J., 2001. Rheological evolution during extension at nonvolcanic rifted margins: onset of serpentinization and development of detachments leading to continental breakup. *Journal of Geophysical Research: Solid Earth,* 106(B3):3961–3975. **http://dx.doi.org/10.1029/2000JB900325**

Reston, T.J., 2009. The structure, evolution and symmetry of the magma-poor rifted margins of the North and Central Atlantic: a synthesis. *Tectonophysics,* 468(1–4):6–27. **http://dx.doi.org/10.1016/j.tecto.2008.09.002**

Shi, H., and Li, C.-F., 2012. Mesozoic and early Cenozoic tectonic convergence-to-rifting transition prior to opening of the South China Sea. *International Geology Review,* 54(15):1801–1828. **http://dx.doi.org/10.1080/00206814.2012.677136**

Sun, Z., Liu, S., Pang, X., Jiang, J., and Mao, S., 2016a. Recent research progress on the rifting-breakup process in passive continental margins. *Journal of Tropical Oceanography,* 35(1):1–16. (in Chinese with English abstract) **http://dx.doi.org/10.11978/2015030**

Sun, Z., Stock, J., Jian, Z., McIntosh, K., Alvarez Zarikian, C.A., and Klaus, A., 2016b. *Expedition 367/368 Scientific Prospectus: South China Sea Rifted Margin.* International Ocean Discovery Program. **http://dx.doi.org/10.14379/iodp.sp.367368.2016**

Sun, Z., Stock, J., Klaus, A., and the Expedition 367 Scientists, 2017. *Expedition 367 Preliminary Report: South China Sea Rifted Margin.* International Ocean Discovery Program. **https://doi.org/10.14379/iodp.pr.367.2017**

Sun, Z., Xu, Z., Sun, L., Pang, X., Yan, C., Li, Y., Zhao, Z., Wang, Z., and Zhang, C., 2014. The mechanism of post-rift fault activities in Baiyun sag, Pearl River Mouth Basin. *Journal of Asian Earth Sciences,* 89:76–87. **https://doi.org/10.1016/j.jseaes.2014.02.018**

Sutra, E., and Manatschal, G., 2012. How does the continental crust thin in a hyperextended rifted margin? Insights from the Iberia margin. *Geology,* 40(2):139–142. **http://dx.doi.org/10.1130/G32786.1**

Wang, P., Prell, W.L., Blum, P., et al., 2000. *Proceedings of the Ocean Drilling Program, Initial Reports,* 184: College Station, TX (Ocean Drilling Program). **http://dx.doi.org/10.2973/odp.proc.ir.184.2000**

Wang, T.K., Chen, M.-K., Lee, C.-S., and Xia, K., 2006. Seismic imaging of the transitional crust across the northeastern margin of the South China Sea. *Tectonophysics,* 412(3–4):237–245. **http://dx.doi.org/10.1016/j.tecto.2005.10.039**

Wei, X.-D., Ruan, A.-G., Zhao, M.-H., Qiu, X.-L., Li, J.-B., Zhu, J.-J., Wu, Z.-L., and Ding, W.-W., 2011. A wide-angle OBS profile across the Dongsha uplift and Chaoshan depression in the mid-northern South China Sea. *Chinese Journal of Geophysics,* 54(6):1149–1160. **http://dx.doi.org/10.1002/cjg2.1691**

Whitmarsh, R.B., Manatschal, G., and Minshull, T.A., 2001. Evolution of magma-poor continental margins from rifting to seafloor spreading. *Nature,* 413(6852):150–154. **http://dx.doi.org/10.1038/35093085**

Yan, P., Zhou, D., and Liu, Z., 2001. A crustal structure profile across the northern continental margin of the South China Sea. *Tectonophysics,* 338(1):1–21. **http://dx.doi.org/10.1016/S0040-1951(01)00062-2**

Zhou, D., Sun, Z., Chen, H., Xu, H., Wang, W., Pang, X., Cai, D., and Hu, D., 2008. Mesozoic paleogeography and tectonic evolution of South China Sea and adjacent areas in the context of Tethyan and Paleo-Pacific interconnections. *Island Arc,* 17(2):186–207. **http://dx.doi.org/10.1111/j.1440-1738.2008.00611.x**

Zhou, X.M., and Li, W.X., 2000. Origin of late Mesozoic igneous rocks in southeastern China: implications for lithosphere subduction and underplating of mafic magmas. *Tectonophysics,* 326(3–4):269–287. **http://dx.doi.org/10.1016/S0040-1951(00)00120-7**

Table T1. Expedition 368 hole summary. — = no data.

Hole	Proposed site	Location	Water depth (m)	Total penetration (m)	Cored interval (m)	Drilled interval without coring (m)	Core recovery (m)	Core recovery (%)	Time on hole (days)	Cores (*N*)	Depth of 10.75 inch casing (m)
U1501A	SCSII-41A	18° 53.0922′N 115° 45.9483′E	2857.11	9.5	9.5	—	9.73	102.42	0.66	1	—
U1501B		18° 53.0922′N 115° 45.9483′E	2852.11	9.5	9.5	—	9.83	103.47	0.05	1	—
U1501C		18° 53.0919′N 115° 45.9485′E	2845.81	461.9	461.9	—	444.77	96.29	3.53	62	—
U1501D		18° 53.0929′N 115° 45.9370′E	2845.82	644.3	210.8	433.5	78.77	37.37	5.15	26	—
			Site U1501 totals:	1125.2	691.7	433.5	523.54	49.09	9.39	90	—
U1502A	SCSII-17A	18°27.8720′N 116°13.8381′E	3763.72	758.2	383.2	375.0	176.81	46.14	5.22	40	—
U1502B		18°27.8798′N 116°13.8409′E	3763.58	920.8	193.1	727.7	131.57	68.14	14.06	36	723.7
			Site U1502 totals:	1679.0	576.3	1102.7	308.38	53.51	19.28	76	
U1503A	SCSII-9B	18° 8.6300′N 116° 18.8456′E	3867.71	995.1		995.1	0.00	0.00	11.88	0	991.5
			Site U1503 totals:	995.1		995.1	0	0.00	11.88	0	—
U1504A	SCSII-27A	18°50.9199′N 116°14.5397′E	2816.57	165.5	165.5	—	52.93	31.98	2.17	21	—
U1504B		18°50.8213′N 116°14.5978′E	2842.97	200	111.8	88.2	21.48	19.21	3.33	19	—
			Site U1504 totals:	365.5	277.3	88.2	74.41	26.83	5.50	40	—
U1505A	SCSII-3D	18°55.0560′N 115°51.5369′E	2916.57	0.3	0.3	—	0.38	126.67	0.59	1	—
U1505B		18°55.0562′N 115°51.5370′E	2918.57	3	3	—	3.23	107.67	0.04	1	—
U1505C		18°55.0570′N 115°51.5491′E	2917.37	480.2	480.2	—	480.15	99.99	4.29	64	—
U1505D		18°55.0458′N 115°51.5501′E	2917.00	184.5	184.5	—	191.43	103.76	1.2	20	—
			Site U1505 totals:	668.0	668.0	—	675.19	101.08	6.12	86	—
			Expedition 368 totals:	4832.8	2213.3	2619.5	1601.08	138.24	52.17	292	—

Figure F1. Seismic data coverage and magnetic anomalies of the South China Sea basin, Expedition 367. Black lines = ocean-bottom seismometer refraction data. Other seismic lines are mostly multichannel seismic reflection data. White stars = Expedition 367 and 368 drill sites. ODP Leg 184 (red squares) and IODP Expedition 349 (red circles) sites are shown with site numbers. For more details, see Figure **F5**.

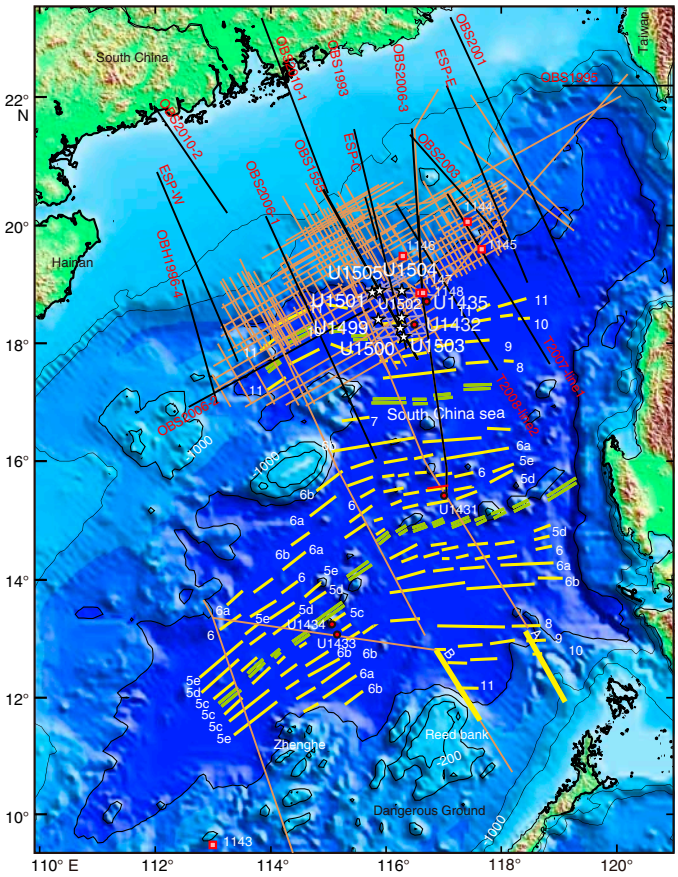

Figure F2. A–D. Schematic development of continental breakup initiated by a simple shear along a deep, low-angle fault. B–D are slightly modified from Huismans and Beaumont (2011) and illustrate modeling-based stages of extension at magma-poor rifted margins of the Iberia-Newfoundland type. Key features of D are thinning of the upper crust, juxtaposition of lower crust and serpentinized mantle between the outer margin and igneous oceanic crust. UP = upper plate, LP = lower plate. The Expedition 367/368 drilling strategy will sample and test whether or not these fundamental crustal units and tectonic relationships are present at the northern SCS rifted margin.

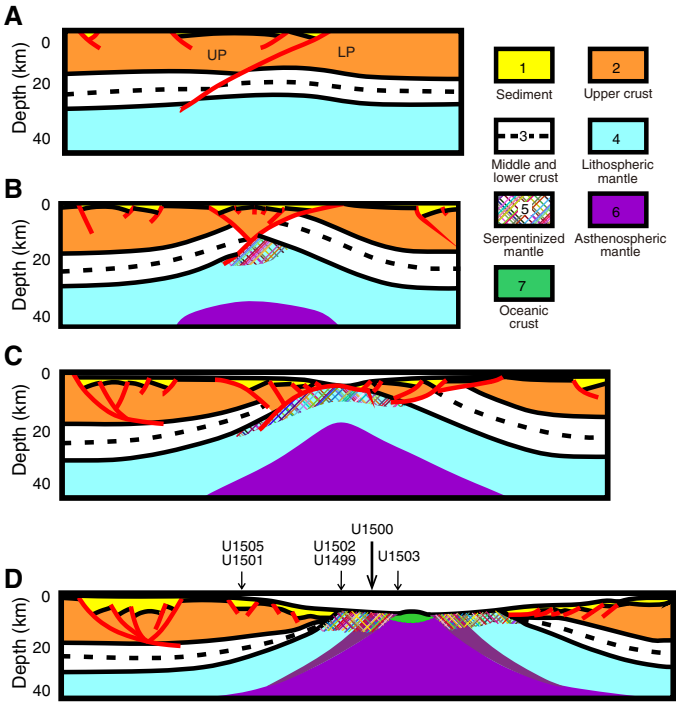

Figure F3. A, B. Expedition 367 and 368 sites (white stars) in the northern South China Sea margin with seismic coverage of 2-D, time-migrated multichannel seismic reflection seismic data and ocean-bottom seismometer data. Magnetic chron number is after Briais et al. (1993). Thick blue lines = key seismic lines used for planning of the drilling transect, red lines = magnetic lineations within the ocean crust.

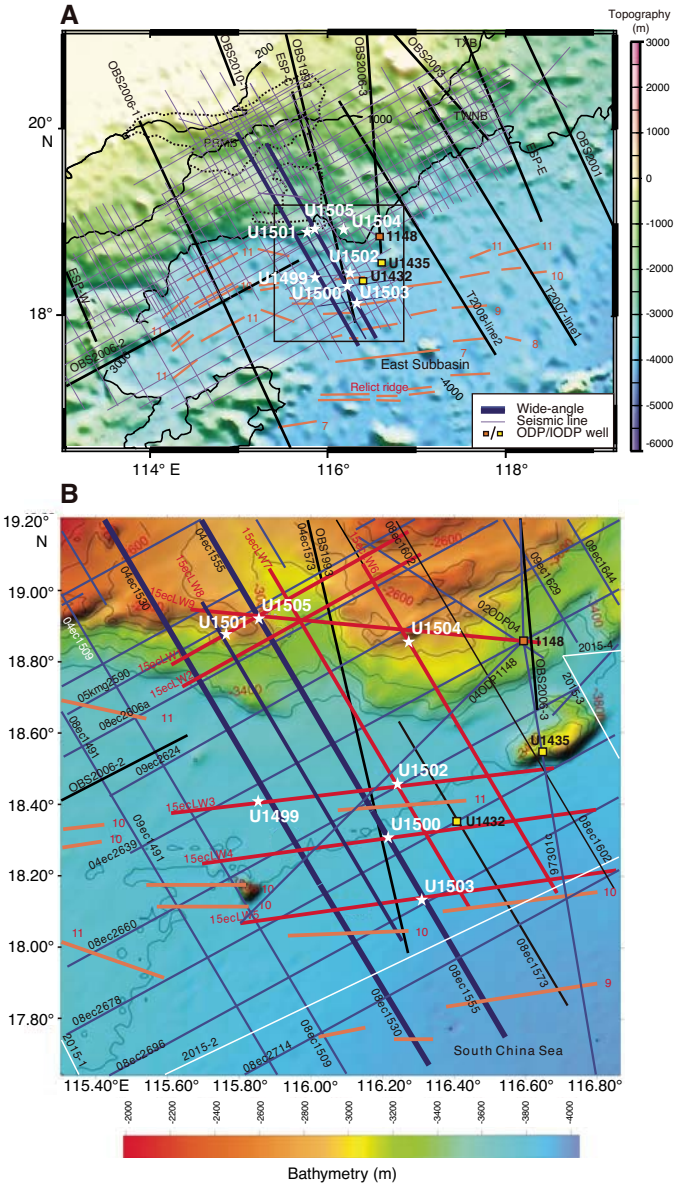

Figure F4. Deep crustal time-migrated seismic reflection data (A) without interpretation and (B) with interpretation. Note the rather thin lower crust (two layers) above a strong Mohorovicic seismic discontinuity (Moho) reflector that can be followed oceanward. Moho reflection is weak to absent seaward from around the interpreted continent–ocean boundary (COT). Wide-angle seismic data (Yan et al., 2001) confirm ~6 km thick ocean crust (OC) to be present seaward of the COT. A large detachment fault ~150 km inland of the COT separates more stable crust landward from that of highly extended crust seaward. An outer margin high (OMH) is a fairly consistent feature margin along this margin segment. Key seismic unconformities are shown in purple (T70; ~32 Ma breakup unconformity?) and blue (T60; ~23 Ma regional basin event). These ages are inferred from long distance (>100 km) correlation of seismic unconformities with industry holes and ODP Leg 184 Site 1148 (T60). These ages need confirmation by coring, and are only tentative. Tg unconformity (green) is basement. Approximate position of seafloor magnetic anomalies with chron numbers are shown by arrows. Seismic data is from Line 04ec1555-08ec1555 (courtesy of the Chinese National Offshore Oil Corporation [CNOOC]). Location of line is shown in Figure **F3**. CDP = common depth point; C11?, C10?, and C9? = possible Chrons. MSB = midslope basin.

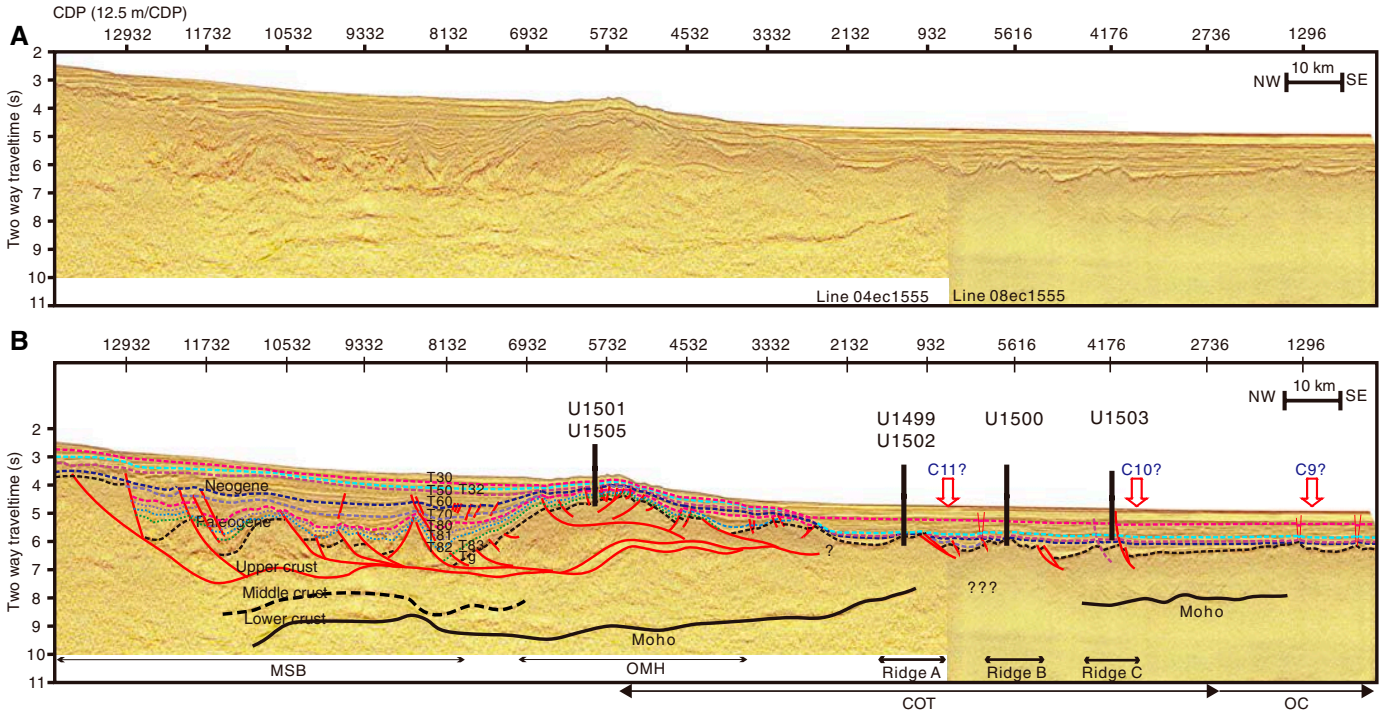

Figure F5. Two-way traveltime to (A) basement (Tg unconformity) and (B) Reflector T60. The proposed drilling transect (thick black line) is located approximately at the center of a margin segment bounded to the southwest by a transform fault. The northeastern boundary of the margin segment is located around IODP Expedition 349 Site U1435. In this location, the outer margin high and Ridge A seem to coalesce, and Ridges B and C of the continent–ocean transition become indistinct toward the northeast within the next margin segment. Note that the outer margin high is slightly oblique to more parallel Ridges A, B, and C.

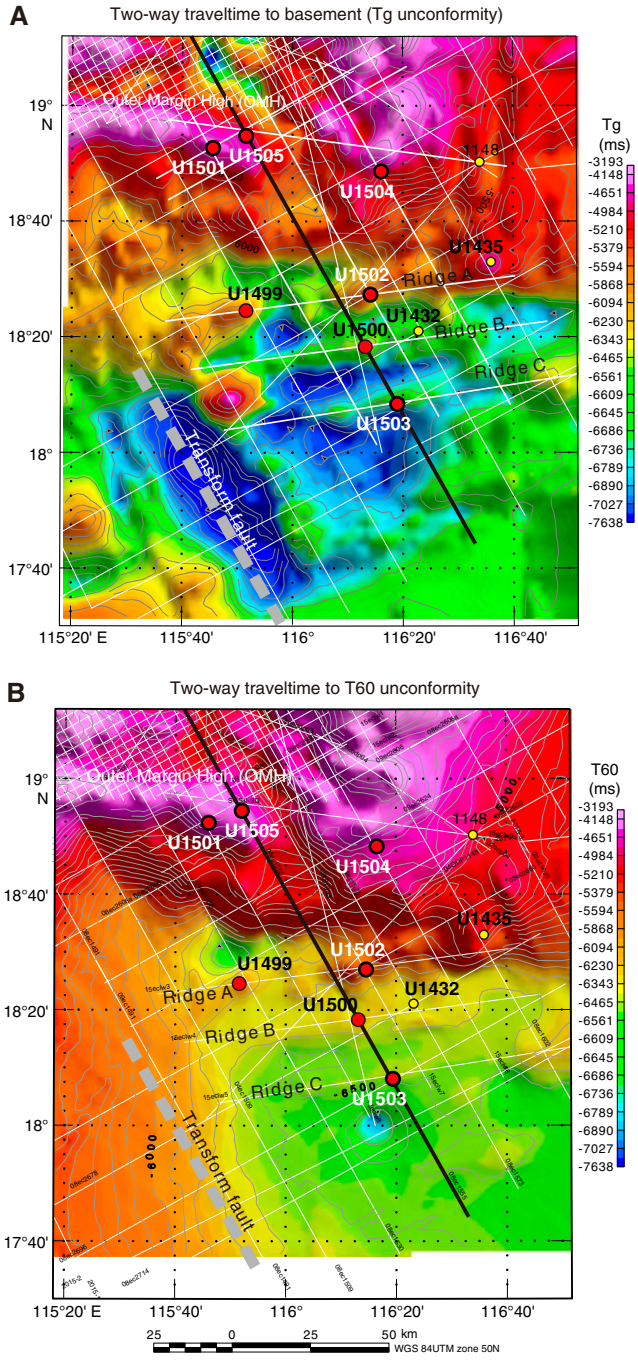

Figure F6. Planned and implemented Expedition 368 operations. APC = advanced piston corer, XCB = extended core barrel, RCB = rotary core barrel.

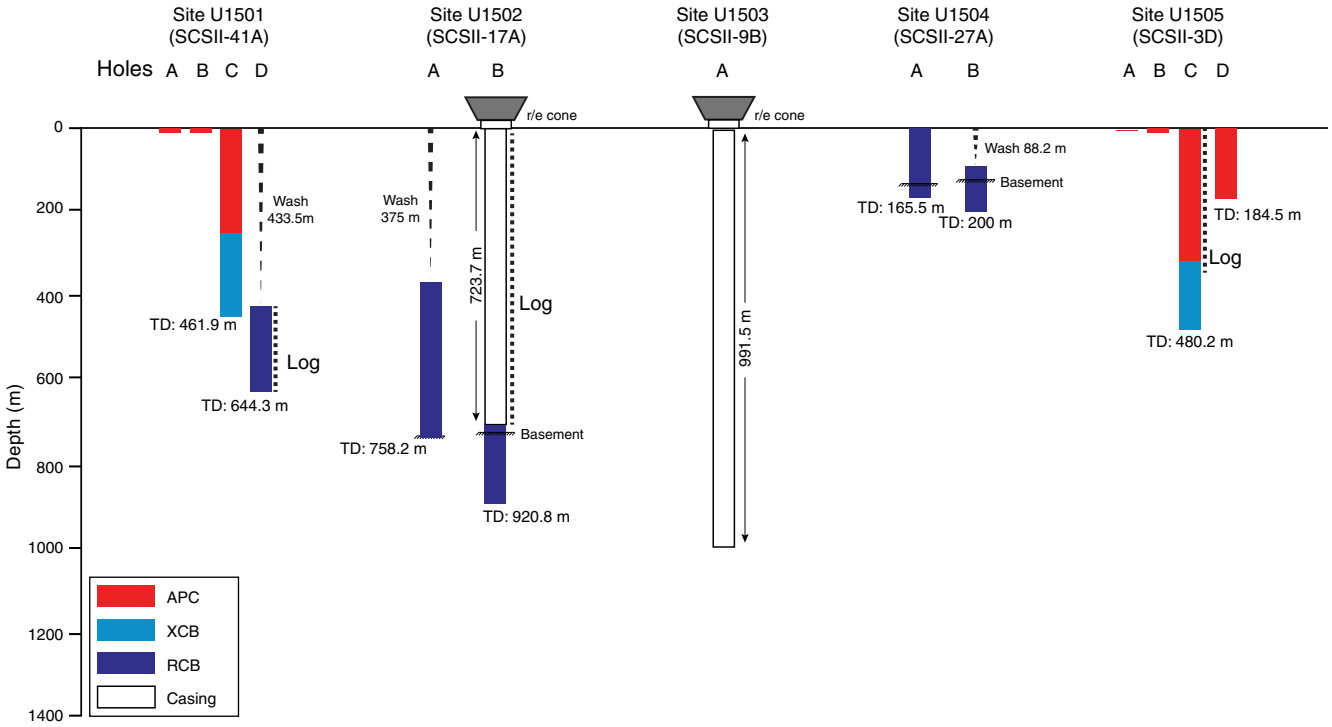

Figure F7. Bathymetry at Site U1501 and location of the site in relation to seismic Lines 15eclw1 and 15eclw8.

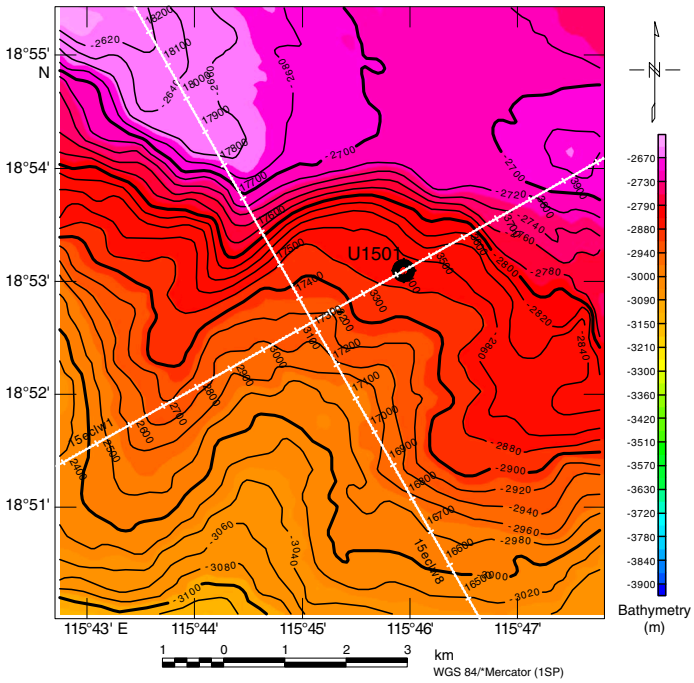

Figure F8. Lithostratigraphic, biostratigraphic, and magnetostratigraphic summary, Site U1501.

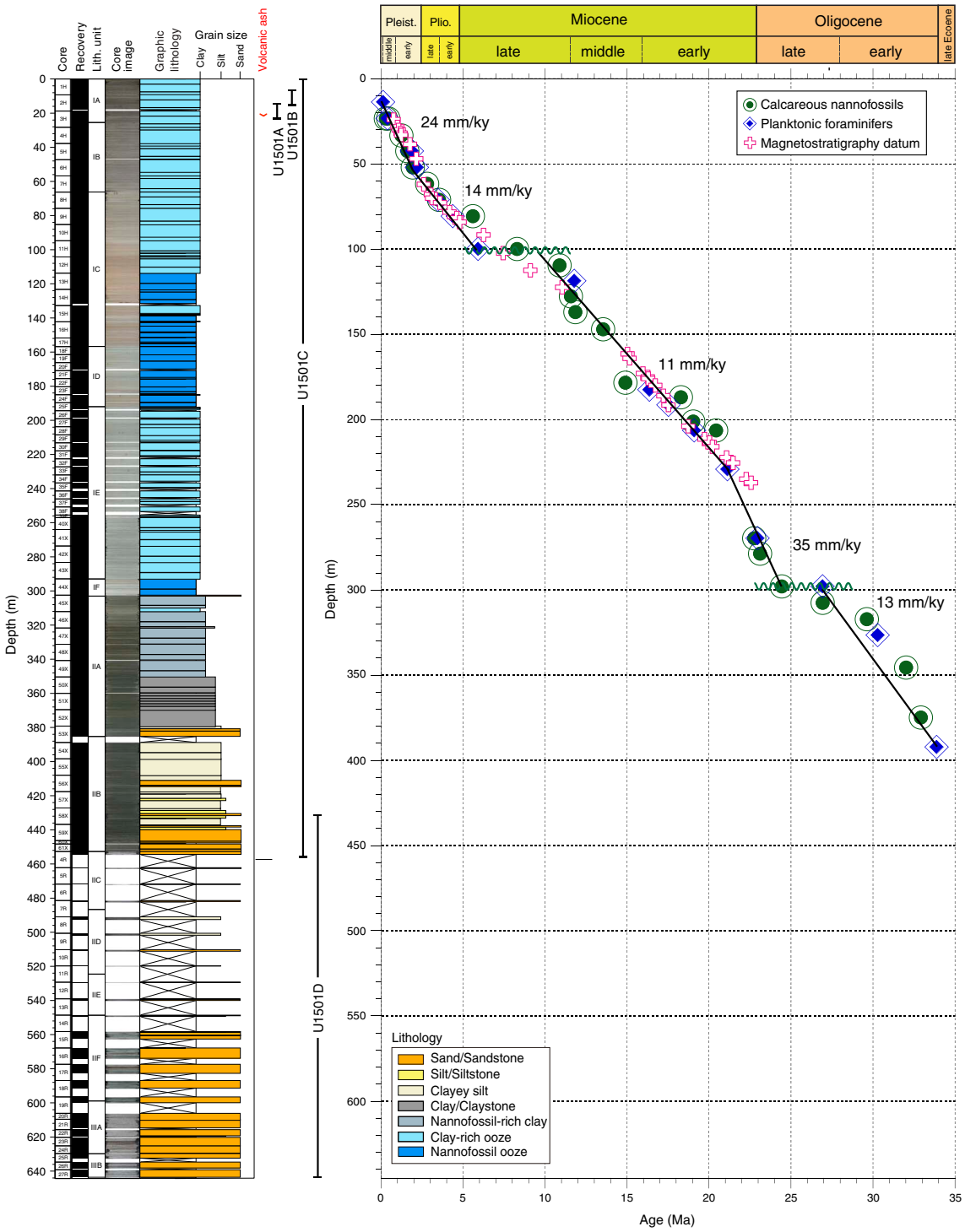

Figure F9. Bathymetry at Site U1502 and location of the site in relation to seismic Lines 15eclLW7, 15eclLW3, and 08ec2660. Note that the site is not at the exact crossing of Lines 15eclLW7 and 15eclLW3.

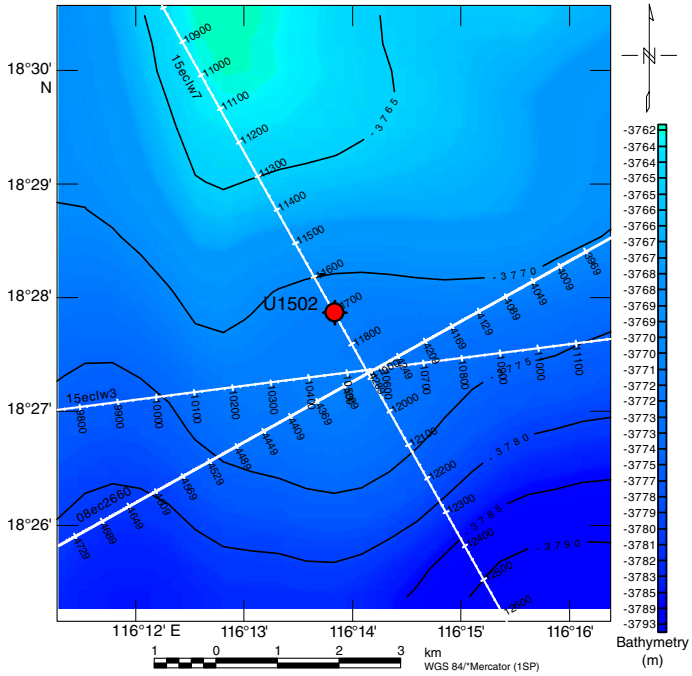

Figure F10. Lithostratigraphic summary of Holes U1502A and U1502B with simplified lithology and unit descriptions.

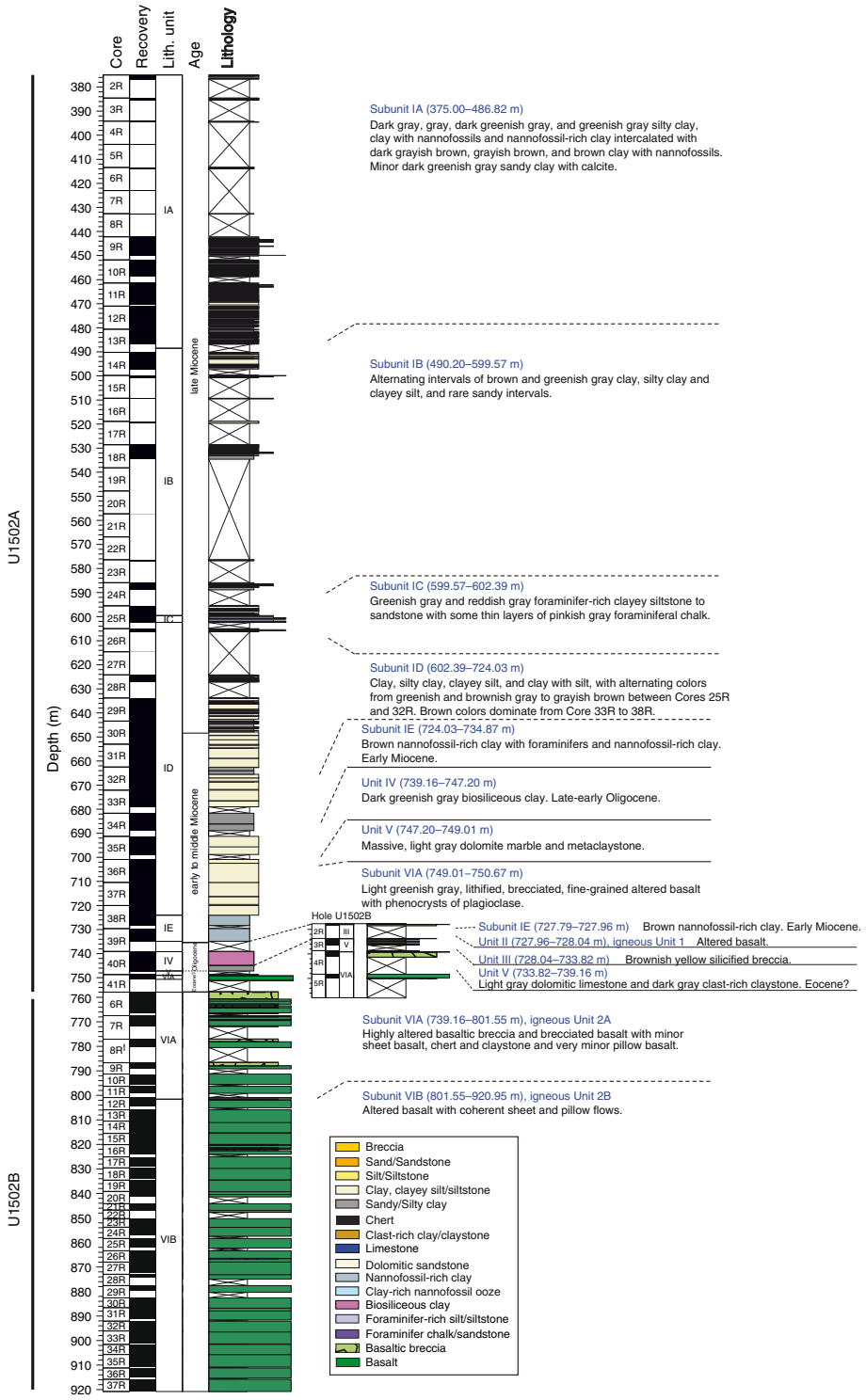

Figure F11. Lithostratigraphic summary of Holes U1502A and U1502B with main igneous lithologies and deformation structures. A. Highly plagioclase-phyric basalt with up to 50% plagioclase phenocrysts. B. Highly altered, sparsely plagioclase phyric pillow basalt with a well-preserved pillow. C. Moderately altered aphyric basalt flow with sparse vesicles. Note the change to a bluish gray color. D. Slump folds. E. Microfaults showing striations/slickensides on exposed surfaces. F. Distributed shear geometries with shear bands and tilted bedding. G. Brecciated basalt. H. Basaltic breccia. I. Network of composite epidote-rich veins.

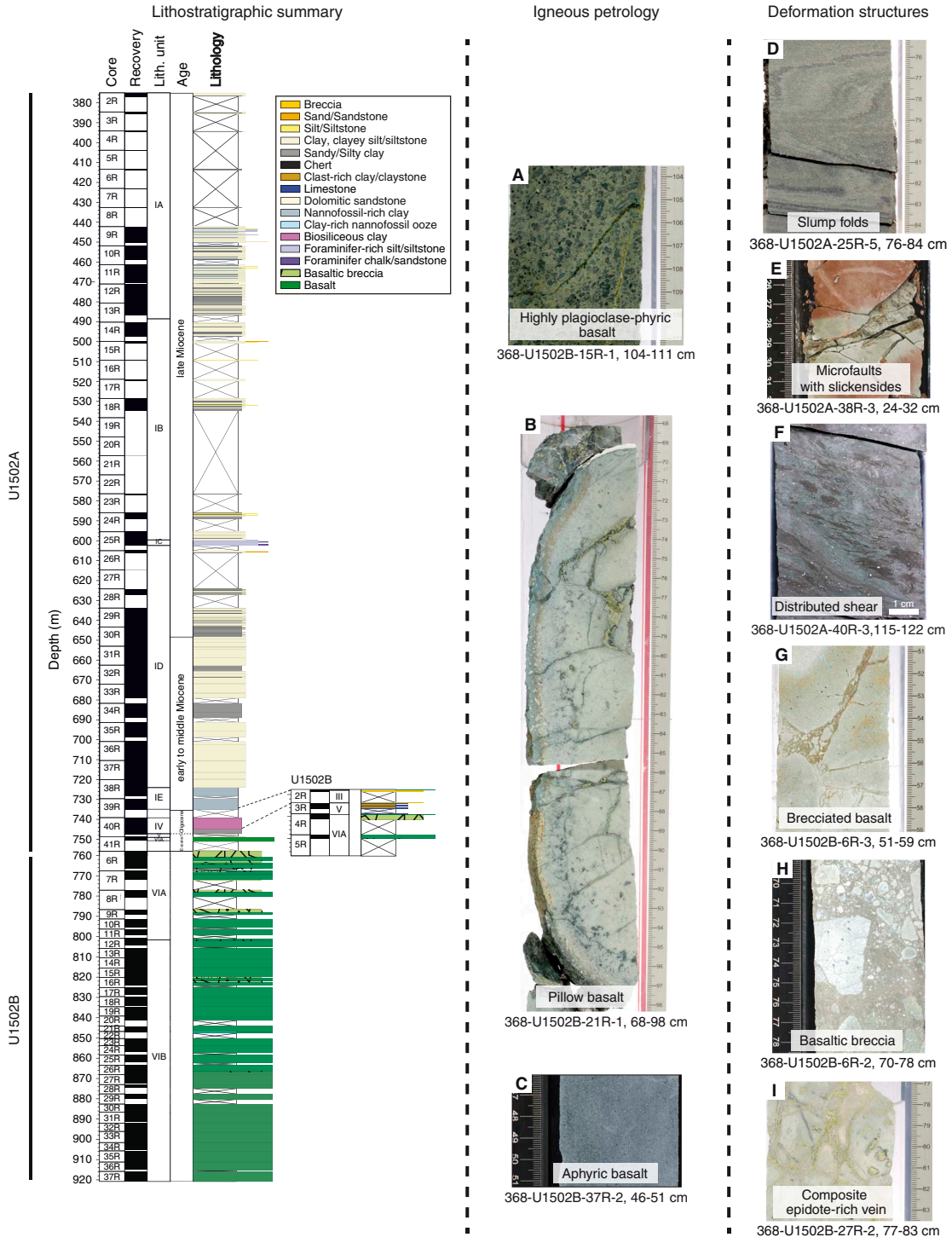

Figure F12. Magnetization intensity vs. inclination showing the effect of the steep drilling overprint. Basalts have higher magnetization intensity than sediments. Green lines represent the expected normal and reversal inclination at present latitudes.

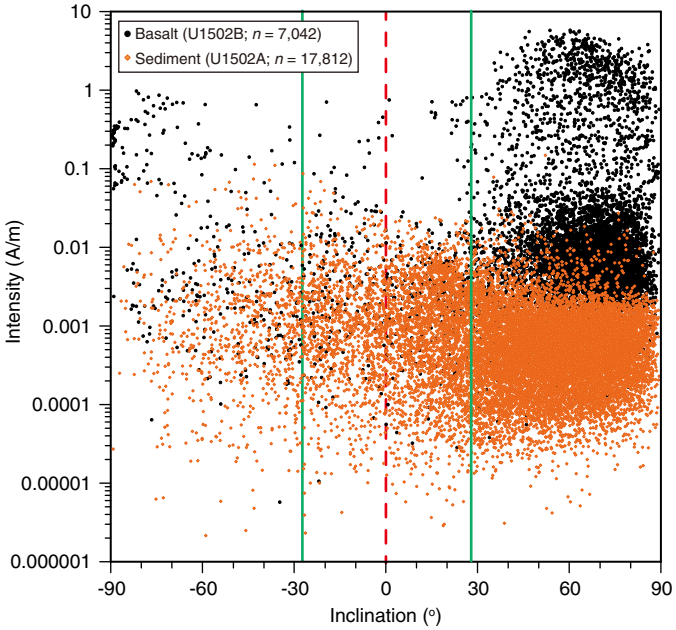

Figure F13. Physical property (PP) records, Site U1502.

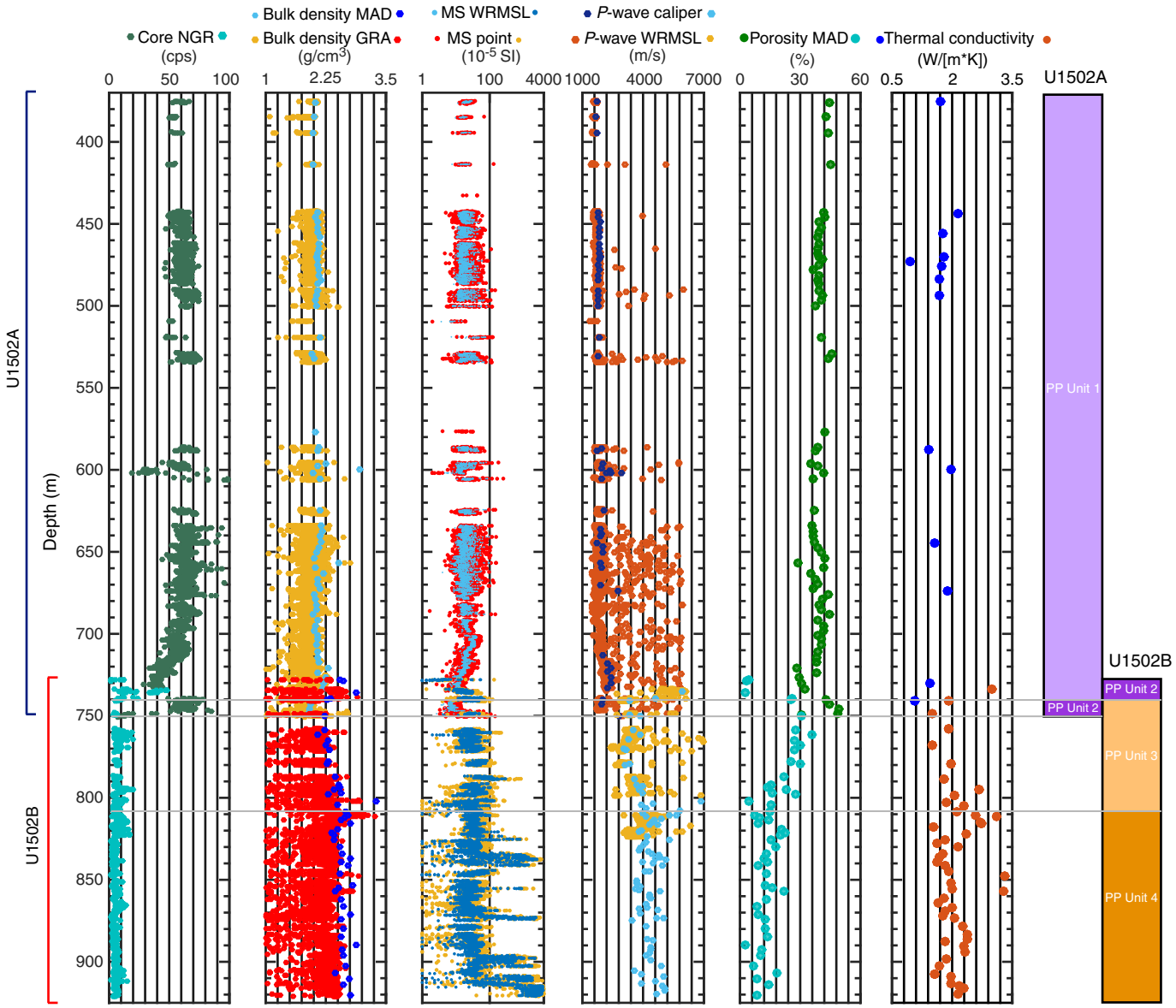

Figure F14. Bathymetry at Site U1503 and location of the site in relation to seismic Lines 15eclw5 and 08ec1555.

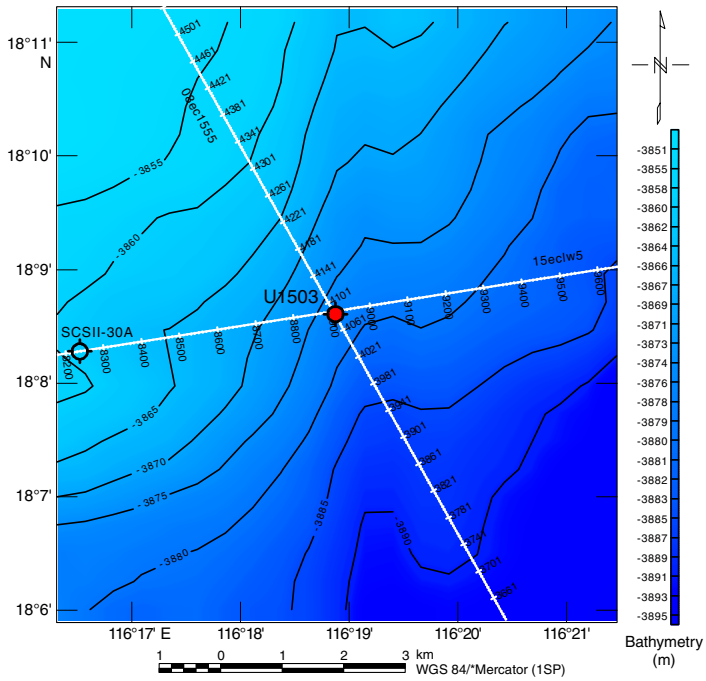

Figure F15. Bathymetry at Site U1504 and location of the site in relation to seismic lines. Note that there is a clear offset in the bathymetry along the margin that may indicate some transform offset within the deeper margin structure.

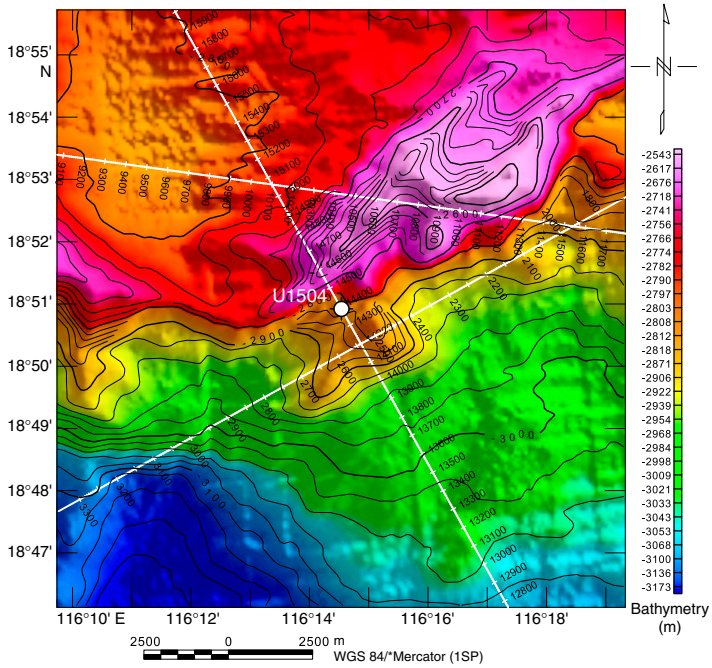

Figure F16. Lithostratigraphic, petrographic/petrological, and structural observations at Site U1504 with strong focus on the metamorphic basement. A, B. Clast-supported limestone with large benthic foraminifers and coral fragments. C. Severely quartz-veined, angular clast of chlorite-epidote granofels enclosed in mylonitic foliation of a typical epidote-chlorite schist. D. Steep (~75°) widely anastomosing foliation in a quartz + feldspar-rich variety of the rock. Arrow = extensively stretched veined clast of chlorite-epidote granofels oriented parallel to the foliation. E. Epidote-chlorite schist with granofels clasts split parallel to the *x*, *y*-plane of finite strain. Large granofels clast is crosscut by a shear band within the epidote-chlorite schist. Several sigma clasts are observed right above the shear band. Both deformation structures indicate normal sense of shear. A late, postkinematic vein crosscuts both the mylonitic foliation and the granofels clast. F. Tight foliation affected by crenulation cleavage in quartz-poor (i.e., more melanochratic) variety of the rock. G. Local occurrence of foliated impure calcite marble. H. Veined and altered aphyric mafic granofels clast (left side) and granofels clast interpreted as protolithic epidote vein (right side). Both clasts are internally undeformed but show synkinematic deformation together with the mylonitic fabric at their rims. I. Rigid (left) and strongly deformed (upper end) granofels clasts embedded in calc-silicate schist. Note the deflection of the mylonitic foliation at the clast boundaries. J. Long piece of core showing the characteristic morphology of the mylonitic foliation in calc-silicate schist of Subunit IIIB. Note the steep inclination and anastomosing geometry enclosing heterolithic clasts that are strongly elongated, folded, and oriented parallel to the foliation.

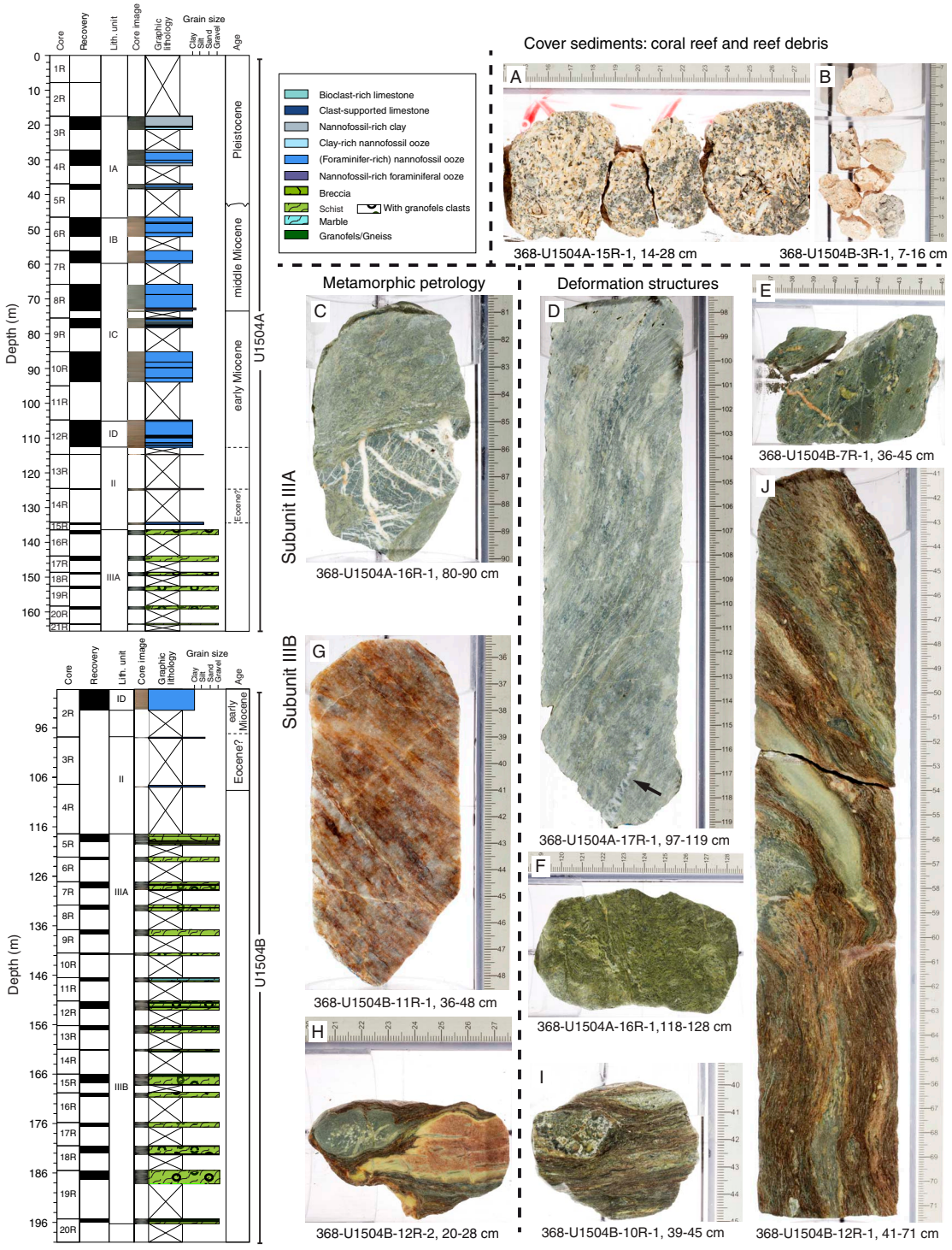

Figure F17. Magnetic measurements, Hole U1504A. Inclination was used to determine polarity. GTS2012 = geomagnetic polarity timescale of Gradstein et al. (2012). NRM = natural remanent magnetization (room temperature), AFD = alternating field demagnetization (archive half), ChRM = characteristic remanent magnetization (discrete samples).

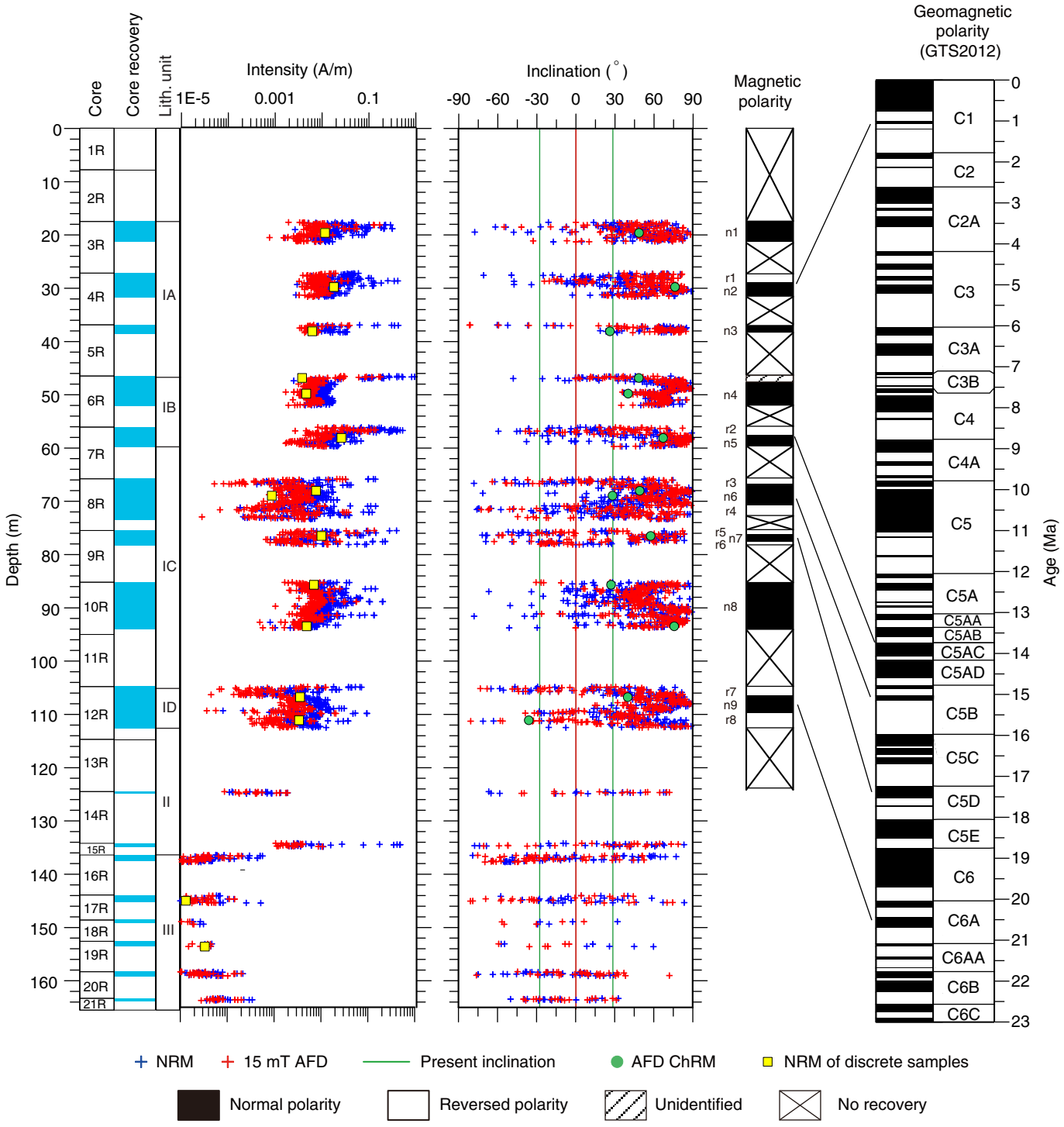

Figure F18. Bathymetry at Site U1505 and location of the site in relation to seismic Lines 04ec1555 and 15eclLW1. Note that the site is not at the exact crossing of Lines 04ec1555 and 15eclLW1.

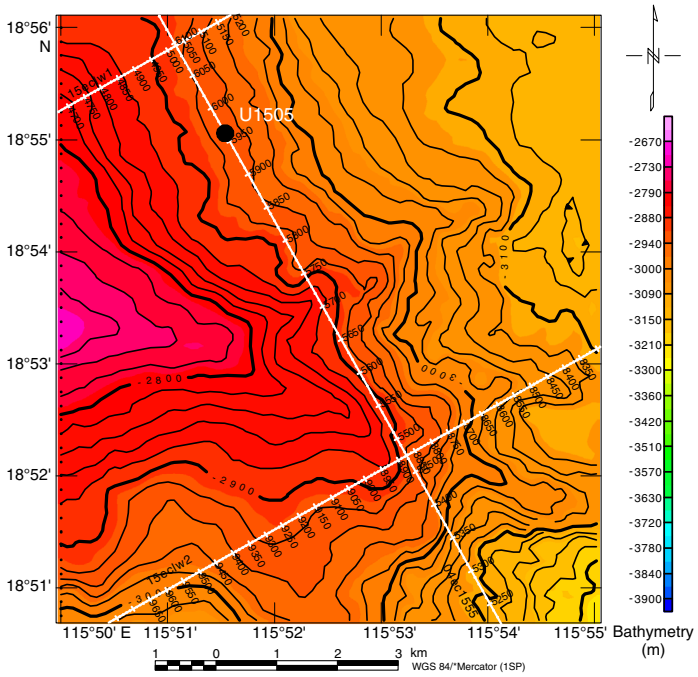

Figure F19. Lithostratigraphic and biostratigraphic summary, Site U1505.

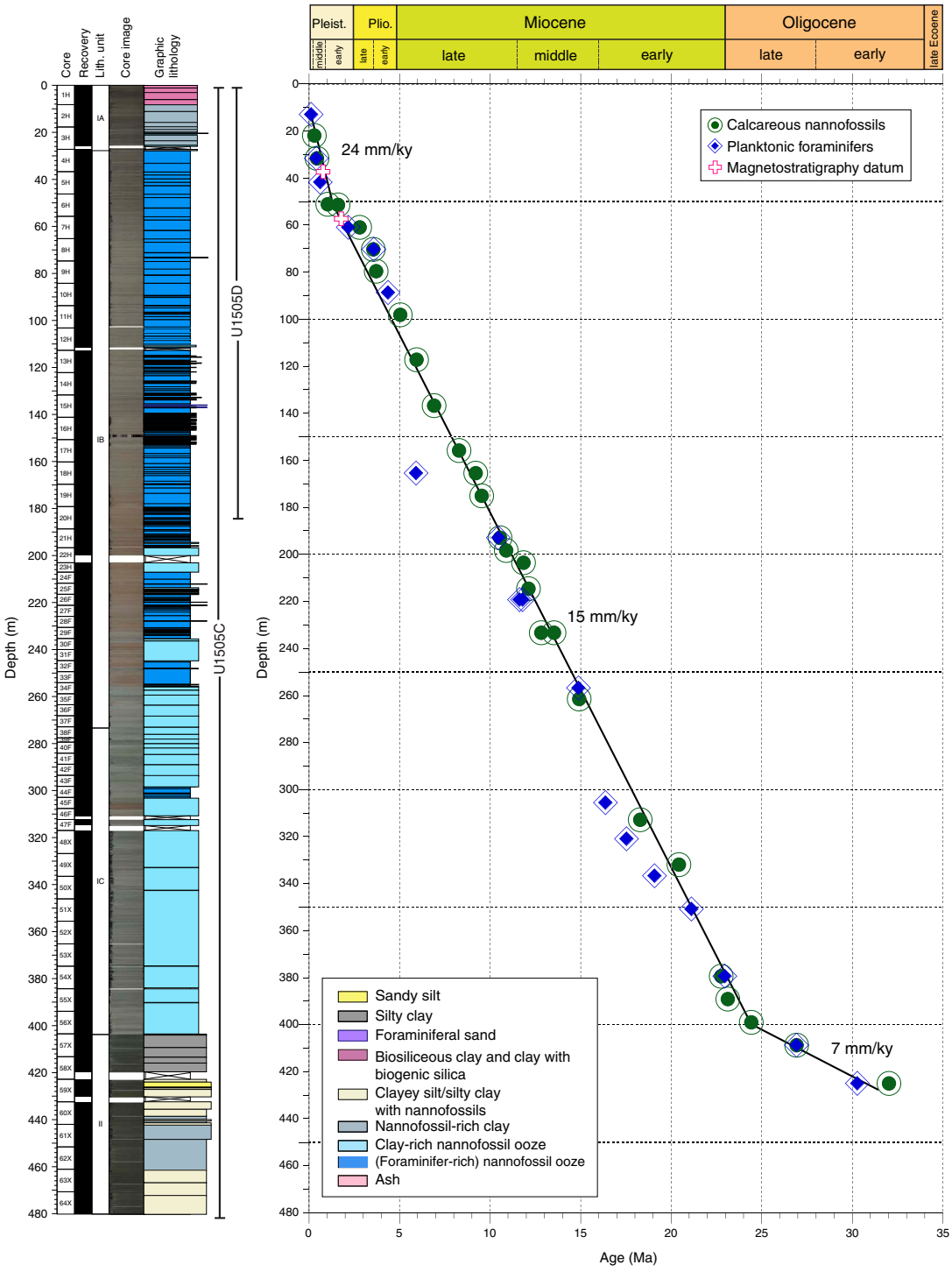

Figure F20. Magnetic measurements, Hole U1505C. Inclination was used to determine polarity. GTS2012 = geomagnetic polarity timescale of Gradstein et al. (2012). NRM = natural remanent magnetization (room temperature), AFD = alternating field demagnetization (archive half), ChRM = characteristic remanent magnetization (discrete samples).

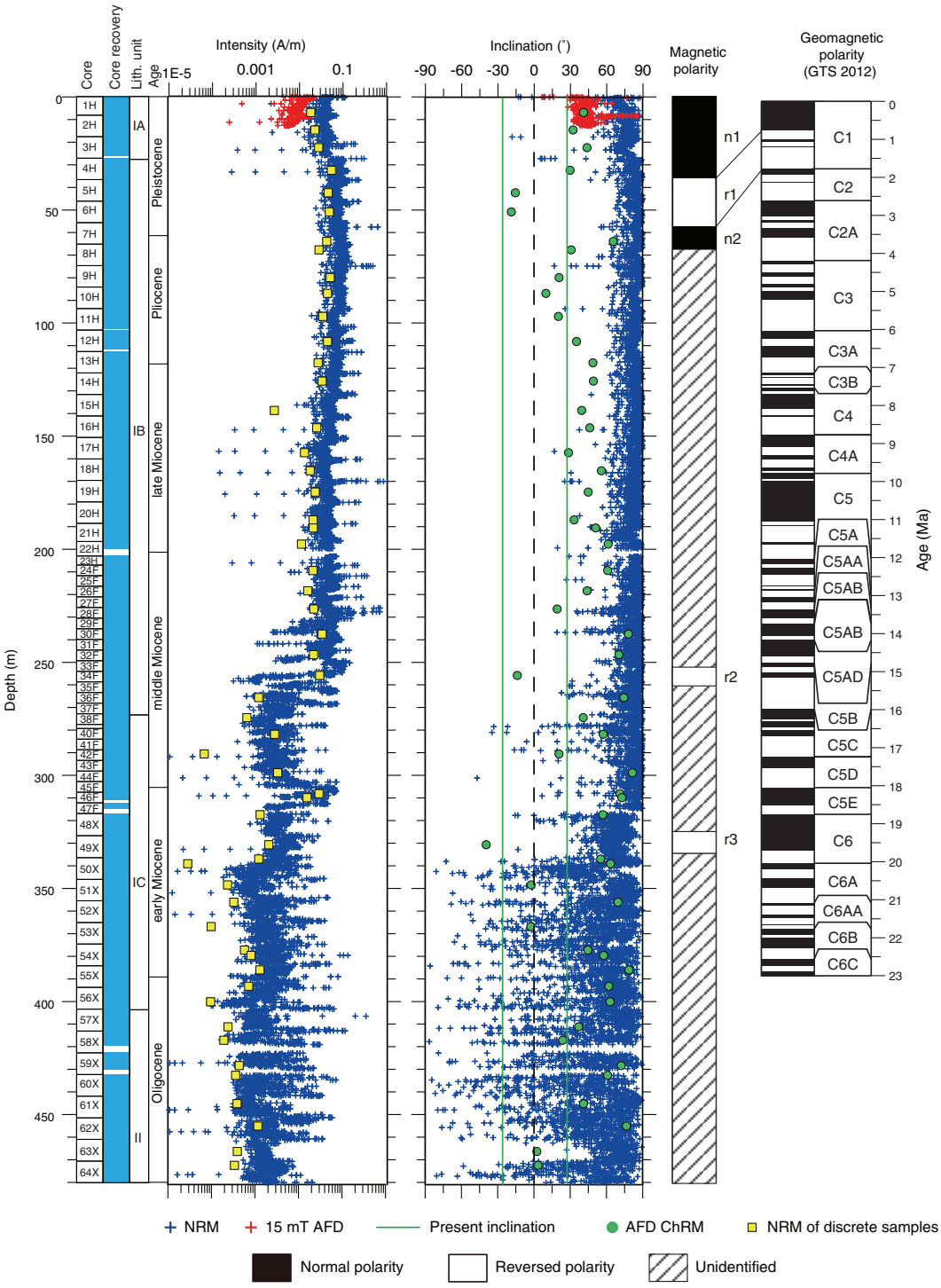

Figure F21. Data characterizing chemical anomalies associated with the T60 regional seismic marker, Site U1505.

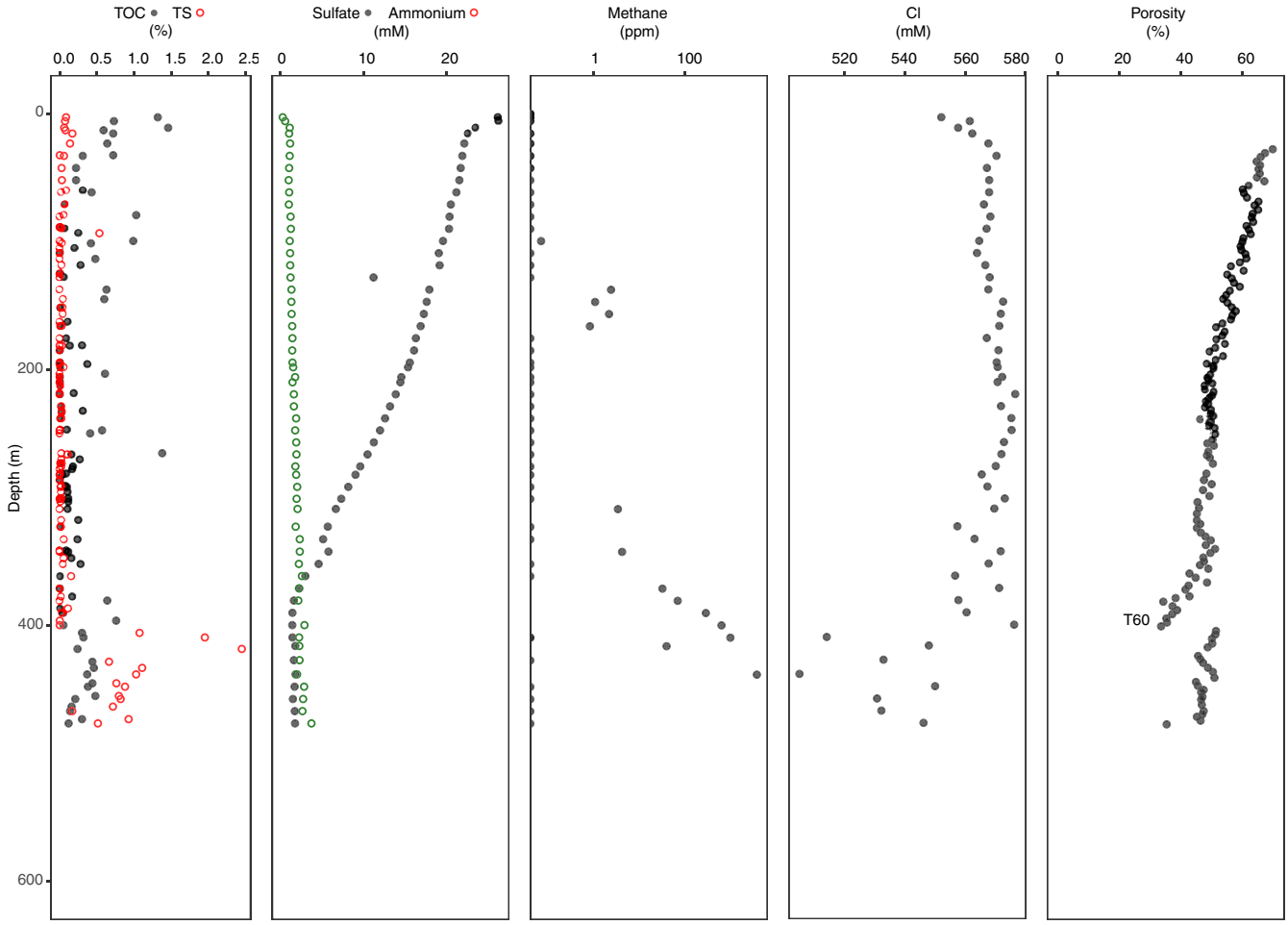

Figure F22. Reentry system and casing, Hole U1502B.

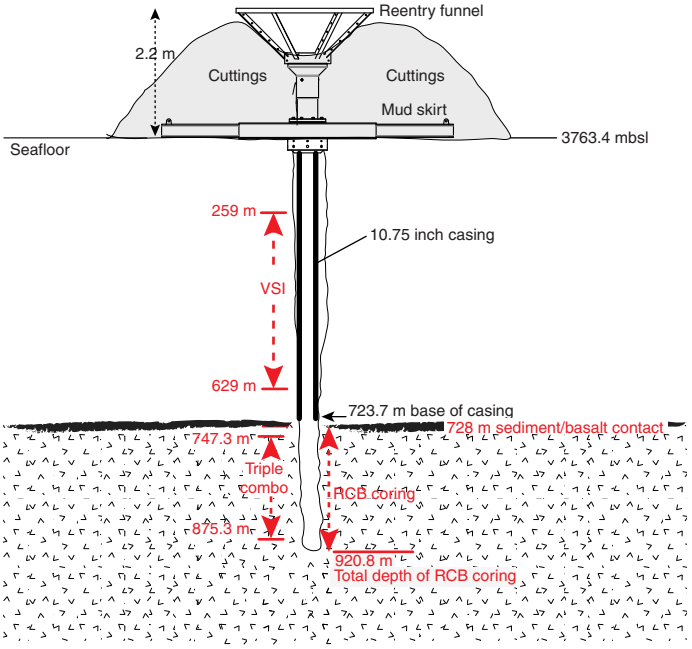

Figure F23. (A) Reentry system on the seafloor after free fall and (B) inspection of reentry cone after casing installation, Hole U1503A. The hole remains unused as a legacy hole for future occupation.

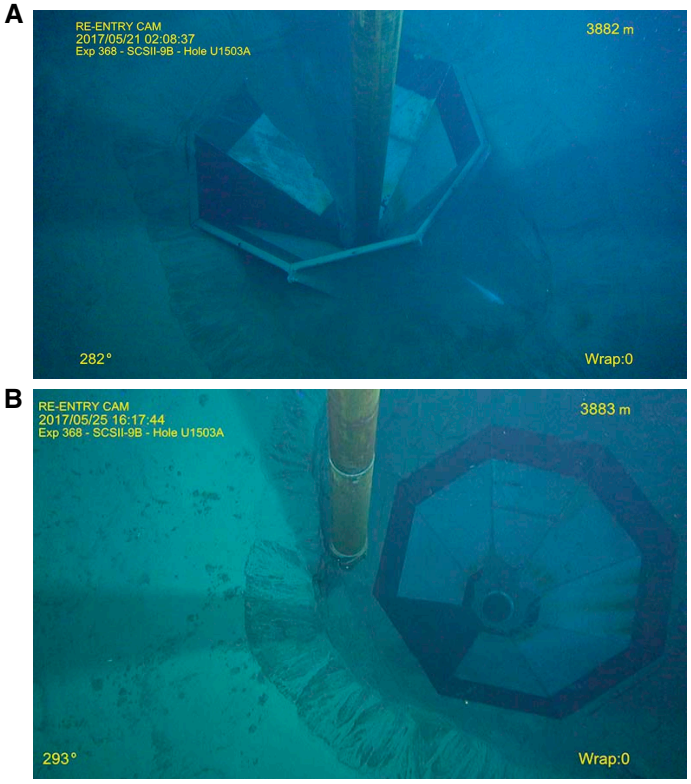

Figure F24. Reentry system and casing after installation, Hole U1503A.